



The Effectivity of Field Research Methods: Microbiological Monitoring of Acid Mine Drainage in Gauteng and Mpumalanga, South Africa

This thesis is submitted in partial fulfillment for the *Bachelor of Science (B. Sc.)* degree in Applied Chemistry

by

Corinna Schwarz

Eichastr. 6

90602 Seligenporten

Supervisors

Prof. Dr. Eberhard Aust

Prof. Dr. Ronald Ebbert

Nuremberg, 26.08.2016 (Summer Term 2016)

Prüfungsrechtliche Erklärung

Ich, Corinna Schwarz, Matrikel-Nr. 2301259, versichere, dass ich die Arbeit selbständig verfasst, nicht anderweitig für Prüfungszwecke vorgelegt, alle benutzten Quellen und Hilfsmittel angegeben sowie wörtliche und sinngemäße Zitate als solche gekennzeichnet habe.

Plagiarism Declaration in Accordance with Examination Rules

I herewith declare that I have worked on this thesis independently. Furthermore, it was not submitted to any other examining committee. All sources and aids used in this thesis, including literal and analogous citations, have been identified.

Nürnberg, 26.08.2016

Unterschrift / Signature

Acknowledgments

First of all, I would like to thank Prof. Christian Wolkersdorfer for giving me the opportunity to discover such a beautiful country and all the tips and tricks he taught me. Further, I would like to thank Prof. Dr. Aust and Prof. Dr. Ebbert for their supervision and support during my studies. At this point, special thanks goes to Prof. Dr. Ebbert and the Tshwane University of Technology for the allowance provided.

A big thank-you goes to Zeynep Weninger and Susanne Ederer for help in word and deed, and for their steady nerves.

For all the advice and ideas during my study, I offer a special word of thanks to Prof. Dr. Lösel. Last but not least, I would like to thank my mother and my boyfriend for cooking hot chocolate and for all their support.

Keywords

Mine Drainage

BART (Biological Activity Reaction Test)

Bacteria

qPCR

Field Research Methods

Schlüsselwörter

Grubenwasser

BART (Biological Activity Reaction Test)

Bakterien

qPCR

Feldmethoden

Abstract

South Africa has a substantial legacy of mining history. Many water sources are affected by mine drainage originating from flooded mines or tailings dams. For the pollution of this water, pyrite oxidation plays a pivotal role. Because of the forming of sulfuric acid and ferrous iron, the conditions for sulfate-reducing, iron-oxidising and iron-reducing bacteria are ideal, which are also catalysing these processes. People who depend on the contaminated water sources, e.g. habitants of townships or farmers, are the main affected parties. Especially because of this fact, the BART test can be helpful. In this thesis, the task was to ascertain the reliability and the handling of the BART test as an easy to apply and cheap field method.

The tests were performed to detect iron-related, sulfate-reducing and slime-performing bacteria at different locations in the regions of Gauteng and Mpumalanga. The results were compared with the results of a quantitative Real-Time PCR, which could detect DNA amounts between 1 ng and 0.1 ng per millilitre. To make further statements, on-site parameters were used as well, in order to verify the detected types of bacteria.

The BART test gave reliable results for the existence of the types of bacteria in the samples, provided that they were performed by the same person and under the same conditions. In three case examples, possible applications of the BART tests are suggested.

Kurzzusammenfassung

Durch seine lange Bergbauhistorie ist Südafrika zu einem großen Vermächtnis gelangt. Viele Wasserquellen sind durch Grubenwasser aus stillgelegten und gefluteten Minen oder durch Sickerwasser von Aushüben bedroht. Durch die Bildung von Schwefelsäure und Eisen(II) ist die Pyritoxidation hauptverantwortlich für die Bildung von saurem Grubenwasser, was den idealen Lebensraum für sulfatreduzierende, eisenoxidierende und eisenreduzierende Bakterien darstellt. Diese Mikroorganismen katalysieren den Prozess zusätzlich. Die daraus entstehende Wasserverschmutzung stellt besonders für Personengruppen ein Problem dar, die zwangsweise darauf angewiesen sind, wie Farmer oder Townshipbewohner. Aus diesem Grund können BART Tests eine hilfreiche Methode zur Observierung der Wasserqualität sein. Es handelt sich um einen leicht durchzuführenden und günstigen Test, der auch Laien zu einem simplen Screening befähigt. In dieser Arbeit soll das Handling und die Zuverlässigkeit dieses Tests untersucht werden.

Dazu wurden drei BART Testtypen – für eisenreduzierende oder -oxidierende, sulfatreduzierende und schleimbildende Bakterien – verwendet. Bei den Probenahmestellen handelte es sich u. a. um stillgelegte Minen, trinkwasserführende Flüsse oder Seen in den Regionen Gauteng und Mpumalanga. Die Testergebnisse wurden mit den Resultaten einer qPCR verglichen, wobei ein DNA-Gehalt zwischen 1 ng und 0,1 ng pro Milliliter in den Proben festgestellt wurde. Um weitere Aussagen treffen zu können, wurden zusätzlich die physikochemischen Parameter vor Ort gemessen und Proben für eine ICP-MS gesammelt.

Mit den BART Tests konnte eine zuverlässige Aussage zur Existenz der getesteten Bakterientypen in den Proben getroffen werden. Jedoch müssen absolut gleiche Versuchsbedingungen gewährleistet sein. In drei Fallbeispielen wurden Anwendungsmöglichkeiten des Tests vorgestellt.

Abbreviations

ADP	Adenosine Diphosphate
AMD	Acid Mine Drainage
AMP	Adenosine Monophosphate
ATP	Adenosine Triphosphate
BART™	Biological Activity Reaction Test
BA	Blackening All in Base and Ball
BB	Blackened Base
BC	Brown Cloudy
BG	Brown Gel
BL	Blackened Liquid
BR	Brown Ring
BT	Blackening around Ball
CG	Cloudy Gel-Like
CL	Cloudy Growth
CP	Cloudy Plates Layering
DS	Dense Slime (Gel-Like)
FO	Foam
GC	Green Cloudy
GY	Greenish-Yellow Glow in UV-Light
PB	Pale Blue Glow in UV-Light
RC	Red Cloudy
SR	Slime Ring around the Ball
TH	Thread-Like Strands
BSA	Bovine Serum Albumin
CARD-FISH	Catalysed Reporter Deposition Fluorescence <i>in situ</i> Hybridization
cfu	Colony Forming Units
DMSO	Dimethyl Sulfoxide
EC	Electrical Conductivity
FID	Floating Intercedent Device
FISH	Fluorescence <i>in situ</i> Hybridization
ICP-MS	Inductively Coupled Plasma Mass Spectrometry
IRB	Iron-related Bacteria
pac	Predictive Active Cells
PES	Polyethersulfon
P _i	Inorganic Phosphate
PLP	Possible Log Population [log (cfu mL ⁻¹)]
RPS	Reaction Pattern Signatures

SLYM	Slime-forming Bacteria
SRB	Sulfate-reducing Bacteria
TDS	Total Dissolved Solids [mg L ⁻¹]
T-RFLP	Terminal Restriction Enzyme Fragment Length Polymorphism
VFR	Vertical Flow Reactor

Contents

1	Introduction	1
1.1	Acid Mine Drainage in South Africa	1
1.2	Microbiological Activity in Acid Mine Drainage	4
1.2.1	Metabolism Basics	4
1.2.2	General Discussion of Microbes in Acid Mine Drainage	5
1.2.3	Microbes in AMD – What was Done until Now	7
1.3	Applied Field Research Methods	7
1.4	What should be Achieved	8
1.5	The Way to Go	9
2	Theory of the Used Methods	11
2.1	Measuring of the On-Site Parameters	11
2.2	What are BART-Tests	13
2.2.1	In General	13
2.2.2	Detailed Information about the IRB-BART Test	15
2.2.3	Detailed Information about the SRB-BART Test	16
2.2.4	Detailed Information about the SLYM-BART Test	17
2.3	Isolation of the DNA	17
2.4	DNA Quantification	18
2.4.1	Quantification by Real-Time PCR (qPCR)	18
2.4.2	Quantification by Photometer	19
3	Material and Methods	20
3.1	Material used in this Thesis	20
3.1.1	For the Performance of the BART Tests	20
3.1.2	For the On-Site Parameters and Sampling	20
3.1.3	For the DNA Isolation	21
3.1.4	For the Real-Time PCR (qPCR)	21
3.1.5	For the Agarose Gel Electrophoresis	22
3.1.6	Other Material	22
3.2	Site Description and Sampling	23
3.3	Performance of the Methods	26
3.3.1	BART-Tests	26
3.3.2	DNA Isolation	26
3.3.3	Photometric Quantification	27
3.3.4	Real-Time PCR (qPCR)	27
3.3.5	Agarose Gel Electrophoresis	28
4	Results and Interpretation	29
4.1	Interpretation of the Measured On-Site Parameters for Further Analysis	29
4.2	BART Tests	33

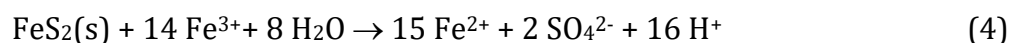
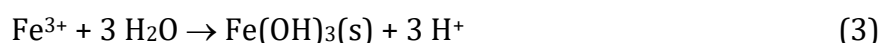
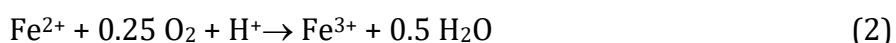
4.2.1	Description of the Visible Reaction and Quantification	33
4.2.2	BART after 21 Days for the Detection of any Weakness	43
4.3	Quantification of the Contained DNA	45
4.3.1	Results of the Photometric Quantification	45
4.3.2	Results of the Real-Time PCR	48
4.4	Results of the Agarose Gel Electrophoresis	55
5	Discussion and Application Possibilities	59
5.1	Comparison of the Quantification Methods	59
5.2	Microbiological Diversity	61
5.3	Example Case 1: Passive Treatment System in Carolina	61
5.4	Example Case 2: Cradle of Humankind – UNESCO World Heritage Site	63
5.5	Example Case 3: Active Mining	63
5.6	Future Work	64
6	Conclusions	65
7	References	66
8	Appendix	i
8.1	Standard Curves of the Agarose Gel Electrophoresis	i
8.2	Process of BART Test	iv

1 Introduction

1.1 Acid Mine Drainage in South Africa

There is a long history of mining connected to South Africa. It started with the discovery of copper fields in the Dryland of Namaqualand in the seventeenth century. In the late 1860, gold was found in the Eastern Transvaal and diamonds were discovered on the north-east border of the Cape Colony. Just a few years later, the gold mother lode of Johannesburg was discovered whereby the foundation for the economic and financial centre of South Africa was laid.¹ However, since this era, the main resources have changed to non-ferrous metals, ferrous metals and minerals (e.g. vanadium, chrome ore, ferro-chrome and chromium). The world's leading gold producer, is now China, and no longer South Africa. Nevertheless, being the sixth largest producer with a production of 154.2 t gold in 2013, gold mining remains important for the country. Especially the areas of Gauteng and Mpumalanga are famous for their gold deposits ².

It is well-known, that mining causes pollution on various spatial and temporal scales. One problem is acid mine drainage (AMD), which is caused by the oxidation of disulfides such as pyrite and pyrrhotite.³ Exposed to oxygen and water, the minerals start to oxidise and sulfuric acid is produced ⁴. Mills ⁵ illustrated the reaction for pyrite-oxidation as following:



After getting in contact with oxygen rich water, the sulfide of the pyrite is oxidized to sulfate. Caused by the oxidation, ferrous iron dissolves in the water and protons are released (1). In the next step, the ferrous iron is oxidized to ferric iron (2) which is hydrolysed afterwards and precipitates as ferric hydroxide (3). In this step, more acidity is released into the water. Another possible reaction to increase the acid is the oxidation of pyrite by ferric iron (4). The oxidation of Fe^{2+} is thermodynamically preferred (ΔG^\ominus is negative), but kinetically inhibited. Because of that, the reaction is very slow under abiotic conditions.^{5,6} An example for oxidised pyrite is shown in Figure 1. Due to microbiological catalysation by some chemolithotrophes,

the reaction can be accelerated by a factor of up to 10^6 times ⁷. A detailed description of the importance of microbiological activity for the genesis of acid mine drainage can be found in the following chapter '*1.2.2. General Discussion of Microbes in Acid Mine Drainage*'.

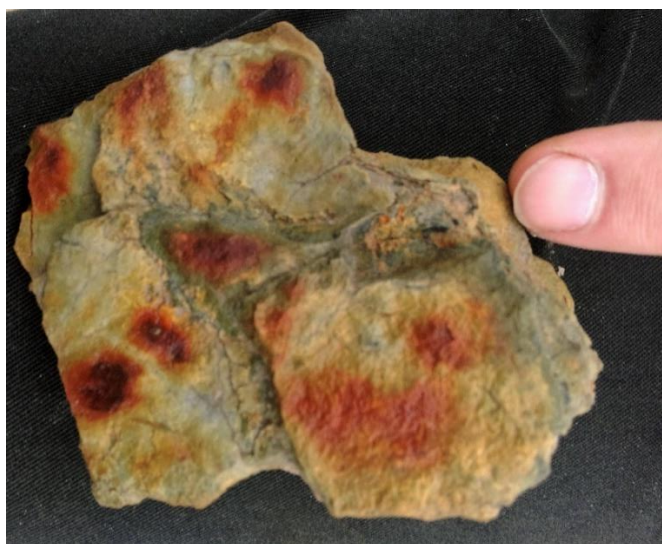


Figure 1: Oxidized pyrite from the Nestor Tailings Dam Pond.

In 2012, an event revealing the danger of AMD and showing environmental and social consequences thereof occurred in the town of Carolina (Mpumalanga).⁸ In this region, coal mining is very widespread, and the coal is contained in layers within sedimentary rocks ⁹. To gain coal, two different ways of mining are possible: opencast and deep mining. During opencast mining, the overburden is removed until the coal layer is laid open. Then, the coal seam is removed and afterwards, the place is due to be recultivated. AMD in this environment is generated, when rainwater percolates through the stockpiled topsoil and overburden and oxidizes the pyrite.⁹

McCarthy and Humphries investigated the incident in Carolina. After an intense rainstorm, a rapid deterioration of the water quality in the Boesmanspruit dam was detected. Inside the water reservoir, a sudden decrease of the pH to 3.7 was noticed. Moreover, the concentrations of iron, aluminium, manganese and sulfate increased, fish were dying and the water turned dark green. Since the dam was built to ensure the drinking water supply of Carolina, the residents depended on potable water from outside resources. The problem was unresolved for seven months and led to protests and vandalism, and one of the protesters was even shot dead. Chemical analyses showed an accumulation of mine water seepage in the wetland area upstream to the dam, and originating from the Witrandspruit sub-catchment. Catchment

basins containing the contaminated run-off from coal mining facilities were flooded during the downpour, and the contents were flushed in the basin.⁸

The impact of AMD resulting from gold mining in the West Rand Gauteng Province was scrutinized by Naicker et al.¹⁰ They confirmed the detrimental effects on the environment, particularly at the quality of ground water in the karst aquifer of the Zwartkrans Compartment. Downstream landowners and agricultural activities depending on ground water are threatened by the contaminated water.



Figure 2: Impact of acid mine drainage on the flora at site MSS (Middleburg Steam & Station), which is close to eMalahleni.

In the Witwatersrand region, gold mining caused a contamination of the ground water with potentially toxic substances (Ni, Co, Cu, Fe, Mn, Cr and Zn) as well as acidification ¹¹. In this area, gold is contained in layers of one metre thickness on average within conglomerate rocks. These rocks are removed and brought to the surface. There, the rocks are crushed and the gold is extracted with different chemical or mechanic methods. After this, the gold free material is brought to waste heaps, forming tailing dumps or slimes. On average, the conglomerate contains approximately 3 % of pyrite, which can be oxidized.⁹

Acid mine drainage occurs at flooded mines as well. Varying oxygen concentrations and redox values associated with the fluctuation in the water level caused by storms or draughts cause the oxidation of pyrite and consequently AMD is generated. It is quite common to flood mines after the lifespan of the mine ended, and for various reasons. Mine flooding prevents the collapse of the mine, unauthorized entry, illegal mining and disulphide oxidation. On account of different environment variables as mentioned above, disulphide oxidation cannot be avoided completely.¹²

1.2 Microbiological Activity in Acid Mine Drainage

1.2.1 Metabolism Basics

Cells need energy to enable processes which are essential for life, such as movement or mass transportation. Therefore, free enthalpy has to be generated, saved and released purposefully. As energy carrier, ATP (adenosine triphosphate) is responsible for the regulation, storage and disposition of energy. ATP consists of three pyrophosphates (Pi) which are linked with to ribose and an adenine rest. To release energy, one or both of the phosphoanhydride bonds are hydrolysed by enzymes. Thereby, adenosine diphosphate (5) or adenosine monophosphate (6) and pyrophosphates are the educts.



To keep the metabolism working, ATP has to be regenerate somehow. Therefore, at least the amount of discharged energy has to be brought up again. How much energy this process really needs is exemplarily calculated for reaction 5.

$$\Delta G_m'^0 = \sum \Delta G_{f,m}'^0 (\text{products}) - \sum \Delta G_{f,m}'^0 (\text{educts}) \quad (7)$$

$\Delta G_m'^0$ standard Gibbs free energy change per mole of reaction, [kJ mol⁻¹]

$\Delta G_{f,m}'^0$ standard Gibbs free energy of formation change per mole of reaction, [kJ mol⁻¹]

Under biological standard conditions (pH = 7, T = 298 K, p = 1 bar), 32 kJ mol⁻¹ of energy are released^{13, 14}. Given that, it must not be forgotten to convert the result in order of the concentrations present in a cell. Under physiological conditions, the amounts of ATP, ADP and Pi in cells are approximately 10 mM ATP, 1 mM ADP and 10 mM inorganic phosphate.¹³ Therefore, equation 8 has to be applied.

$$\Delta G' = \Delta G_m'^0 + RT \ln \left(\frac{c_p}{c_E} \right) \quad (8)$$

$\Delta G'$ Gibbs free energy change, [kJ mol⁻¹]

$\Delta G_m'^0$ standard Gibbs free energy change per mole of reaction, [kJ mol⁻¹]

R ideal gas constant

c_p concentration of products, [mol]

c_E concentration of educts, [mol]

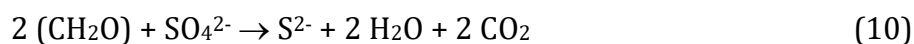
With $\Delta G_m'^0 = -32 \text{ kJ mol}^{-1}$, $R = 8.31451 \text{ J mol}^{-1} \text{ K}^{-1}$ and $T = 298 \text{ K}$:

$$\begin{aligned} \Delta G' &= -32 \text{ kJ mol}^{-1} + R \cdot 298 \text{ K} \cdot \ln \left(\frac{0.01 \text{ M} \cdot 0.001 \text{ M}}{0.01 \text{ M}} \right) \\ &= -32 \text{ kJ mol}^{-1} - 17.12 \text{ kJ mol}^{-1} = -49.12 \text{ kJ mol}^{-1} \end{aligned} \quad (9)$$

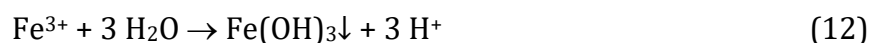
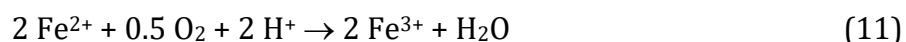
The hydrolysis of ATP is an exergonic process ($\Delta G < 0$), which means energy is released. To recreate ATP, the cell needs at least the same amount of energy what is set free. This is especially true given that since cells need 75 – 80 kJ mol⁻¹ to regenerate ATP.¹³ For this purpose, different metabolic pathways had developed by evolution. Pyrite oxidation is caused by chemolithotrophic bacteria, which uses a redox reaction (*chemo*-) as energy source and inorganic compounds (*-litho*-) as electron donor. In the case of acid mine drainage, the FeS₂ or other metal sulfides (e.g. marcasite or pyrrhotite) are the source of electrons.¹²

1.2.2 General Discussion of Microbes in Acid Mine Drainage

As mentioned before, microorganisms play a pivotal role in the generation of acid mine drainage. For some time, the microbiological influence in the forming of AMD was underestimated. Since then, it has been ascertained, that the biological oxidation rate of pyrite is 10⁶ - 10⁷ times higher than the chemical oxidation rate ^{15,16}. In first instance, key roles in this process are played by iron-oxidizing and sulfate-oxidizing bacteria. Almost all reactions of sulfur oxidation are chemolithoautotroph. For Microbes, there are two different ways of how to attack metal sulfides. When the microorganism is located directly on the mineral, enzymes react with the surface of the crystal corn. For the indirect way, the mineral dissolves and the sulphur is oxidized to sulfate by the microbes. Under anaerobe conditions, some microorganisms are able to oxidize organic material while reducing sulfate.



In equation 10, the organic material is symbolized by CH_2O . Sulfids originating from sulfate reduction builds pyrite, when ferrous iron is released at the same time. Due to the formation of sulfids in coal layers, the sulfate reduction is also an important geochemical process. For the oxidation from ferrous to ferric iron, the iron has to be diluted first. Afterwards it is oxidized by different microbes (e.g. *Acidithiobacillus ferrooxidans*) and precipitates as iron hydroxide, which is responsible for the red – yellow colour of rocks.



These reactions are part of the pyrite oxidation. The full reactions therefore can be found in ‘1.1 Acid Mine Drainage in South Africa’ (reaction 1 - 4). The more ferrous iron is released and the more iron-(III)-hydroxide precipitates, the more acid the water becomes, as can be seen in reaction 11 and 12. A high concentration of iron in groundwater is caused by high activity of microbes. Iron can be reduced directly, when it serves as electron acceptor during the oxidation of organic material. It can also be reduced indirectly by bacteria, caused by the production of suitable reducing agents. However, it becomes difficult to distinguish between sulfur- and iron-oxidation when it comes to reactions with iron sulfids.^{5,17}



Figure 3: Typical red colour from acid mine drainage caused by the precipitation of iron-(III)-hydroxide

1.2.3 Microbes in AMD – What was Done until Now

Currently, ample research on the microbiology of acid mine drainage and mine water in general has been done. On the one hand, research was focused on analysing the biodiversity. Therefore, FISH (fluorescent *in situ* hybridization), CARD-FISH (catalysed reporter desposition – fluorescent *in situ* hybridization), T-RFLP (terminal restriction enzyme fragment length polymorphism), qPCR (quantitative polymerase chain reaction), SYBR Green II direct counting and pyrosequencing were the methods of choice.^{3,18,19} On the other hand, the use of different microbes in a variety of water treating plants is quite common ²⁰⁻²². Phylogenetic analysis has been performed as well. Therefore, iron oxidizing bacteria cultures originating from the Bundesanstalt für Geowissenschaften und Rohstoffe (Hannover, Germany) were used ¹⁵. Due to the fact that only a fractional amount of bacteria contained in a sample can be cultivated, there are still a lot of unknown bacteria which cannot be considered in culture based studies. However, a study focused on an easy to perform and apply routine check method has not been undertaken yet.

1.3 Applied Field Research Methods

Cheap and easy to use field research methods for the analysis of acid mine drainage have been widely tested ^{23,24}. Fyffe et al. concluded their studies within the limits of a High School research project on AMD. There, the influence of gold and uranium mining in the upper Wonderfonteinspruit catchment on other water sources was examined. Macherey and Nagel Quantifix test kits for pH, sulfate, aluminium, carbon hardness and the total iron concentration were used. To verify the results, samples were sent to the Council for Geoscience Environmental Laboratory as well. The results showed, that the simple kits could reliably discriminate between polluted and unpolluted water.²⁴

Coetzee used test strips in his works, which indicated the pH and different concentrations of sulfate and iron through a colour reaction. His intention was to set up a field screening protocol to evaluate the water quality, especially for sites which are not or only slightly in need of rehabilitation and no detailed chemical analysis is necessary. The test strips are also a reliable source of information, although here are some limitations. Different individuals may see the colour changes in different ways and for a complete characterisation, laboratory analysis cannot be avoided.²³

BART Tests have been used before to inspect the effectivity of biological source treatment of AMD ²⁵ or to estimate the population size in rough habitats. ²⁶ In these studies, especially the SRB BART was used and its usability was verified.

1.4 What should be Achieved

As a newly industrialised country and a young industrial nation, South Africa does not have the full capacities in laboratories and well-trained staff. Problems already start at school, where chemicals and laboratory equipment are often not available due to financial constraints.²⁷ Despite this, the country has a severe legacy of pollution originating from mine workings ^{28 29 30}. Besides active mines, over 6000 mine sites are abandoned and primarily in the Witwatersrand region ²³.

In addition, South Africans are becoming more aware of the environmental impact and the consequences, as was evident with the Carolina incident. Because of the large number of mines, the negative impact of mining areas and from mining influenced areas with human habitat is unavoidable. A perfect example is the mine water discharge in the Wetland West of Transvaal and Delagoa Discharge Point (Sample TDW) (Figure 4) which is situated next to a township. In addition, there is a rivulet close by in which children play.



Figure 4: The Wetland West of Transvaal and Delagoa Discharge Point, sampling location of TDD and TDW. In the background, the township KwaGuqa can be seen clearly.

That is only one of many cases and as in many times, the poor are the most affected. Especially during draughts, people need to use every available source of water that exists. However, not only inhabitants of townships are affected. Mine water can also have an agricultural impact, since most plants cannot grow in soil polluted by acid mine drainage. This means that farmers are affected as well.

The measuring of the on-site parameters (e.g. pH, electrical conductivity, redox potential) combined with a microbiological monitoring can give valuable information about the water quality, especially for obtaining a first impression or for routine checks. Therefore, it is necessary to enable non-laboratory working people, e.g. mine workers, farmers and officials, to examine the water quality. Using methods which are easy to apply and to understand are essential to establish a continuous monitoring of a large number of sites. The aim of this work is to examine the BART tests, to determine whether they are a reliable and representative method to examine the microbial consortia at a sampling location. Based on the results of the BART tests of frequently taken samples, recognizing a change in the water quality should be possible.

1.5 The Way to Go

In order to reach a clear statement and achieve the aim of this study, various steps need to be followed. The results of the BART tests will be compared with the results of the qPCR. In the end, three example cases will be created to show up a possible application of the BART test. The single work steps are listed in [Figure 5](#).

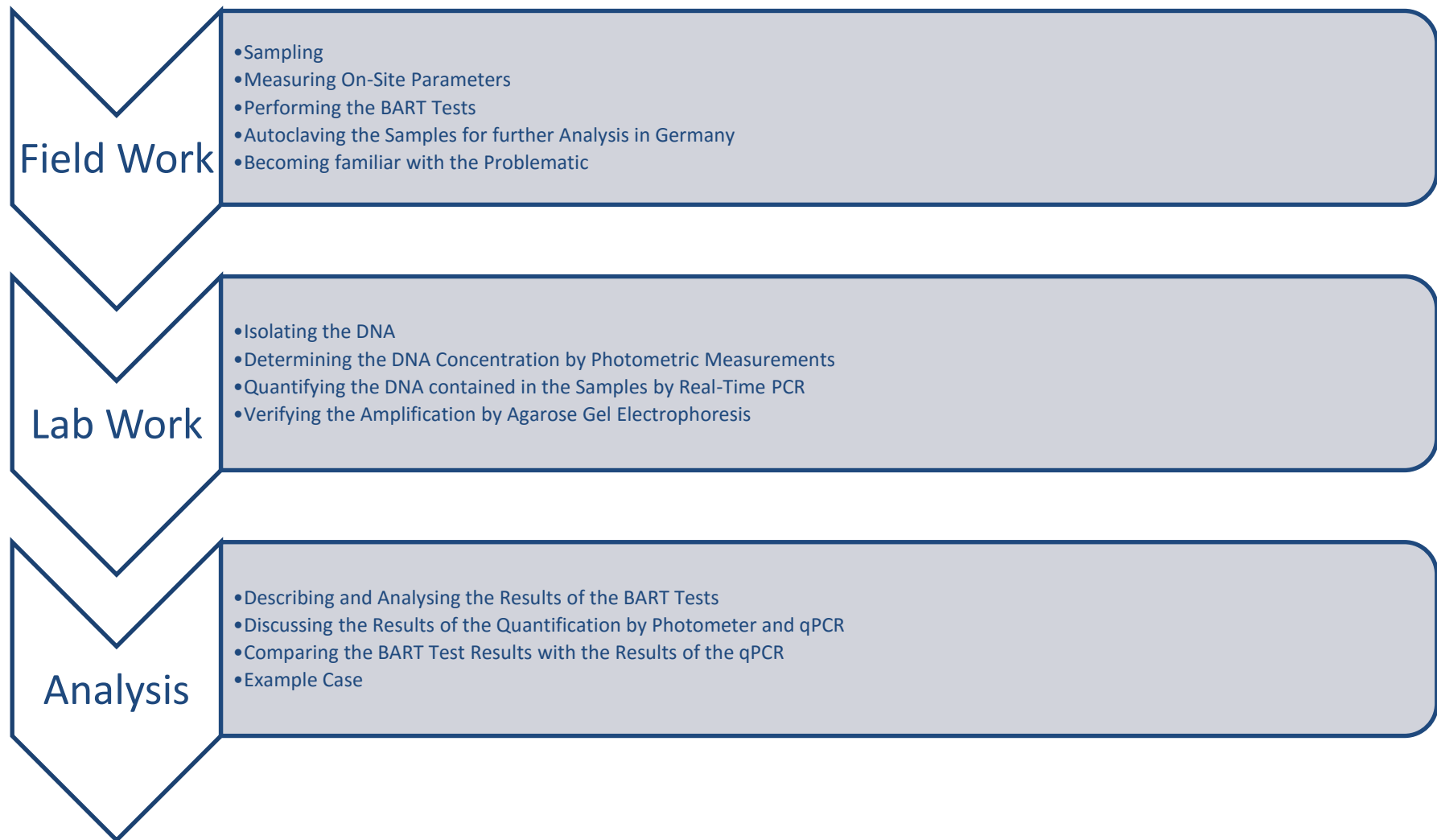


Figure 5: General overview of the work steps.

2 Theory of the Used Methods

2.1 Measuring of the On-Site Parameters

To determine the water quality, it is important to understand some basic parameters, e.g. pH, redox potential or the electrical conductivity. These parameters are also helpful to recognize sudden changes in the water, resulting from new influences. Since the parameters are measured directly on the site, they are called on-site parameters. Because the standard-H₂-probe cannot be used in the field, the measured redox potential has to be corrected to the standard hydrogen probe potential. Therefore, Wolkersdorfer ¹² combined the traditionally used terms into one equation:

$$E_{H(25\text{ }^{\circ}\text{C})} = E - 0.198 (\vartheta - 25) + \sqrt{a - b\vartheta} \quad (13)$$

- E_h redox potential, [mV]
- E measured redox potential at temperature ϑ , [mV]
- ϑ measured temperature, [$^{\circ}\text{C}$]

The coefficients a and b depend on the type of electrode that was used. The HACH PH20101 is an Ag/AgCl-electrode (3 M KCl) wherefore $a = 50230$ and $b = 295$.

This equation is based on the Nernst Equation, which explains the correlation between the probe potential and the concentration of the oxidised or reduced particles.

$$E = E^{\ominus} + \frac{R T}{z F} \cdot \ln \frac{a_{ox}^{v_{ox}}}{a_{red}^{v_{red}}} \quad (14)$$

- E probe potential, [V]
- E^{\ominus} standard potential, [V]
- T measured temperature, [K]
- R ideal gas constant, [8.3145 J K⁻¹ mol⁻¹]
- z number of transferred electrons
- F Faraday constant, [96,500 C mol⁻¹]
- $a_{ox}^{v_{ox}}$ activity of the oxidised particles, [mol L⁻¹]
- $a_{red}^{v_{red}}$ activity of the reduced particles, [mol L⁻¹]

To measure the redox potential, an electron electrode is used. This means, the phase boundary between probe and electrolyte is not conquered by ions, it is conquered by electrons. So the electrolyte and the inside of the probe have their own potential. The Galvani potential $\Delta\phi$ is the difference between both potentials. Due to the fact, that electrons cannot exist in an aqueous solution, ions for transporting them are needed. Thereby, the Galvani potential

depends on the activity of ions contained in the solution. The activity is connected with the ion concentration (equation 15).

$$a_i = \gamma_i c_i \quad (15)$$

a_i ion activity, [mol L⁻¹]
 γ_i activity coefficient
 c_i ion concentration, [mol L⁻¹]

Therefore, the concentration dependence of the Galvani potential is described by the following Nernst equation:

$$\Delta\phi = \Delta\phi^\ominus + \frac{RT}{zF} \cdot \ln a(\text{Me}^{+z}) \quad (16)$$

$\Delta\phi$ Galvani potential, [V]
 $\Delta\phi^\ominus$ standard Galvani potential, [V]
 $a(\text{Me}^{+z})$ activity of the metal ions

The Galvani potential of electrodes cannot be measured directly, so a reference electrode is needed. As a consequence, a hydrogen probe is used, which has a Galvani potential of 0 V by definition. This context is used for correcting measured redox potentials to the standard hydrogen probe potential.

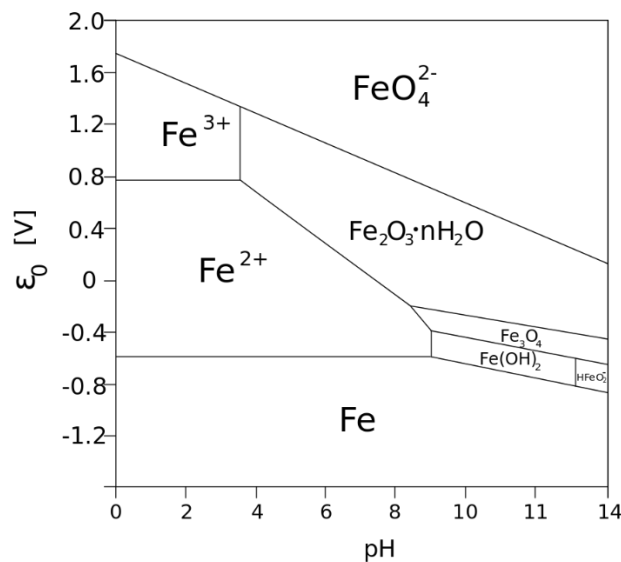


Figure 6: Pourbaix diagram of iron (from wikipedia.org)

Pourbaix diagrams can be constructed by the help of the Nernst equation as well. An generic diagram can be found in Figure 6. Thereby, the pH as a function of the redox potential of chemical equilibria is plotted. These types of diagrams help to show, which type of chemical species is stable or not and they can also explain in a simple manner, what these circumstances

mean for the aquatic system. For each element and for each sampling location, a single Purbaix diagram can be constructed with the measured on-site parameters and the ICP-MS results. Therefore, software like Geochemist's Workbench® can be used. Such a diagram can be constructed manually as well. An instruction can be found in Stumm and Morgan's '*Aquatic Chemistry*'⁶.

2.2 What are BART-Tests

2.2.1 In General

The following sections are based on Cullimore's '*Microbiology of Well Biofouling*'³¹.

Cullimore describes the functionality of the BART (Biological Activity Reaction Test) test, which is a patented test to detect biological activity in water samples using the activities and reactions of microbes. The activity of microorganisms is related to their growth, which can be expressed by the formation of clouds, slime or gels in the tubes. The reaction is linked to the manner in which the microbes behave within the tube. An indication thereof can be provided by gas development, colour change and precipitation. All these indicators together can identify the sort and the amount of some microorganisms in a water sample. The main difference between the BART test and common-used agar techniques is the use of the sample itself. The BART test uses the whole water sample as it is, so that the bacteria can remain and grow within their natural environment. By comparison, microbes have to take the water out of the agar for their growth. Not all microbes can do this and some microbes may consequently be missed.

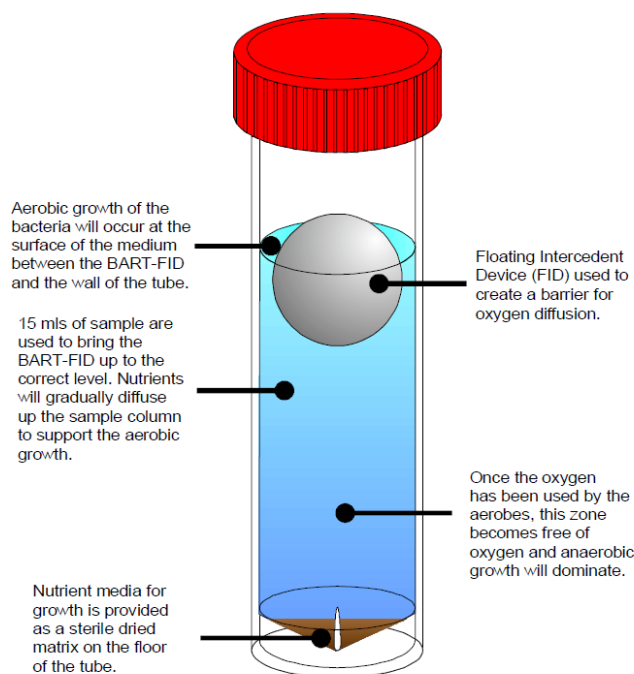


Figure 7: General set-up of a BART test tube (from dbi.sk.ca).

Furthermore, the design of the BART test enables the formation of different habitats within one tube (Figure 7). The floating ball (floating intercedent device - FID), restricts the oxygenation of the sample in the lower parts of the tube. Thus, an anaerobic area builds up in the base of the bio detector. One tube can contain an aerobe (oxidative) area and an anaerobe (reductive) area with a transitional zone, containing a reduction-oxidation gradient, in between. Growth in this intermediate area proves the existence of facultative anaerobes. To determine different groups of microbes, selective media are necessary (Table 1). The medium resides as a sterile dried matrix at the bottom of the tube. After filling the sample tube with water, the nutrients dilute slowly upwards. This progression can take as long as two days. Within these two days, the microbes get used to the increasing concentration of nutrients and begin to grow, if suitable for them.

Table 1: Selective media used to differentiate between groups of microbes (from Microbiology of Well Biofouling³¹)

	Microbial Community	Selective Culture Medium^a
IRB	Iron-related Bacteria	Winogradsky's Medium
SRB	Sulfate-reducing Bacteria	Postgate's Medium
SLYM	Slime-forming Bacteria	Glucose Peptone Medium

^a Media have been modified to maximize the potential for recovery of the microbes using the BART-system

The BART-Test for field work consists of an inner and an outer tube. The outer tube protects the sample inside, in case there is any damage at the inner tube. For taking a sample, the outer tube is filled with the water, to be tested. Afterwards, the inner tube is filled with 15 mL of the sampled water and closed. Since the tubes were observed inside, there was no need to place these back into the outer tube. The test tube needs to be stored away from direct sunlight and not moved vigorously at all during the test period of nine days.

2.2.2 Detailed Information about the IRB-BART Test

In order to analyse iron-related bacteria, several facts need to be taken into consideration. At first, IRBs prefer to grow at surfaces and not directly in water. Therefore it has to be ensured, that the bacteria have detached, and are suspended. Over and above that, several bacteria exist, which are able to metabolize iron in different ways. Because of the ability of the test to create two different habitats (aerobe and anaerobe), iron-reducing as well as iron-oxidizing bacteria can grow inside the tube. To select iron-related bacteria from others, the BART test contains as crystallized matrix a medium, based on the original composition of Winogradsky's medium. The essential component of this medium is ferric ammonium citrate. Due to the gradual increase of nutrients upwards in the bio detector, this diffusion front can change into different colours. If there is no chemical reaction and oxygen is present, the water turns yellow which means that the sample is oxidative. Should the sample become green, then it is reductive and contains a relatively high concentration of calcium and magnesium. If the contained bacteria start to utilise the nutrients and become active, different reaction patterns will occur (e.g. the sample becomes cloudy, gas or slime is formed or the colour changes).

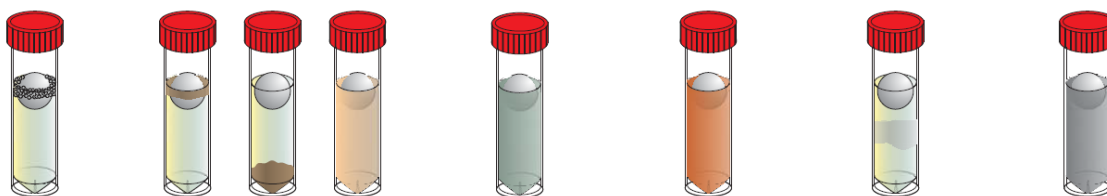


Figure 8: Overview of possible reaction patterns of the IRB BART. The patterns are described in order of figures. Foam (FO) around the ball is caused by anaerobic bacteria and can often give a hint to the presence of sulfate-reducing bacteria. The occurrence of brown rings (BR), brown gel (BG), and/or brown clouds (BC) prove the presence of iron related bacteria. A green cloudy solution (GC) shows the presence of some pseudomonads, a red cloudy solution (RC) shows the presence of enteric bacteria and a colourless cloudy solution (CL) shows the presence of heterotrophic bacteria. A black solution (BL) means the presence of pseudomonads and enteric bacteria (from dbi.sk.ca).

2.2.3 Detailed Information about the SRB-BART Test

For the SRB-BART test, Cullimore sees the challenge in the anaerobe conditions needed for the growth. Sulfate-reducing bacteria tend to live deep inside biofilms as part of a consortium. Short chain fatty acids are used by this BART test as a substrate. The sulfate contained in Postgate's medium becomes reduced to hydrogen sulfide, which reacts with the diffusing ferrous iron, and iron sulphides are formed. However, heterotrophic anaerobic bacteria can grow there, too. They often grow faster than the sulfate-reducing bacteria, and the sample within the tube becomes cloudy. It can also happen, that the sample turns black within half an hour. If that occurs, there is too much hydrogen sulfide contained in the water and the sample needs to be stripped under sterile conditions.



Figure 9: Overview of possible reaction patterns of the SRB BART. The patterns are described in order of figures. If only the base dyed black (BB) occurs, a dense anaerobic consortium of sulfate-reducing has to be present. If the tube shows a reaction only around the ball/top black (BT), the consortium has to be aerobic. Both patterns prove the presence of aerobic and anaerobic sulfate-reducing bacteria. When the solution is cloudy but colourless, other anaerobic bacteria are present (from dbi.sk.ca).

2.2.4 Detailed Information about the SLYM-BART Test

Furthermore, Cullimore describes the specific characteristics of the BART test for slime-producing bacteria. The glucose peptone medium used in this test is very enriching and causes a wide and fast growth. Slime-forming bacteria grow under different redox-conditions. In doing so, slime can be detected where the redox gradient is optimal for them. The SLYM-BART test can be used as simple presence or absence test. To some extent, the population size and the sort of microbe can be determined as well.

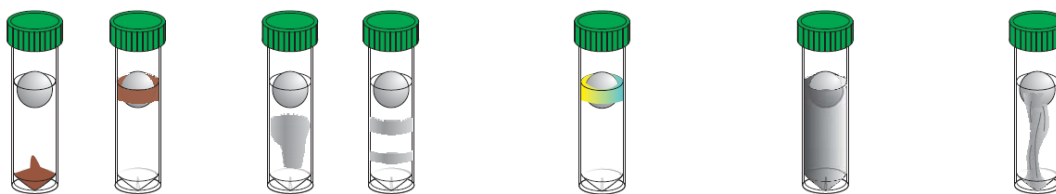


Figure 10: Overview of possible reaction patterns of the SLYM BART. The patterns are described in order of figures. A dense slime (DS) in base or a slime ring (SR) around the ball prove a dense consortium of slime bacteria. Slime-forming bacteria are also present, when there is a cloudy (CL) growth, or layered plates (CP) inside. A pale blue glowing (PB) under UV-light around the ball proves the presence of fluorescing pseudomonads. Is the liquid blackened (BL), pseudomonads and enterics are contained in the samples. Thread-like strands (TH) prove a tight consortium of slime bacteria (from dbi.sk.ca).

2.3 Isolation of the DNA

For the isolation of genomic DNA, the decomposition of cell walls is the first step. Which method is used depends on the organism. For bacteria, lysozyme and proteinase K are applied. The lysozyme degrades the cell walls and proteinase K degrades the cell wall proteins proteolytically. Afterwards, the DNA is precipitated with ethanol. Instead of phenol extraction, buyable kits (e.g. DNeasy Blood & Tissue, which was used in this thesis) use anion exchanger columns for isolation and purification. The anion exchanger material in this kit is prepared in spin columns through which the solutions are centrifuged.³² In general, the procedure consists of the lysis of the base material, scrubbing to remove contaminations, eluting, precipitating and resuspending of the nucleic acid.³³

2.4 DNA Quantification

2.4.1 Quantification by Real-Time PCR (qPCR)

In contrast to a qualitative PCR, where only the result can be analysed, it is possible to follow the amplification while it is happening with the quantitative PCR or RT-PCR (Real-Time PCR). Thereby a fluorescent dye is used to follow the amplification progress with different methods. If the detection of special fragments or regions is not necessary, an intercalating dye (e.g. SYBR Green) is used to measure the number of copies. The dye is intercalated in the double-strand of the product.

The fluorescence signal increases with the growing number of amplicates. That means, the measured signal is proportional to the amount of copies³⁴ and the number of cycles is indirect proportional to the logarithm of the template DNA copies³⁵. This signal is shown in a sigmoidal curve (Figure 11), which is typical for enzymatic reactions.

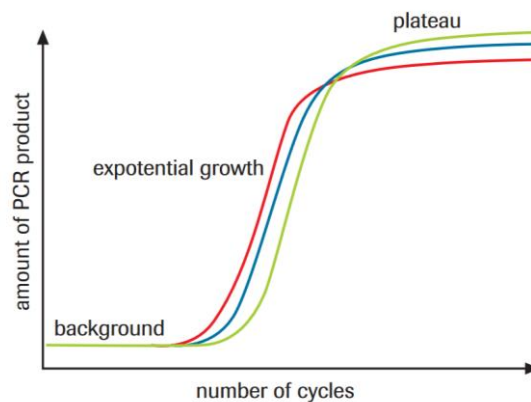


Figure 11: Sigmoidale curve of a qPCR run (from LightCycler Real-Time PCR Systems – Application Manual, Roche).

Important for the calculation of the concentration of the template DNA is the crossing point (C_p). At this point, the fluorescence signal of the sample is obviously higher than the background signal. Given DNA templates with a known concentration, a standard curve can be calculated with the corresponding C_p 's.

2.4.2 Quantification by Photometer

After the isolation of the DNA, the concentration can be determined by measuring the optical density of the sample at 260 nm. For the calculation, equation 17 was used.

$$c(\text{dsDNA}) = F \cdot OD_{260 \text{ nm}} \cdot 50 \mu\text{g mL}^{-1} \quad (17)$$

F dilution factor
 $OD_{260 \text{ nm}}$ optical density at 260 nm

If a solution containing $50 \mu\text{g mL}^{-1}$ of dsDNA is measured at 260 nm, the optical density is 1. To determine the pureness of the isolated DNA, the maximum absorption of proteins at 280 nm needs to be considered as well. The absorption at 280 nm is based on the absorption of the aromatic rests of the contained amino acids.

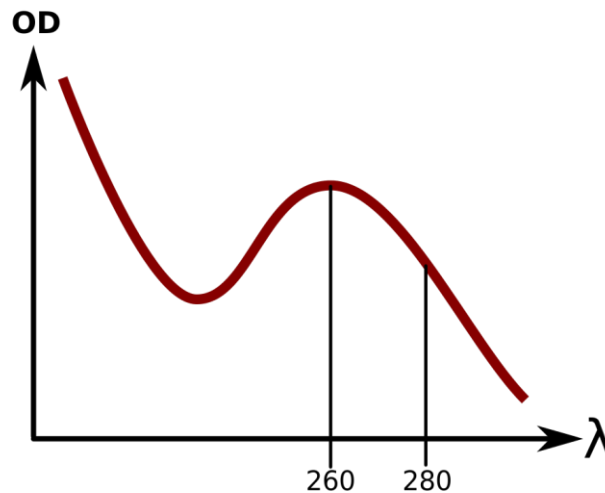


Figure 12: Optical density for the quantification of DNA. 260 nm is the absorption maximum of DNA. To determine the pureness of the extract, the sample is also measured at 280 nm, the absorption maximum of proteins. (from wikipedia.org).

The pureness is calculated by the ratio R of both wavelengths:

$$R = \frac{OD_{260 \text{ nm}}}{OD_{280 \text{ nm}}} \quad (18)$$

A pure DNA solution has a ratio of 1.8. In general, a ratio between 1.8 and 2.0 is accepted. If the ratio is less than 1.8, the sample is contaminated with proteins or phenol. When the ratio is higher than 2.0, a pollution with RNA is present.

3 Material and Methods

3.1 Material used in this Thesis

3.1.1 For the Performance of the BART Tests

The BART tests were developed by the Canadian company Droycon Bioconcepts Inc. To ensure a consistent quality of the medium, each test of one test type originates from the same batch:

- SRB-BART (Batch #: 0807-C,D)
- SLYM-BART (Batch #: 0773-O,Q)
- IRB-BART (Batch #: 0502-P)
- BART Software

3.1.2 For the On-Site Parameters and Sampling

In the field, the samples were collected in different types of bottles, depending on the treatment to be followed. Samples for the ICP-MS scan were collected in/with:

- 1.5 L PE bottles
- 100 mL PE bottles, acidified with 20 % HNO₃ (pH < 2)
- 50 mL syringe
- 0.22 µm PES syringe adapter filters (Sartorius)

The parameters were measured with:

- Multimeter HQ40d multi (HACH)
- LDO101 oxygen probe (HACH)
- PCH 201 pH probe (HACH)
- ORP-REDOX MTC 101 redox probe (HACH)
- CDC 401 electrical conductivity probe (HACH)

For the further analysis in Germany, the samples had to be autoclaved as well. For this reason, the water samples were taken with sterile and autoclavable 50 mL reaction tubes and sterilised afterwards with a Haxley HL340 autoclave (Already Enterprise Inc.) in a laboratory at the Tshwane University of Technology (Pretoria). The following performance was done in the laboratory for biochemistry of the University for Applied Research Georg-Simon-Ohm (Nuremberg).

3.1.3 For the DNA Isolation

To isolate the DNA from the bacteria contained in the water sample, a pre-treatment was necessary. Therefore, the following material and chemicals were used:

- 5 µm Chromafil® Xtra PES-500/25 syringe adapter filters (MARCHEREY-NAGEL)
- 50 mL Injekt® syringe, sterile (BRAUN)
- 1 % H₂SO₄
- 1x PBS (pH 7.3, c(NaCl) = 136.9 mM, c(KCl) = 2.7 mM, c(Na₂HPO₄ · 7 H₂O) = 43 mM, c(Na₂HPO₄) = 114 mM)

Afterwards, the DNeasy Blood & Tissue Kit (Qiagen) was used for the isolation, concentration and purification.

3.1.4 For the Real-Time PCR (qPCR)

The polymerase chain reaction was performed with the LightCycler® 2.0 system (Roche). The system contains:

- LightCycler® 2.0 with sample carousel (32 positions)
- LightCycler® glass capillaries
- LightCycler® centrifuge adapters, capping tool and capillary releaser
- LightCycler® Software 4.1

The ZymoResearch Femto™ Bacterial DNA Quantification Kit was used. The kit contains a premix, a no template control and seven bacterial DNA standards. The premix contains SYTO® 9 as fluorescence dye and a primer mix, which is targeting the 16S rRNA. Referring to Turner et al. ³⁶ the bacterial primers 8F/357R (Table 2) were used in the premix. Other components are not known.

Table 2: Primer sequences

Primer	Sequence 5' – 3' ^{37,38}	16S regions ³⁷
8F	AGTTTGATCCTGGCTCAG	V2 - V3
357R	CTGCTGCCTYCCGTA	

Bacterial DNA purified from *E. coli* strain JM109 is used as standards.

Table 3: Bacterial DNA Standards

Standard	Amount of Bacterial DNA ng / Reaction Well
1	20
2	2
3	0.2
4	0.02
5	0.002
6	0.0002
7	0.00002

3.1.5 For the Agarose Gel Electrophoresis

For the gel electrophoresis, a customary horizontal electrophoresis cell was used with a Bio-Rad PowerPac™ Basic. After the staining process, the gel was observed under a Transilluminator BIO View UV-Light UXT-20M-8K (wavelength: 312 nm) from Biostep. Furthermore, the following reagents were used:

- LE Agarose (Biozym)
- 1x TBE buffer (pH 8, c(Tris) = 88 mM, c(H₃BO₃) = 88 mM, c(EDTA) = 2 mM)
- Quick-Load Purple 100 bp DNA Ladder (New England Biolabs)
- 6x DNA loading buffer (50 % (w/v) glycerine, 0.25 % (w/v) bromophenol blue)
- ethidium bromide solution ($\rho(\text{EtBr}) = 10 \text{ mg mL}^{-1}$)
- HDGreen Plus DNA Stain (INTAS Science Imaging)

3.1.6 Other Material

Additionally, the following facilities were used:

- Microwave
- Camera and photographic system (Uvitec)
- UV transparent cuvettes, DNA/RNA/protein free (Sarstedt)
- UviLine 9400 photometer (Schott Instruments)
- 5415D centrifuge for 1.5 mL reaction tubes (Eppendorf)
- 3K30 centrifuge for 50 mL reaction tubes (Sigma)
- Vortex mixer
- freezer (-25 °C)
- ice bath
- other typical lab material

3.2 Site Description and Sampling

Samples were taken from shafts, adits, surface outflow, cave lakes and by acid mine drainage influenced surface water in the Gauteng and Mpumalanga provinces.

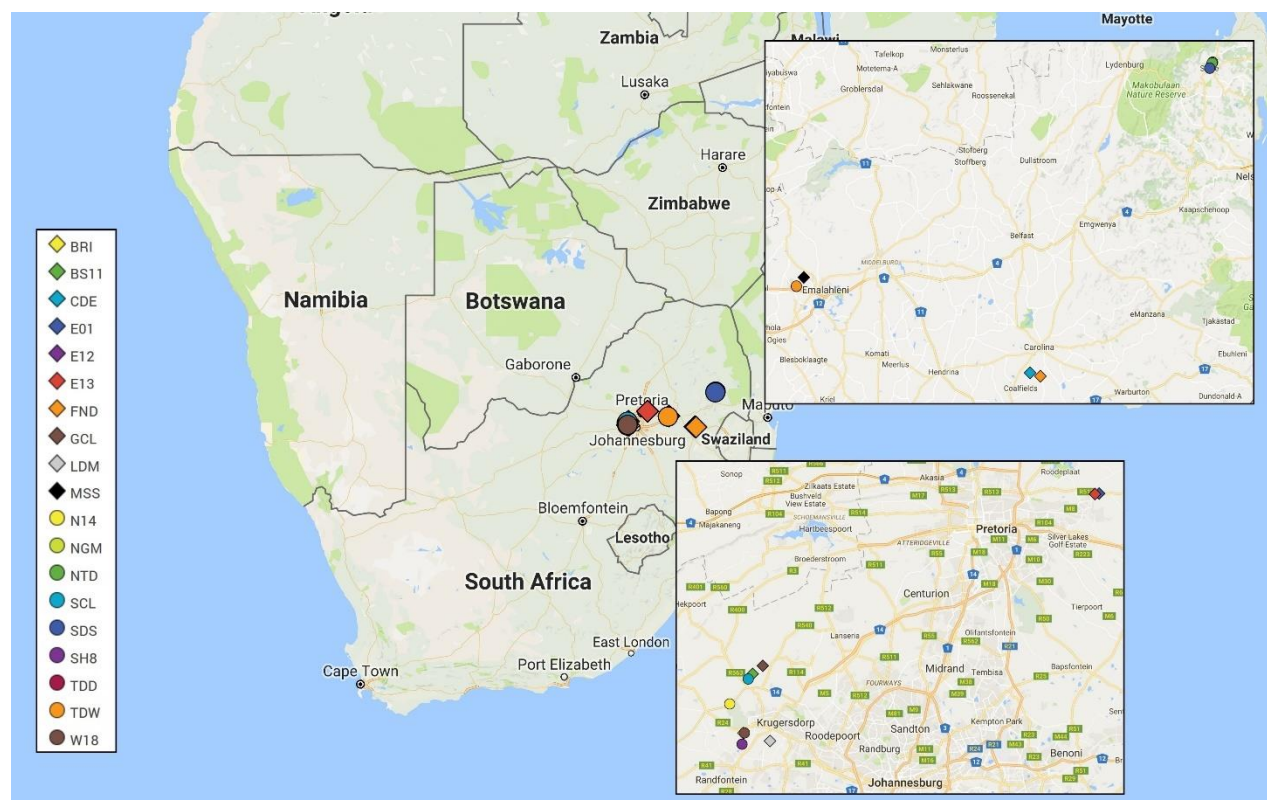


Figure 13: Sampling locations in South Africa (from Google Maps). CDE also contains FND, V2I, V2O and VFO.

Close to Edendale in the Pretoria-Witbank area, samples were taken from shafts of the Union Silver and Lead Mine. The mine is located on the farm Nooitgedacht 333 JR (formerly Nooitgedacht 458) and consists of two separate mines. The Central Discharge and the Fanie Nel Discharge are located south of Carolina in the Chief Albert Luthuli Municipality. At both places, the water originates from hard coal mining. Fanie Nel Discharge is a passive treatment system that has been set up to clean the acid mine drainage. The samples collected around Sabie originate from mine water influenced by gold mining. The sample 'Sabie Drinking Water Supply' was taken at an adit of the Glynn Underground Complex. The others were collected from the adit and the tailings dam of the Nestor Gold Mine. The region around eMalahleni is also well-known for its coal deposits. The open pit lake of Middelburg Steam & Station can be found in the northwest region of the town. In the same area, another sample was taken from a mine water discharge in the wetlands west of the Transvaal and Delagoa discharge point.

Another famous region for gold mining is the Witwatersrand, a range of hills through the provinces North West, Gauteng and Mpumalanga. There, the “Cradle of Humankind” World Heritage Site is located, a karst landscape close to Krugersdorp northwest of Johannesburg. Samples were taken from two different cave lakes (Sterkfontein Cave and Glibers’ Cave) and two rivulets (Bloubankspruit and Tweelopiespruit) in a region that is potentially influenced by mine water from gold mining³⁹. Close to Krugersdorp is the Lancaster Dam of the Lancaster Mine, holding acid mine drainage from gold mining activities. At the Westrand Goldfield in the Western Pool of the Witwatersrand, samples were taken from three different shafts: Black Reef Incline, Winze 18 and Shaft 8. Except for some sampling spots in Carolina, locations were named after the name of the associated farm, landmarks close-by, companies or sites. The sampling places FND, V2I, V2O and VFO are inside a pilot passive treatment system.

Table 4: Sampling locations

Code	Name	Location	Resource	Sampling Place
E01	Number 2 Mine Main Shaft	Edendale	lead, silver	shaft
E12	Number 1 Mine Main Shaft	Edendale	lead, silver	shaft
E13	Number 1 Mine Shaft 2	Edendale	lead, silver	shaft
CDE	Central Discharge	Carolina	hard coal	spring
FND	Fanie Nel Discharge	Carolina	hard coal	spring
VFO	Vertical Flow Reactor Outflow, Fanie Nel Discharge	Carolina	hard coal	passive treatment system
V2I	Vertical Flow Reactor 2 Inflow, Fanie Nel Discharge	Carolina	hard coal	passive treatment system
V2O	Vertical Flow Reactor 2 Outflow, Fanie Nel	Carolina	hard coal	passive treatment system
SDS	Sabie Drinking Water Supply	Sabie	gold	adit
NTP	Nestor Tailings Dam Pond	Sabie	gold	tailings dam
NGM	Nestor Gold Mine	Sabie	gold	adit
MSS	Middleburg Steam & Station	eMalahleni	hard coal	open pit lake
TDD	Transvaal and Delagoa Discharge Point	eMalahleni	hard coal	mine water discharge
TDW	Wetland West of Transvaal and Delagoa Discharge Point	eMalahleni	coal	mine water discharge
SCL	Sterkfountain Cave Lake	Cradle of Humankind World Heritage Site	-	dolomite cave lake
GCL	Glober's Cave Lake	Cradle of Humankind World Heritage Site	-	dolomite cave lake
BS1	Bloubankspruit	Cradle of Humankind World Heritage Site	-	rivulet
N14	Tweelopiespruit	Krugersdorp	-	rivulet
LDM	Lancaster Dam	Krugersdorp	gold	dam
BRI	Black Reef Incline	Krugersdorp	gold	shaft
W18	18 Winze	Krugersdorp	gold	shaft
SH8	Shaft 8	Krugersdorp	gold	shaft

Except the samples for the laboratory analysis, samples were taken twice, in March and in April 2016. The samples for the laboratory analysis were only taken in March 2016. On site, samples for chemical analyses (Waterlab, Pretoria, South Africa) were taken in 1.5 L bottles. In the lab, TDS, ammonia, nitrate, nitrite, chloride, sulfate, fluoride and bromide were determined with a discrete analyser. The samples for the ICP-MS (Waterlab, Pretoria, South Africa) were taken with a 50 mL syringe and transferred into an acidified 100 mL bottle with

a 0.22 μm syringe filter. All sample containers (except the acidified bottles for the ICP-MS) were rinsed three times before taking the samples and filled without head space.

For the qPCR and the BART tests, three sterile 50 mL falcon tubes were filled up with water without head space. After the trip, the sample was filled in a SRB-BART, a SLYM-BART and an IRB-BART. The other two falcon tubes were immediately autoclaved at 121 °C. On-site parameters were measured at the site. The probes for measuring the pH and the electrical conductivity were calibrated daily.

3.3 Performance of the Methods

3.3.1 BART-Tests

The BART tube was filled each with 15 mL sample and kept in half shade at ambient temperature (20 – 28 °C) for nine days. The tests were checked every 24 h. Differences were noticed with the recommended abbreviations. Furthermore, photographs were taken from each sample each day to prove the changes.

To see if there are huge changes in the results, when the tests are not started as soon as possible another two IRB and SRB BART tests were performed for each sampling site. The first tests were filled up as mentioned before, directly at the site. Samples for the remaining IRB and SRB BART tests were taken with a sterile 50 mL falcon tube (as mentioned in ‘3.2 Site Description and sampling’). Afterwards the tubes were stored in a fridge for 21 days. Then, BART tests were started again.

3.3.2 DNA Isolation

Due to the fact, that the samples were taken in the field from a natural source of water, the challenge was to remove disturbing pollutions and to concentrate the DNA. Especially the precipitated $\text{Fe}(\text{OH})_3$ constituted an obstacle. Therefore a pre-treatment was developed, basing on the works of Wu et al. ⁴⁰ and Kesberg and Schleheck ⁴¹. Wu et al. isolated *Acidithiobacillus* strains from different environmental areas for phylogenetic analysis. They removed the ferric iron precipitate by washing the cells after centrifugation with diluted sulfuric acid water. Kesberg and Schleheck cleaned the cells by filtering them through filters with different pore sizes and backflushing the 0.1 μm syringe filter in which the cells were kept.

Therefore, each sample containing 50 mL falcon was centrifuged for 30 min at 10 000 rpm at 25 °C first, and the water was decanted. Where necessary, 5 mL of 1% sulfuric acid was added to dissolve the precipitated Fe(OH)₃. Afterwards, the tube was centrifuged under the same conditions as before and decanted as well. Next, 1.5 mL of PBS were added to solve the precipitate. To remove other contaminants, the solution was filtered through a 5.0 µm syringe filter and transferred in a 1.5 mL reaction tube. Then, the tube was centrifuged for 10 min at 6 600 rpm and the supernatant was decanted. The precipitated cells were solved with 200 µL PBS. From then on, the instruction manual of the DNeasy Blood & Tissue Kit was followed.

3.3.3 Photometric Quantification

To verify the purity of the extracted DNA, a spectrum (240 nm – 320 nm) was recorded with a UV-Vis photometer. Therefore, 50 µL of the AE buffer from the DNeasy Blood & Tissue Kit were filled in a cuvette and the baseline was recorded first. Afterwards, 50 µL of each sample were measured as well.

3.3.4 Real-Time PCR (qPCR)

For the quantification of the contained DNA, the Femto™ Bacterial DNA Quantification Kit was used. The instruction manual was followed and the parameters were set as mentioned in *Table 3*. All steps were performed under sterile conditions. For the analysis, LightCycler Software 4.1 was used.

Table 5: The thermocycling parameters in step 2 according to the instruction manual.

		Temperature / °C	Time / min
Step 1:	Initial Denaturation	95	10
Step 2:	Denaturation	95	0.5
(40 cycles)	Annealing	50	0.5
	Extension	72	1
Step 3:	Melting	95	
		65	1
		95	

Due to some organisational reasons, only one extract of each sampling location was used.

3.3.5 Agarose Gel Electrophoresis

A gel electrophoresis was performed to control the amplification. After the qPCR run, the glass capillaries were opened and put upside down into 1,5 mL reaction tubes and centrifuged for 1 min at 800 rpm. 3.4 μ L 6x loading buffer were added to each reaction tube.

For a 1.5 % gel, 0.75 g agarose were dissolved in 50 mL 1x TBE. Once the gel was cured (after 20 min), the gel was loaded with 10 μ L DNA ladder and 18 μ L of the samples. The electrophoresis run for 45 min at a constant voltage of 80 V.

As soon as the run was completed, the agarose gel was put into an ethidium bromide bath for 5 min. Afterwards, the gel was placed under UV light and a picture was taken.

The gel with the samples from the run "Schwarz Samples 2 03082016" was coloured with DNA stain. 3 μ L of the stain were added to the dissolved agarose at a temperature of 50 – 60 °C before the gel was poured. After the run, the gel was placed immediately under the UV light.

4 Results and Interpretation

4.1 Interpretation of the Measured On-Site Parameters for Further Analysis

The average of the measured on-site parameters can be found in Table 6. At the second sampling trip, the water source of NTD was dried out, so no sample was taken then. The water discharge TDD was found by chance at the second field trip.

Table 6: Average on-site parameters of the two sampling campaigns from 2016-03-08 to 2016-03-16 and 2016-04-16 to 2016-04-20. The redox potential is corrected to the standard H₂-electrode and 25 °C according to equation (13).

Sample	pH	E _H / mV	EC / $\mu\text{S cm}^{-1}$	ϑ / °C	c(O ₂) / mg L ⁻¹	O ₂ / %
E01	6.32	430	345.5	23.4	4.54	63.5
E12	6.64	323	600.5	23.7	0.89	12.3
E13	6.65	383	369.5	25.7	1.97	27.8
CDE	4.30	346	1480.5	19.4	0.27	3.5
FND	3.22	564	1905.0	19.1	0.57	7.5
VFO	3.02	658	2008.5	18.7	3.00	38.6
V2I	3.68	549	1879.0	20.8	7.07	96.1
V2O	3.65	577	1885.5	19.5	4.60	60.4
SDS	6.75	392	228.0	20.7	7.83	97.4
NTD ^a	3.60	723	460.0	21.7	6.98	90.5
NGM	6.19	433	124.1	18.2	7.83	94.3
TDW	3.57	586	11780.0	30.8	0.67	10.6
TDD ^b	3.60	549	12190.0	31.5	3.09	50.0
MSS	2.55	728	3764.0	23.9	4.15	58.5
SCL	6.96	401	792.0	18.6	6.16	77.7
GCL	6.90	389	557.0	20.6	6.55	85.8
BS1	7.30	413	1542.0	22.2	5.23	71.3
N14	5.95	439	3067.0	21.6	7.06	95.8
LDM	2.60	732	3886.0	23.1	4.95	70.6
BRI	6.14	153	3469.0	22.3	0.14	1.9
W18	6.23	113	3541.0	22.9	0.23	3.3
SH8	6.07	155	3552.5	23.1	0.69	9.8

^a only measured during the sampling in March 2016

^b only measured during the sampling in April 2016

Almost all samples taken from a discharge of water in aerobic conditions have a very low oxygen percentage (< 15 %). E01 and E13, both samples taken from a shaft, that reaches into a flooded mine, have a high content of oxygen. Especially E01 is far too high. E13 belongs to the same mine as E12. It is possible, that there is an oxygen source under the surface close by or the variance originates in natural fluctuation. However, a handling mistake is more likely to be the cause, because from the moment, that the sample gets in contact with oxygen, the percentage rises. Normally if a sample has to be collected with a bucket, the first measured parameter is the content of oxygen, to keep errors as low as possible. Having a closer look at the original data, (E01: 72.2 % (March) and 54.8 % (April); E12: 12.9 % (March) and 11.7 % (April); E13: 13.4 % (March) and 42.2 % (April)) this shows also a strong difference at E01 and E13 between both sampling trips. Due to the fact that the measurements were carried out by different people, neither a handling mistake nor a natural fluctuation can be excluded. Samples with an oxygen content around 90 % were taken from rivulets (N14, SDS), from lakes or another type of water discharge. These lakes are not only open to the air; the flow is very low as in an old gold mine (NGM) or in a cave lake (GCL).

Comparing the electrical conductivity with the amount of TDS from the ICP-MS scan, a correlation can be seen clearly.

Table 7: Abstract of the ICP-MS results from Waterlab. The results of E01, E12, E13, FND and TDD are missing, because the name was not identifiable or the results were not available. The TDS were measured at 180 °C.

Sample	TDS / mg L ⁻¹	SO ₄ ²⁻ / mg L ⁻¹	NO ₃ ⁻ / mg L ⁻¹	Fe / mg L ⁻¹	Mn / mg L ⁻¹	Al / mg L ⁻¹	Ni / mg L ⁻¹
CDE	1420	1006	<0.1	3.89	21	1.13	0.243
VFO	1802	1198	<0.1	18	23	49	1.51
V2I	1798	1163	<0.1	126	21	<0.1	1.55
V2O	1724	1147	<0.1	119	20	6.49	121
SDS	130	10	0.70	0.051	<0.025	<0.1	<0.010
NGM	126	102	1.30	0.3350	0.171	0.045	0.041
MSS	3928	2652	<0.1	131	29	114	2.88
TDW	10314	7090	<0.1	36	12	7.23	0.506
SCL	498	168	6.80	0.031	<1	<0.1	0.003
GCL	334	73	4.20	<0.025	<1	<0.1	<0.010
BS1	996	576	2.90	0.133	4	0.042	0.102
N14	3068	2122	1.10	0.065	18	<0.1	0.165
LDM	4788	3400	<0.1	174	30	252	14
BRI	3714	2449	<0.1	81	33	0.086	0.888
W18	3770	2455	<0.1	49	31	<0.1	0.422
SH8	3588	2410	<0.1	54	22	<0.1	0.606
NTD	100	99	<0.1	18	0.185	2.09	0.148

With the help of the pH, the redox potential and the corresponding ion concentration, a Pourbaix diagram can be constructed.

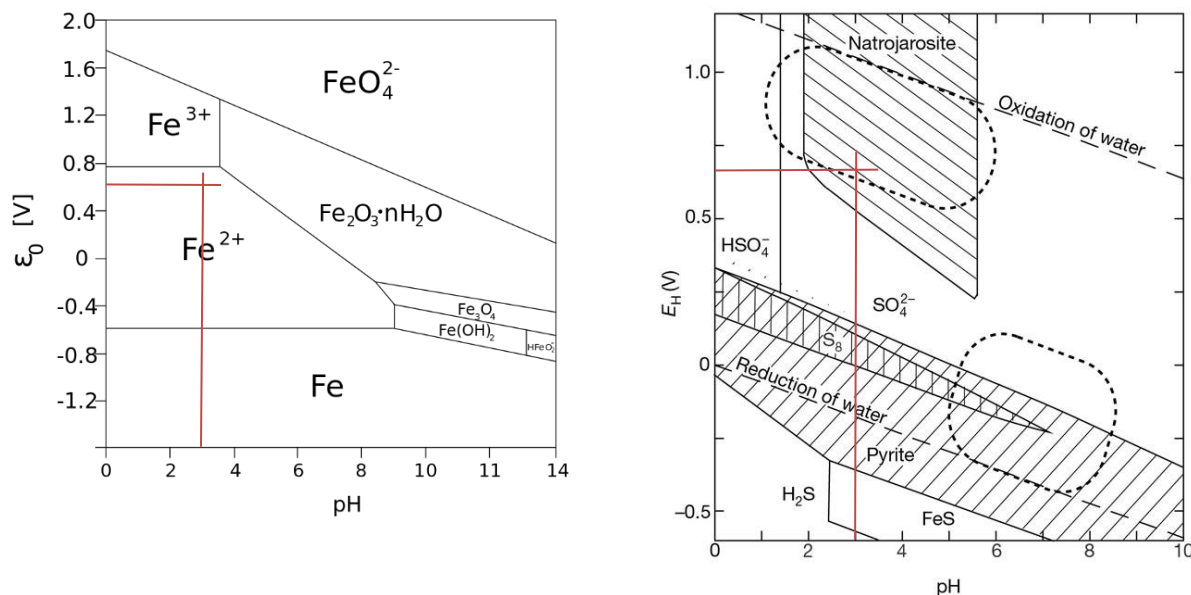


Figure 14: Pourbaix diagram of iron (from wikimedia.org) and of sulfur with iron and sodium ions ⁴². The red lines mark the crossing point of the pH (3.02) and the redox potential (658 mV) of the samples from VFO, roughly guessed.

Figure 14 shows two Pourbaix diagrams. As an example, the pH and the redox potential of VFO are marked in each diagram. In the stability diagram of iron, the two lines are crossing at the stability field of Fe^{2+} . That means, the water contained ferrous iron. Having a look at the diagram of sulfur, together with iron and sodium, sulfate is also stable under the given conditions. Having equation 4 in mind, the result is not surprising. The contained ferrous iron and the sulfate ions result from the pyrite oxidation, as well as the sulfate. Despite the content of oxygen, the ferrous iron is stable due to the acidic conditions. Therefore, this environment would be perfect for iron-oxidising and sulfate-reducing bacteria.



Figure 15: Test passive treatment system of Carolina. The sampling spots VFO, V2O, V2I and FND can be found there.

4.2 BART Tests

4.2.1 Description of the Visible Reaction and Quantification

After nine days, the test period is over and the results can be analysed. Figure 18 shows the change over these nine days of the sampling location E12 in Edendale. An aerial photo of the sampling area in Edendale can be seen in Figure 16.

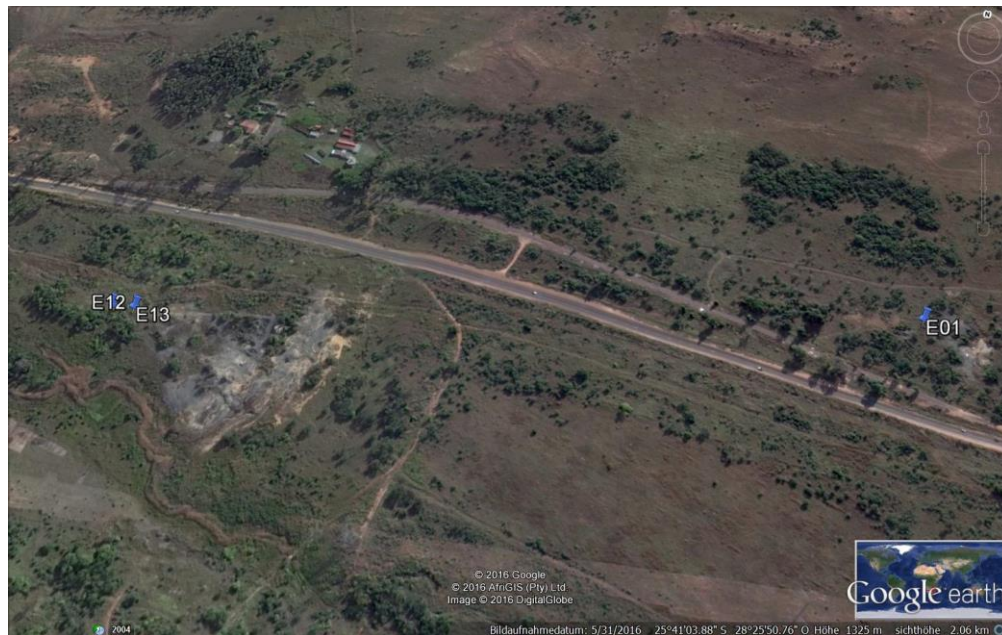
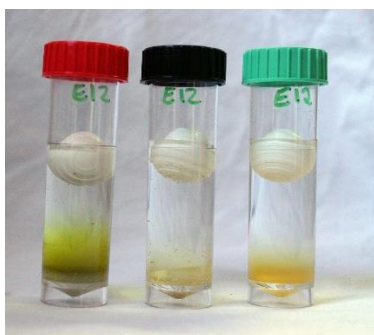


Figure 16: The sampling locations of Edendale at one glance.

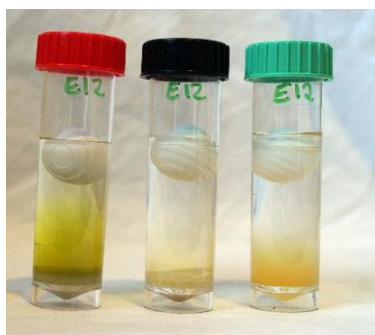


Figure 17: Sampling at E01 in Edendale. E12 can be found on the other side of the street. Both locations belong to the same mine complex of mines as mentioned in '3.2 Site Description and Sampling'.



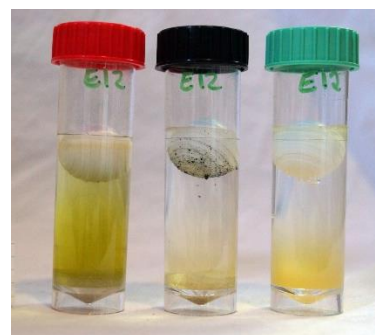
Day 1

IRB: Cloudy
SRB: Cloudy Gel-Like
SLYM: Dense Slime, Cloudy Plates layering



Day 2

IRB: Cloudy
SRB: Cloudy Gel-Like
SLYM: Dense Slime, Cloudy Plates layering



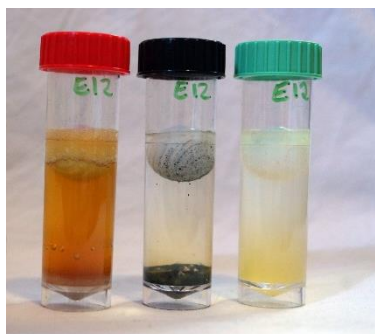
Day 3

IRB: Cloudy
SRB: Cloudy Gel-Like, Black Top
SLYM: Dense Slime, Cloudy Plates layering, Pale Blue Glow



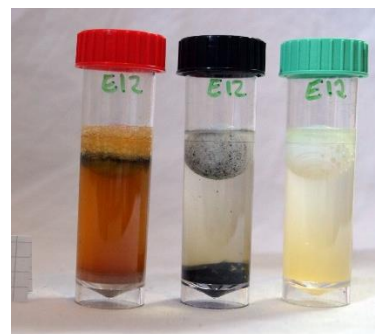
Day 4

IRB: Cloudy, Brown Ring
SRB: Cloudy Gel-Like, Black Top, Black Base
SLYM: Dense Slime, Cloudy Plates layering, Pale Blue Glow



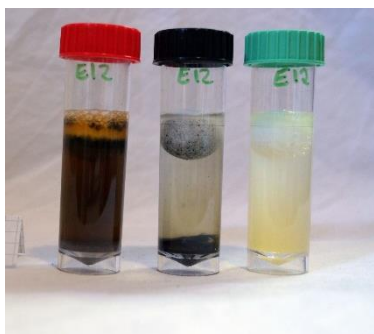
Day 5

IRB: Cloudy, Brown Complete, Foam
SRB: Cloudy Gel-Like, Black Top, Black Base
SLYM: Dense Slime, Cloudy Plates layering, Pale Blue Glow



Day 6

IRB: Cloudy, Brown Complete, Foam
SRB: Cloudy Gel-Like, Black Top, Black Base
SLYM: Dense Slime, Cloudy Plates layering, Pale Blue Glow



Day 7

IRB: Cloudy, Blackened Liquid, Foam
SRB: Cloudy Gel-Like, Black Top, Black Base
SLYM: Dense Slime, Cloudy Plates layering, Pale Blue Glow



Day 8

IRB: Cloudy, Blackened Liquid, Foam
SRB: Cloudy Gel-Like, Black Top, Black Base
SLYM: Dense Slime, Cloudy Plates layering, Pale Blue Glow



Day 9

IRB: Cloudy, Blackened Liquid, Foam
SRB: Cloudy Gel-Like, Black Top, Black Base
SLYM: Dense Slime, Cloudy Plates layering, Pale Blue Glow

Figure 18: Progress of the BART test of E12. The test for the iron-related bacteria has the red cap, the test for the sulfate-reducing bacteria has the black cap and the one with the green cap is for the detection of slime-producing bacteria. An overview of the other tests can be found in the appendix.

The test for iron-related bacteria starts with cloudy growth after one day. The first IRB related reaction occurs at day 4 with a brown ring at the top. At day 5, foam started to show up and the whole liquid turned brown. At the next day, a black ring started to occur around the ball and over the next days, the whole liquid blackened. Except for some jelly clouds, the BART test for sulfate-reducing bacteria showed no reaction until the third day. Then, black spots could be detected at the underside of the floating device. Two days later, a black layer started to grow at the bottom of the tube. With a dense slime at the bottom and plates in the tube, the SLYM test showed the first reactions at day 1. At day 3, a pale blue glow on the liquid surface was visible under UV-light. From day 4, the glow was visible with the bare eye.

In Table 8 - Table 10, the development of the BART tests is noted down with the recommended short cuts.

Table 8: Results IRB-BART tests

Sample	1	2	3	4	5	6	7	8	9
E01	-	-	-	-	BR	BR	BR, FO	BR, FO	BR, FO
E12	CL	CL	CL	CL, BR	CL, BC, FO	CL, BC, FO	CL, BL, FO	CL, BL, FO	CL, BL, FO
E13	CL	CL	CL	CL, BR	CL, BR	CL, BR, FO	CL, BR, FO	CL, BR, FO	CL, BR, FO
CDE	-	-	-	BR	BR	BR	BR	BR	BR, FO
FND	-	-	-	-	BR	BR	BR	BR	BR
VFO	-	-	-	-	BR	BR	BR	BR	BR
V2I	CL	CL	CL	CL	CL	CL, BR	CL, BR	CL, BR	CL, BR
V2O	-	-	-	-	-	-	-	-	-
SDS	-	-	-	BR	BR	BR	BR	BR, FO	BC, FO
NGM	CL	CL	CL	CL, BR	CL, BR	CL, BR	CL, BR	CL, BR	CL, BC
TDW	-	-	-	-	-	-	-	-	-
TDD	-	-	-	-	-	-	-	-	-
MSS	CL	CL	CL	CL	CL	CL	CL	CL	CL
SCL	CL	CL	CL	CL, BR	CL, BR	CL, BR	CL, BR	CL, BR	CL, BR
GCL	CL	CL	CL	CL, BR	CL, BR	CL, BR	CL, BR	CL, BR	CL, BR
BS1	CL	CL	CL, BR	CL, BR	CL, BC, FO	CL, BC, FO	CL, BL, FO	CL, BL, FO	CL, BL, FO
N14	CL	CL	CL	CL	CL	CL	CL	CL, BC, FO	CL, BC, FO
LDM	CL	CL	CL	CL	CL	CL	CL	CL	CL
BRI	CL	CL	CL, BR	CL, BR	CL, BR	CL, BR	CL, BR	CL, BR	CL, BR, FO
W18	CL	CL	CL, BR	CL, BR	CL, BR	CL, BR	CL, BR	CL, BR	CL, BR
SH8	-	-	-	BR	BR	BR	BR	BR	BR

Table 9: Results SRB-BART tests

Sample	1	2	3	4	5	6	7	8	9
E01	CG	-	-	-	-	-	-	-	-
E12	CG	CG	CG, BT	CG, BT, BB	CG, BT, BB	CG, BT, BB	CG, BT, BB	CG, BT, BB	CG, BT, BB
E13	CG	CG	CG	CG	CG	CG	CG	CG	CG
CDE	-	-	-	-	-	-	-	-	-
FND	CG	CG	CG	CG	CG	CG	CG	CG	CG
VFO	CG	CG	CG	CG	CG	CG	CG	CG	CG
V2I	CG	CG	CG	CG	CG	CG	CG	CG	CG
V2O	CG	CG	CG	CG	CG	CG	CG	CG	CG
SDS	CG	CG	CG	CG	CG	CG	CG	CG	CG
NGM	CG	CG	CG	CG	CG	CG	CG	CG	CG
TDW	CG	CG	CG	CG	CG	CG	CG	CG	CG
TDD	CG	CG	CG	CG	CG	CG	CG	CG	CG
MSS	CG	CG	CG	CG	CG	CG	CG	CG	CG
SCL	CG	CG	CG, BT	CG, BT	CG, BT	CG, BT, BB	CG, BT, BB	CG, BT, BB	CG, BT, BB
GCL	CG	CG	CG	CG	CG	CG	CG	CG	CG
BS1	CG	CG	CG, BT	CG, BT	CG, BT, BB	CG, BT, BB	CG, BT, BB	CG, BT, BB	CG, BT, BB
N14	CG	CG	CG	CG	CG	CG	CG, BT	CG, BT, BB	CG, BT, BB
LDM	CG	CG	CG	CG	CG	CG	CG	CG	CG
BRI	CG	CG	CG	CG	CG	CG	CG	CG	CG
W18	CG	CG	CG	CG	CG	CG	CG	CG	CG
SH8	CG	CG	CG	CG	CG, BT	CG, BT	CG, BT	CG, BT	CG, BT

Table 10: Results SLYM-BART tests

[illegible]

To simplify the analysis of the results, diagrams which show the reaction pattern were developed. In the diagrams, only the pattern of the bacteria specifically tested were used.

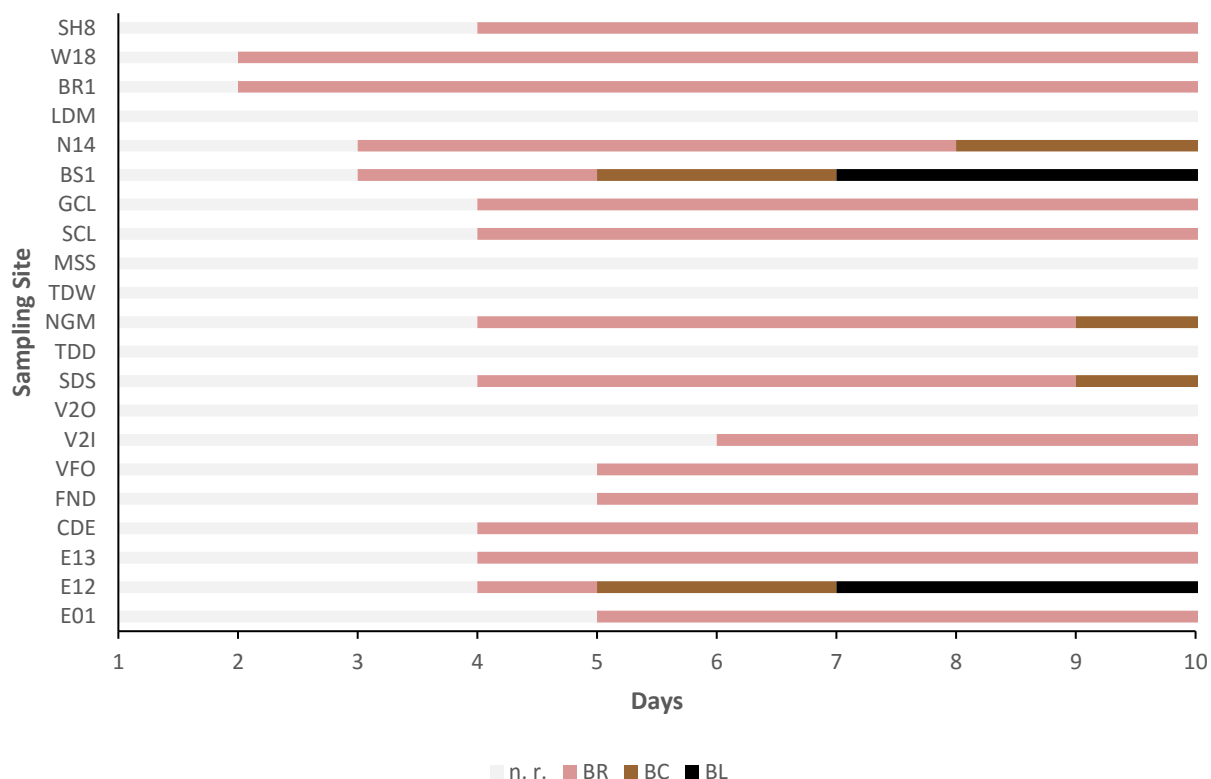


Figure 19: Reaction pattern of the IRB BART test of sampling in April 2016 for the comparison with qPCR. Only the pattern related to iron-related bacteria are shown.

In Figure 19, the reaction pattern of the IRB BART test can be seen. Each shown pattern is marked in a different colour or with a different pattern. For the IRB BART tests, the forming of a brown ring (BR), brown cloudy growth (BC) or the colour change to a blackened liquid (BL) was recorded. If there was no reaction linked to iron-related or sulfate-reducing bacteria (n. r.), a light grey bar is pictured. The samples MSS, LDM, TDW, TDD and V20 showed no reaction related to iron-oxidising or iron-reducing bacteria. The other samples started sooner or later with the appearance of a brown ring around the floating ball. That means the reaction started in the aerobic area. Five samples (E12, SDS, NGM, BS1 and N14) turned brown completely and the liquid of two of them (E12 and BS1) blackened as well. The blackening process from E12 started at the ball and spread out to the bottom of the tube. BS1 reacted vice versa.

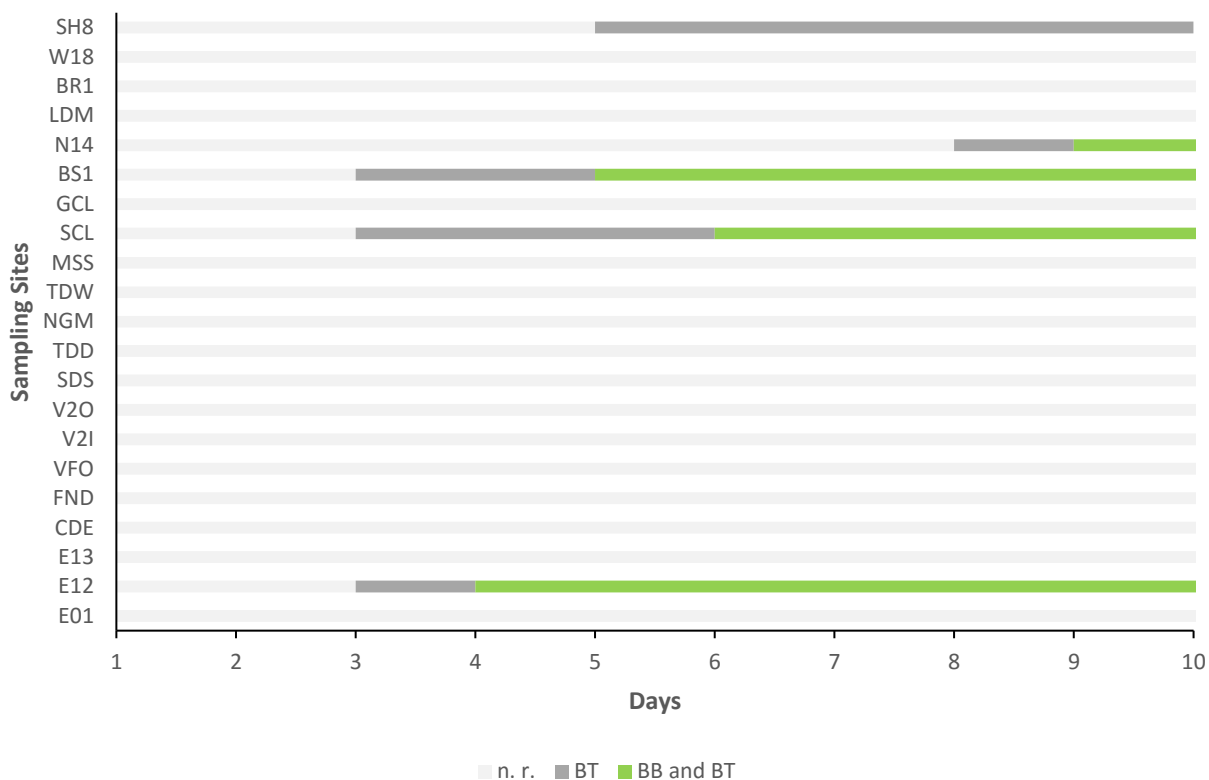


Figure 20: Reaction pattern of the SRB BART test of sampling in April 2016 for the comparison with qPCR. Only the pattern related to sulfate-reducing bacteria are shown.

The reaction pattern for the sulfate-reducing bacteria in the diagram (Figure 20) are symbolised as following: a black top (BT) is symbolized by grey bars. If the bottom and the top blackened, the bar is light green. Only five tests for sulfate-reducing bacteria showed a reaction: SH8, N14, BS1, SCL and E12. All of them started to blacken at the floating device. Except SH8, all of them developed a black base as well.

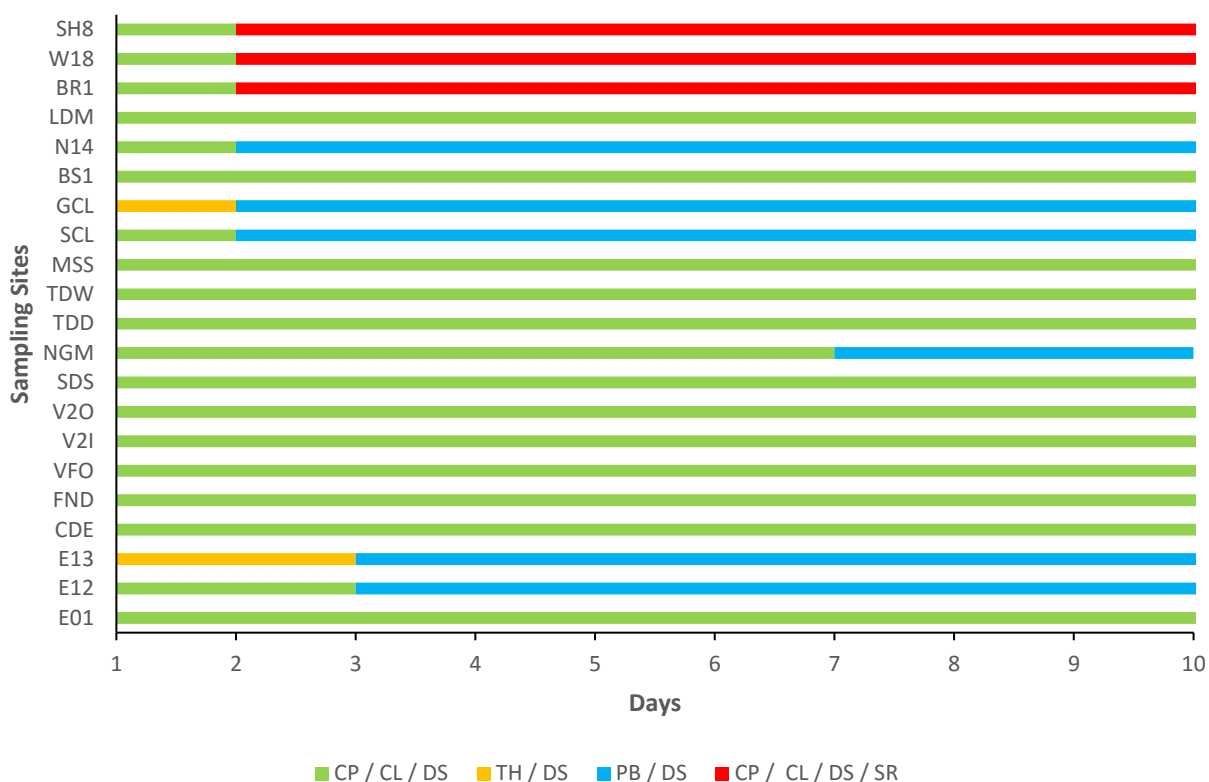


Figure 21: Reaction pattern of the SLYM BART test of sampling in April 2016 for the comparison with qPCR. Only the pattern related to slime-forming bacteria are shown.

In Figure 21, the results of the test for slime-forming bacteria can be seen. Dense slime with cloudy plates and layers (CP/CL/DS) is symbolised with a light green bar. Dense slime with thread-like strings (TH/DS) occur. Pale blue glow is marked with a blue bar (PB) and if a slime ring (SR) occurred, a red bar is marked. Since the first day, all samples showed dense slime at the bottom. The bacteria in E13 and GCL formed thread-like strings in the tube, the others showed plates and layers. N14, GCL, SCL, NGM, E13 and E12 started to glow blue under UV-light. Some of the samples glowed extremely strong, so that it was possible to see the fluorescence with the naked eye. SH8, BRI and W18 also developed a slime ring around the floating device.

The BART Software uses the reaction pattern to calculate the amount of contained bacteria. By doing that, it is not important which pattern occurs first and which pattern follow. Only the day when the first reaction occur, is important, since this forms the basis for the calculation. The result is expressed in predictive active cells per millilitre (pac mL^{-1}).

Table 11: Results BART Software

Sample	IRB / T pac mL⁻¹	SRB / T pac mL⁻¹	SLYM / M pac mL⁻¹
E01	2.2	-	8.81
E12	566	5.21	8.81
E13	566		8.81
CDE	8.82	-	8.81
FND	2.2	-	8.81
VFO	2.2	-	8.81
V2I	566	-	8.81
V2O	-	-	8.81
SDS	8.82	-	8.81
NGM	566	-	8.81
TDW	-	-	8.81
TDD	-	-	8.81
MSS	566	-	8.81
SCL	566	46.6	8.81
GCL	566	-	8.81
BS1	566	46.6	8.81
N14	566	75 pac mL ⁻¹	8.81
LDM	566	-	8.81
BRI	566	-	8.81
W18	566	-	8.81
SH8	8.82	910 pac mL ⁻¹	8.81

According to the software, all of the samples contained at least 8.81 million active cells per millilitre, which are slime-forming bacteria. BS1 and GCL contain the highest number of predictive active cells in total.

4.2.2 BART after 21 Days for the Detection of any Weakness

To have reliable results which can be replicated, it is important to know how the results will differ, if there is a change in the test conditions. Therefore, samples were stored for 21 days at 4°C before the BART tests started. For this test, only the SRB and IRB BART were used.

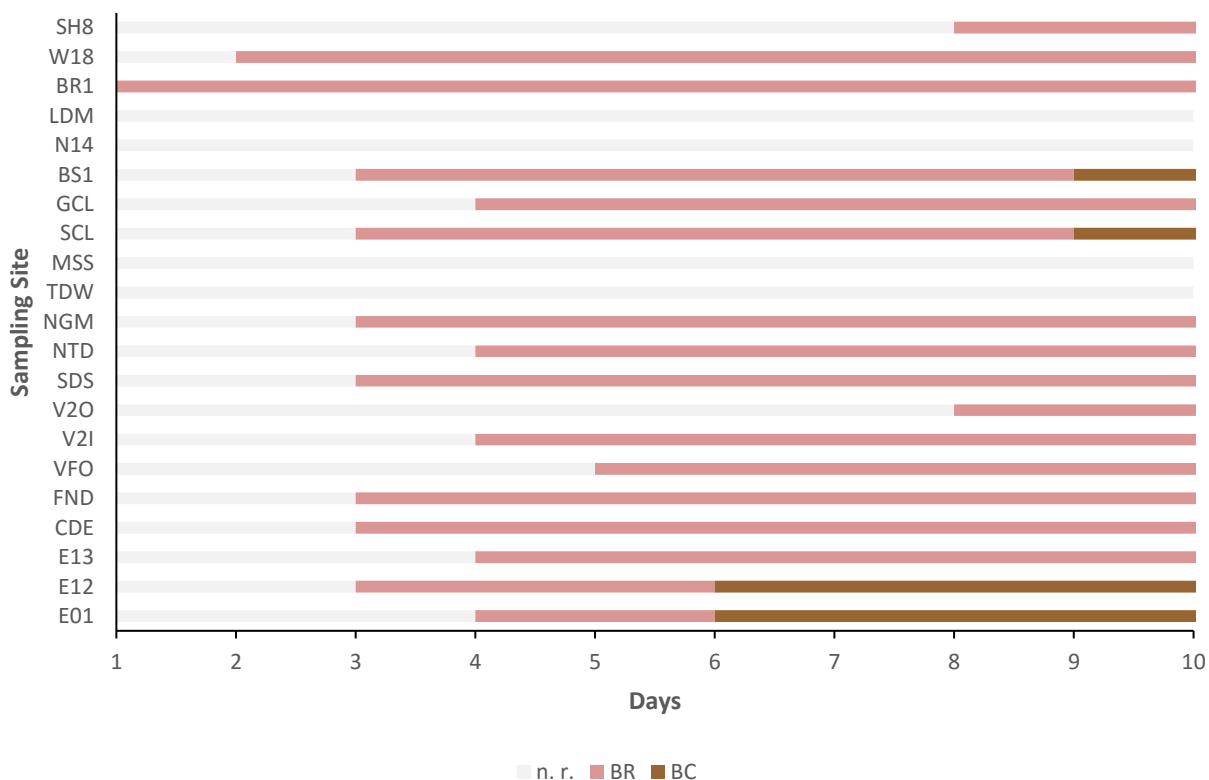


Figure 22: Reaction pattern of the IRB BART test started 21 days after sample taking. Only the pattern caused by iron-related bacteria are shown.

In Figure 22 the reaction pattern caused by iron-related bacteria after 21 days chilled storing are shown. LDM, N14, MSS and TDW showed no reaction. In all of the other samples, a brown ring occurred. Furthermore, BS1, SCL, E12 and E01 turned completely brown after a few days. In general, a huge difference can be seen between the two runs. At first, more samples showed a reaction after 21 days of storing and the reaction started earlier. The second thing is, most of the 21-days-samples showed a brown ring only. Just a few of them turned brown completely and none of them turned black.

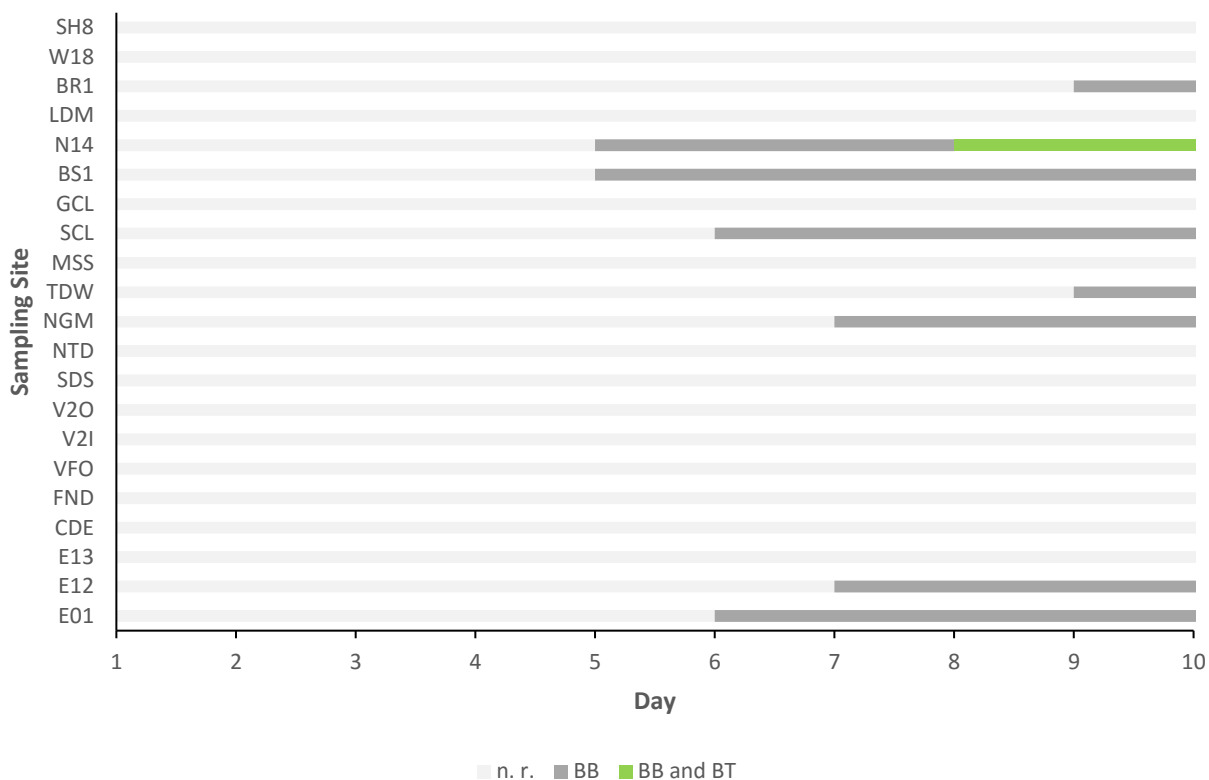


Figure 23: Reaction pattern of the SRB BART test started 21 days after sample taking. Only the pattern caused by sulfate-reducing bacteria are shown.

BRI, N14, BS1, SCL, TDW, NGM, E12 and E01 had a black base. The first of them turned black after five days. Only one of them, N14, got a black top as well. Contrary to the other SRB BART test, the reaction started at the bottom instead at the top of the tube. Additionally, more samples showed a blackening.

4.3 Quantification of the Contained DNA

4.3.1 Results of the Photometric Quantification

Two of the recorded spectra are shown here. The red line marks the absorption maximum of DNA. BS1 and SCL were chosen because of their BART results. According to the results of the BART Software, both contain the biggest number of cells: 566 T pac mL⁻¹ of iron-related bacteria, 46.6 T pac mL⁻¹ of sulfate-reducing bacteria and 8.81 M pac mL⁻¹ of slime-forming bacteria.

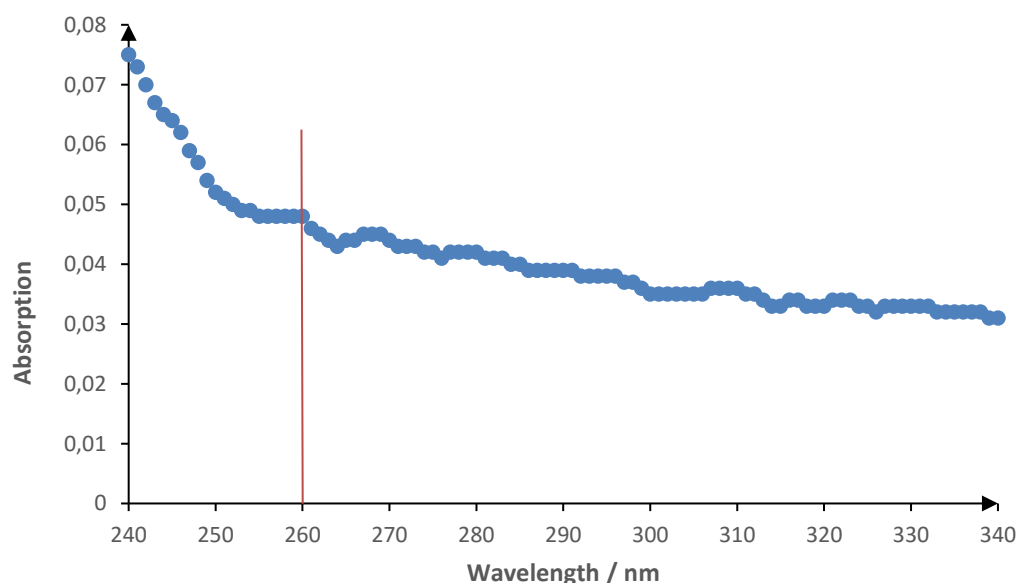


Figure 24: Spectrum of BS1 I

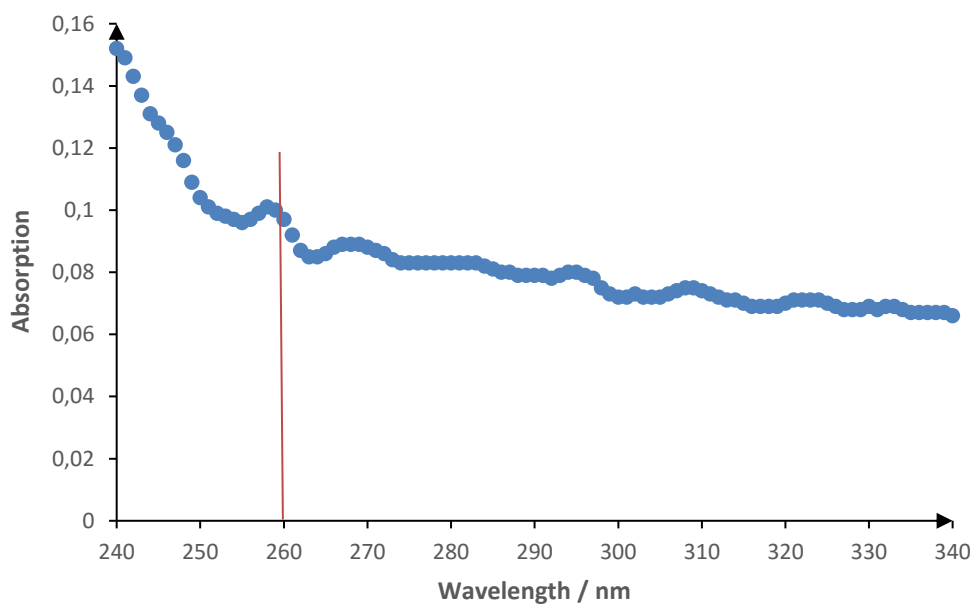


Figure 25: Spectrum of SCL I

Having a closer look at the spectrum of BS1 I, no absorption maxima at 260 nm can be recognized. The spectrum of SCL I shows a tiny peak close to 260 nm.

The Absorption at 260 and 280 nm was read off and the ratio was calculated as mentioned in equation 18. The results are noted in Table 12.

Table 12: Results of the photometer

Sample	260 nm	280 nm	260 nm/280 nm
E01 I	0.025	0.018	1.39
E01 II	0.112	0.093	1.20
E12 I	0.075	0.065	1.15
E12 II	0.027	0.022	1.23
E13 I	0.129	0.117	1.10
E13 II	0.033	0.027	1.22
CDE I	0.035	0.029	1.21
CDE II	0.055	0.047	1.17
N14 I	0.072	0.063	1.14
N14 II	0.050	0.040	1.25
LDM I	0.120	0.096	1.25
LDM II	0.083	0.065	1.28
SH8 I	0.093	0.072	1.29
SH8 II	0.088	0.072	1.22
BRI I	0.098	0.082	1.20
BRI II	0.095	0.075	1.27
BS1 I	0.048	0.042	1.14
BS1 II	0.046	0.039	1.18
LDM I	0.121	0.105	1.15
LDM II	0.099	0.086	1.15
V2I I	0.061	0.055	1.11
V2I II	0.062	0.053	1.17
V2O I	0.058	0.050	1.16
V2O II	0.050	0.042	1.19
FND I	0.182	0.148	1.23
FND II	0.162	0.132	1.23
VFO I	0.100	0.082	1.22
VFO II	0.147	0.130	1.13
SDS I	0.094	0.084	1.12
SDS II	0.064	0.056	1.14
MSS I	0.627	0.494	1.27
MSS II	0.352	0.288	1.22
GCL I	0.094	0.082	1.15
GCL II	0.095	0.083	1.14
SCL I	0.097	0.083	1.17
SCL II	0.068	0.060	1.13
NGM I	0.129	0.113	1.14
NGM II	0.092	0.008	1.15
TDW I	0.103	0.09	1.14
TDW II	0.098	0.079	1.24
TDD I	0.514	0.419	1.23
TDD II	0.097	0.078	1.24
W18 I	0.100	0.083	1.20
W18 II	0.093	0.071	1.31

The ratio varies between 1.4 and 1.0. Due to the fact, that a ratio of 1.5 means, 50 % of the sample are proteins ³², the concentration of the contained DNA was not calculated.

For a photometric quantification, a minimum of 0.25 $\mu\text{g mL}^{-1}$ of DNA ³² has to be contained in the sample. Having a look at the qPCR results, a fluorescence signal of the first samples that is higher than the background is measured after or at the same time as standard 4, which contains 0.02 ng of DNA per reaction well. Each capillary contains 20 μL reaction mix. To proceed at the assumption that the standard has a concentration of 1 ng mL^{-1} , the samples are clearly under the detection limit.

4.3.2 Results of the Real-Time PCR

In the beginning, some trouble was experienced by performing the qPCR. The LightCycler Software received an error message (*'Fluorescence 3 Min. error'*) from the instrument. This means that, the fluorescence signal measured in channel 3 at 705 nm is out of the detection range.

In the premix of the Femto™ Bacterial DNA Quantification Kit, Syto® 9 is contained as fluorescence dye.

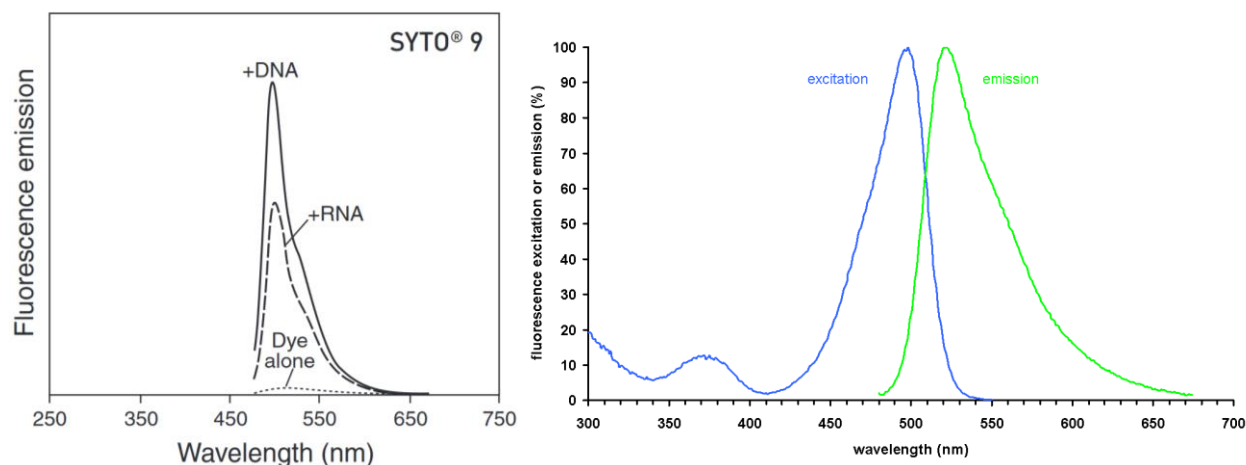


Figure 26: Spectra of the emission of Syto® 9 (from ThermoFisher Scientific) and SYBR Green (from [wikimedia.org](https://commons.wikimedia.org/wiki/File:SYBR_Green_Spectra.png))

Looking at the emission wavelength (Figure 26), the emission spectrum of SYBR Green is shifted to the bigger wavelengths compared to Syto 9. So the fluorescence signal at 705 nm is out of the detection limit of the LightCycler. According to different publications ^{43,44} dyes out of the Syto family have many advantages compared to SYBR Green. Syto 9 is far less inhibitory than SYBR Green and it also produces DNA melting curves with a higher reproducibility over

a broader range of concentrations. Additionally, additives like BSA or DMSO have to be added to a master mix containing SYBR Green to improve the effectivity. All these together can be a reason for the decision of the manufacturer of the qPCR Kit, to use Syto 9 for the kit. Since the LightCycler Software 4.1 used in the Laboratory for Biochemistry cannot use only one or two channels for data analysis, neither a standard curve could be calculated nor the quantification of the DNA samples was possible. Moreover, the derivation of the melting curve could not be produced as well.

For this reason, a test version of the new software (480LightCycler® Software) was ordered from Roche and the results from the run could be analysed.

Table 13: Settings to compile the standard curve

Run	Background	Noiseband	Fit Points	Threshold
1	2 - 6	0.8500	2	2.1500
2	2 - 6	0.3200	2	2.1500

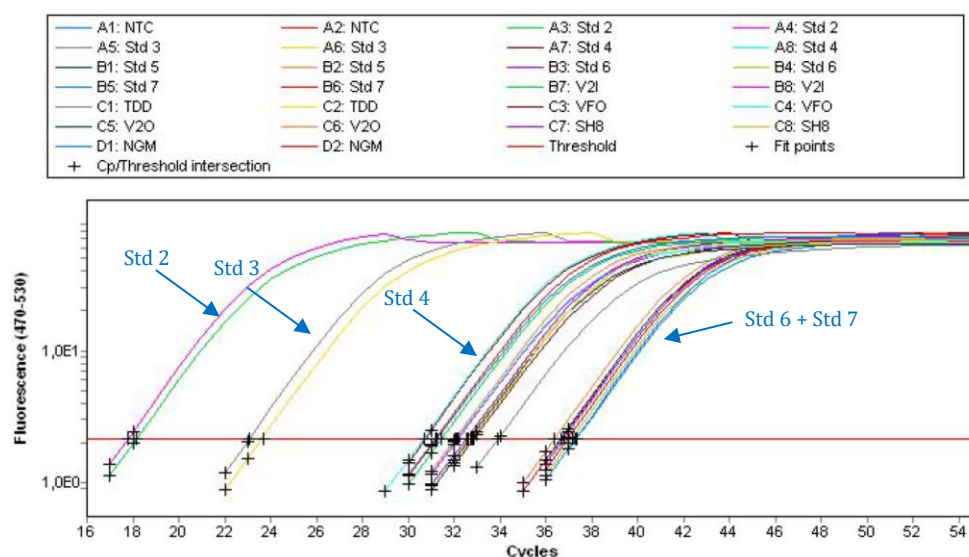


Figure 27: Amplification curve containing the standards to create the standard curve. The standards are marked by the blue arrows from left to right. Std 6 and Std 7 can be found in the bundle, Std 5 is not clearly detectable and not marked.

With an error higher than 1, the standard curve (Figure 28) cannot be used for a reliable quantification.

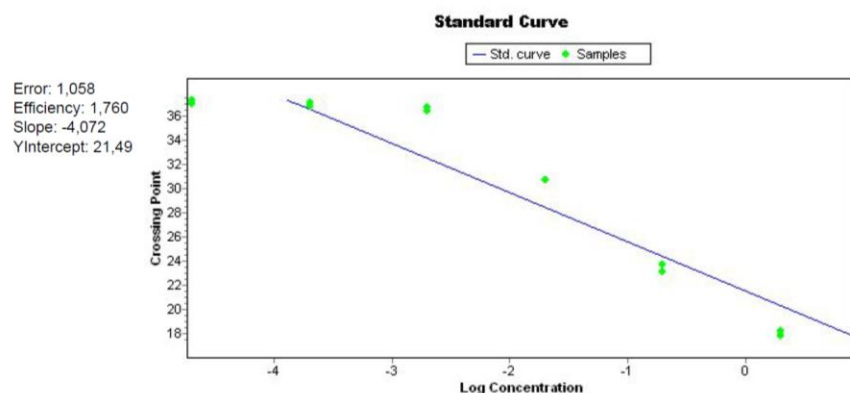


Figure 28: Standard curve produced with the test version of the new software.

Before the test version was achieved, data from a single standard curve was sent to the customer service of Roche (Figure 29). On closer inspection, the curve has the same trend as the curve in Figure 28.

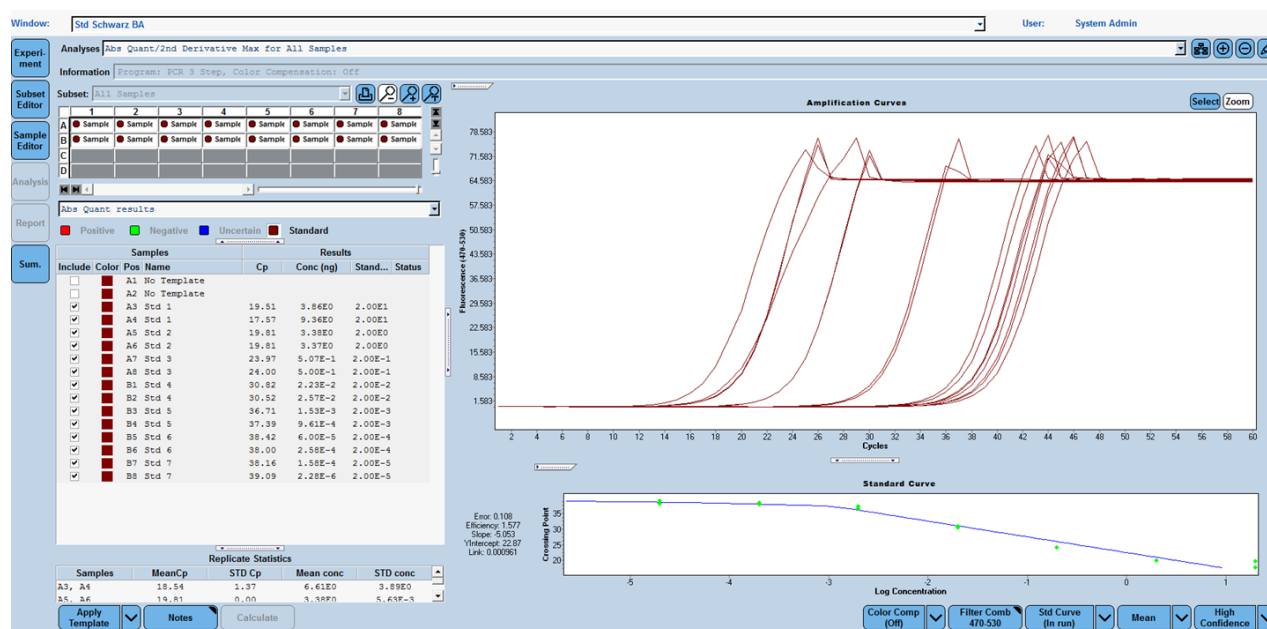


Figure 29: Screen shot of a test run for a standard curve with the Femto Kit, analysed with the new software from a Roche employee.

For a dilution at a ratio of 1:10, the amplification curves of the small standards are too close together. This is especially since the distances between the other curves differ as well. Comparing these results with the curves from Zymo Research (Figure 30), it is clear that something went wrong with the amplification. To check that, an agarose gel electrophoresis was performed after each run. The results can be seen in the following chapter ('4.4 Agarose Gel Electrophoresis').

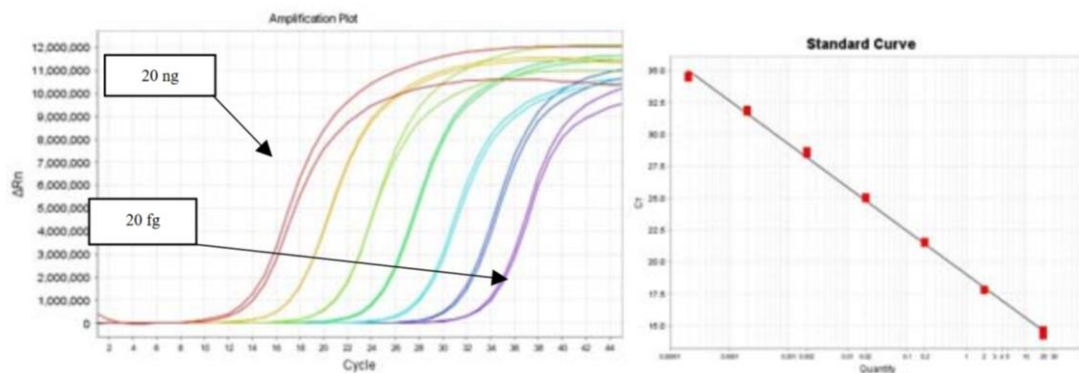


Figure 30: Standard curve and amplification plot of the Femto™ Bacterial DNA Quantification Kit produced by Zymo Research (from the Kit Instruction Manual)

For this reason, a qualitative-quantitative way of analysing the curves was chosen. Therefore, the average C_p of the sample and its replicate was used to list the standards and the samples from the lowest to the highest crossing point (Table 14). So it was possible to say, between which concentrations the samples range.

Despite of this, the results were also analysed quantitatively to give an example. Therefore, the standard curve (Figure 31) was plotted in Microsoft Excel. The formula of the straight line was used to calculate the DNA concentration of each sample (Table 14).

Table 14: Results of the qPCR

Sample	C _p	c(DNA) / ng mL ⁻¹	c(DNA) ^a / ng mL ⁻¹
Std 2	17.96	100	368.0
Std 3	23.36	10	17.36
Std 4	30.71	1	0.2717
NGM	31.22		0.2036
BS1	31.45		0.1788
N14	31.47		0.1767
CDE	31.66		0.1587
V2I	31.82		0.1450
GCL	31.91		0.1378
E12	31.96		0.1340
SDS	31.97		0.1332
E13	32.20		0.1170
V2O	32.39		0.1050
SCL	32.40		0.1044
W18	32.42		0.1033
VFO	32.49		0.0993
TDW	32.66		0.0902
SH8	32.67		0.0897
BRI	32.80		0.0833
MSS	32.85		0.0809
FND	33.01		0.0740
TDD	33.25		0.0646
E01	33.55		0.0545
LDM	36.10		0.0129
Std 5	36.53	0.1	0.0101
Std 6	36.95	0.01	0.0080
NTC Run 1	37.00		0.0077
Std 7	37.14	0.001	0.0072
NTC Run 2	37.71		0.0052

^a exemplary quantification according to Figure 31

According to the crossing points, all samples contain between 1 ng mL⁻¹ and 0.1 ng mL⁻¹.

Except TDD, SH8 and W18, each sample and each standard has only one melting peak. That means, the amplification process brought out two products, one obviously with a higher and one with a smaller GC-concentration.

The results of the exemplary calculation are in the right column of Table 14. Comparing the calculated concentration of DNA in the standards with the concentration according to the manufacturer, it is obviously that the results of this run are not reliable.

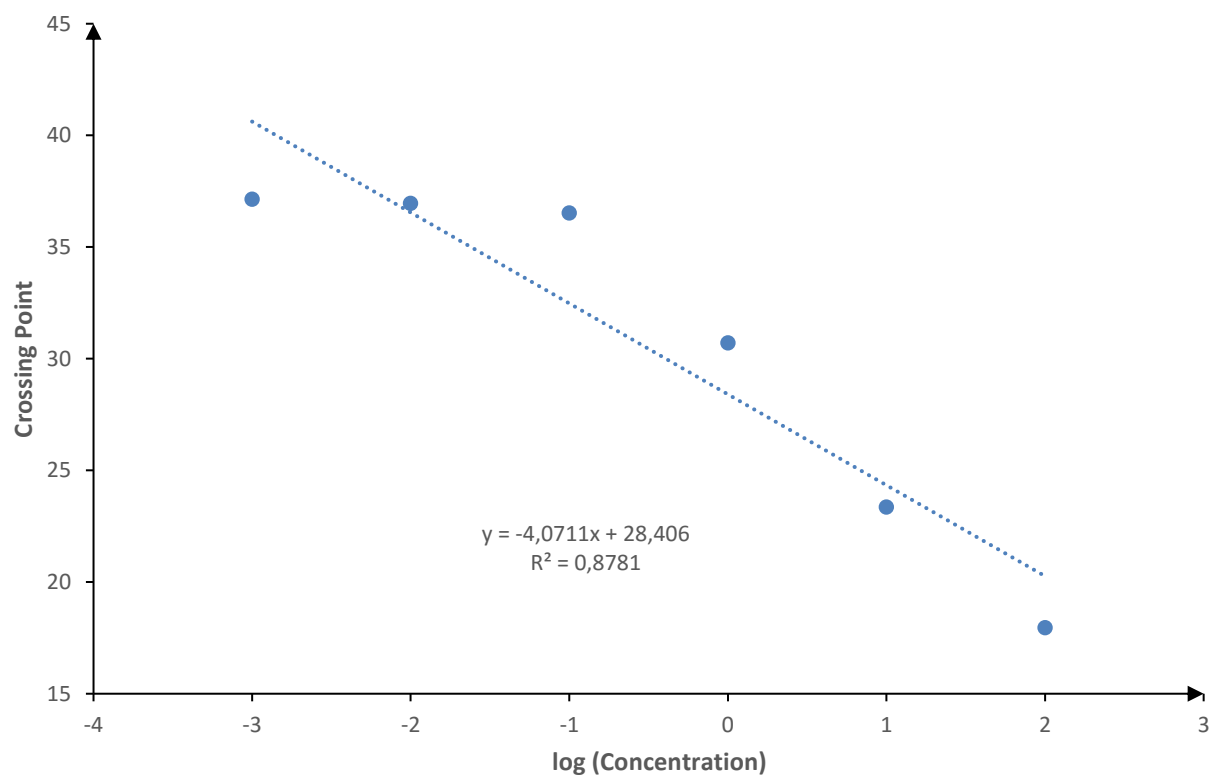


Figure 31: Standard curve of the DNA standards. The formula of the straight line can be found as well.

Table 15: Average maximum melting temperature of the standards and the NTC's.

Sample	T _m / °C
Std 2	84.47
Std 3	84.53
Std 4	84.57
Std 5	85.20
Std 6	85.13
Std 7	85.41
NTC Run 1	85.21
NTC Run 2	85.42

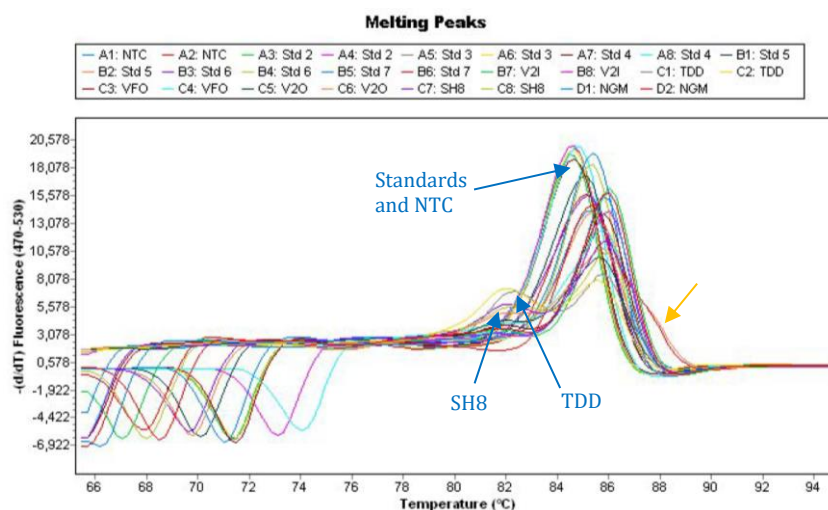


Figure 32: Melting curve of the standards and the first part of the samples. The peaks of the standards and the NTC are marked with a blue arrow. The first one of the double peak of TDD (yellow and grey) and of SH8 (light green and purple) are also marked. The orange arrow marks two peaks with a tailing to the right.

The NTC has also a melting peak with a high fluorescence signal. The maximum melting temperature of the NTC is in the range of the smallest DNA standards. A possible explanation therefore is the formation of primer dimers. This belief is also corroborated by the similarity of the crossing points of the smallest DNA standards and the NTC. In a first test, an agarose gel was made, which was loaded with the NTC and the DNA standards. Both NTC tracks showed no bands, the standards showed two bands. The photograph is not available anymore due to some technical reasons. Another conspicuity is marked by the orange arrow in Figure 32. Because of the repeating colours, the peaks cannot be identified. However, both belong to two different sampling sites. A contamination during the sample preparation for the qPCR is also not very likely, because the samples were not close together. Such a tailing can be seen in Figure 33 as well, but it is also not possible to say, to which sample the peak belongs.

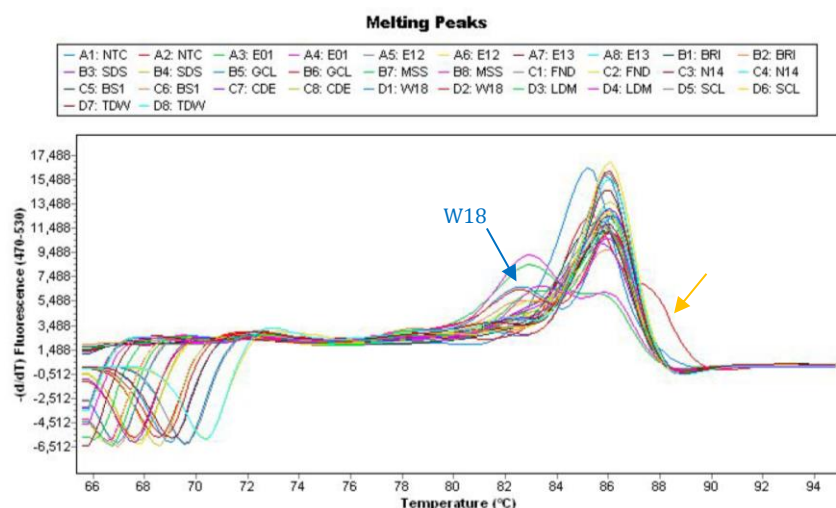


Figure 33: Melting curve of the rest of the samples. The double peak of W18 is marked with a blue arrow.

4.4 Results of the Agarose Gel Electrophoresis

The agarose gel electrophoresis was performed to verify the amplification. Therefore, a 100 bp DNA ladder was used as standard. Two different methods of dyeing were tried as well.

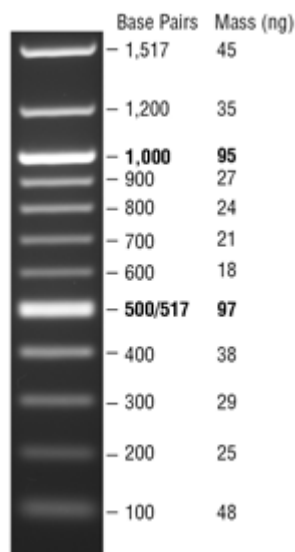


Figure 34: 100 bp Quick Purple DNA Ladder. (from neb.com)

In the upper line of the gel in Figure 35, the DNA standard 2 is plotted. During the amplification two products developed, one with a fragment length of 291 bp and one with 645 bp.

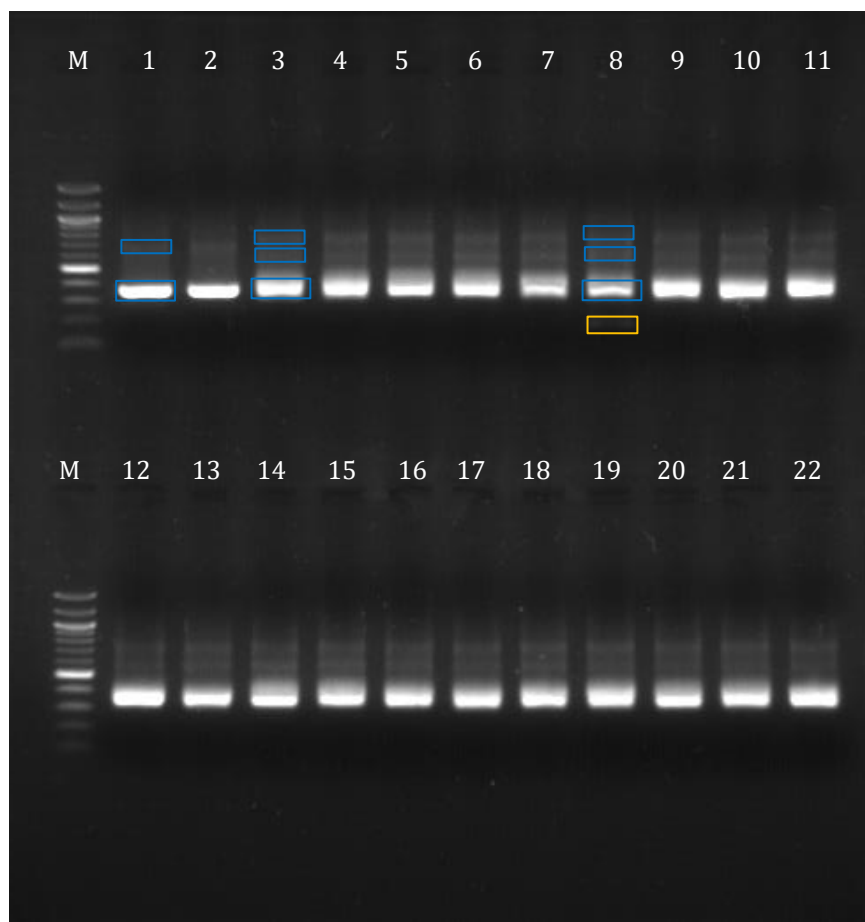


Figure 35: Agarose gel coloured with DNA stain under UV-light. M is the marker, tracks 1 and 2 belong to the DNA standard 2 and its replicate. Further assignment: CDE I and replicate (3, 4), W18 I and replicate (5, 6), LDM I and replicate (7, 8), SCL I and replicate (9, 10), TDW I (11), V2I I and replicate (12, 13), TDD I and replicate (14, 15), VFO I and replicate (16, 17), V20 I and replicate (18, 19), SH8 I and replicate (20, 21) and NGM (22). Due to the lack of space on the gel it was decided, to run NGM and TDW without their replicates, especially since the first gel did not show any variations.

In the sample tracks, three amplification products were found: 329 bp, 540 bp and 736 bp. Only in line 8 (LDM I replicate), one more product with 177 bp is visible (orange frame in Figure 35). Comparing this result with the melting curve (Figure 33), the LDM curve shows an additional peak in the front, similar to a bump in the NTC curve. Having the fragment length in mind, this product can be primer-dimers. Contamination can be excluded. All work steps were performed sterile and the product occurs only once.

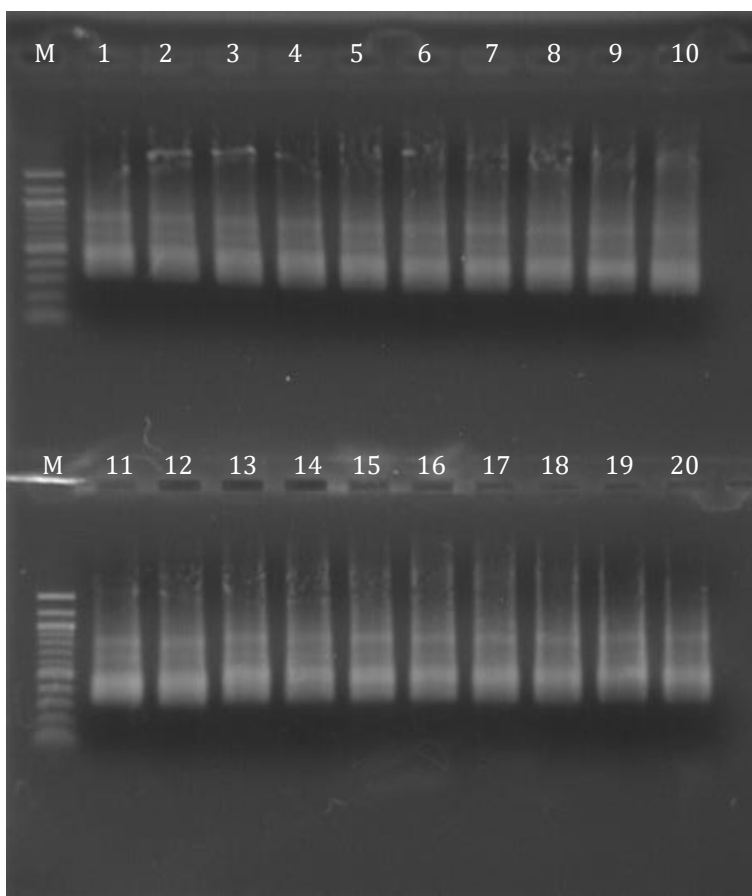


Figure 36: Agarose gel coloured with ethidium bromide under UV-light. M is the marker, tracks 1 and 2 belong to the sample E01 I and its replicate. Further assignment: E12 and replicate (3, 4), E13 and replicate (5, 6), BRI and replicate (7, 8), SDS and replicate (9, 10), GCL and replicate (11, 12), MSS and replicate (13, 14), FND and replicate (15, 16), N14 and replicate (17, 18) and BS1 and replicate (19, 20).

The upper part of the agarose gel in Figure 36 shows a curve. Whereas each single sample track in each gel contains the same products and there are no curves in the other half of the gel, it is conceivably, that the gel was not fully immersed with buffer. Apart from that, all samples contain three amplification products as well.

It is conspicuous, that the gel electrophoresis shows three different products whereas only one melting curve exists. Having a closer look at the bands, the first two are not as bright as the third one. It is very likely, that the concentration of the third product is that much higher, that the other products do not occur in the melting curves or they are responsible for the tailing of some curves.

Comparing the colouring methods, the DNA stain should be preferred in the future by the way. It is less dangerous than ethidium bromide and the bands are sharper and better detectable.

Despite of the order shown in this thesis, the qPCR run of the samples in the gel 2 and the electrophoresis were performed one day earlier than the run of gel 1, because of some organisational reasons. In doing so, it was decided to use the DNA stain for the second run to get sharper bands.

5 Discussion and Application Possibilities

5.1 Comparison of the Quantification Methods

To discuss the effectivity of the quantification by BART test, Table 16 was used. There, the samples were ordered from the highest measured amount to the lowest measured amount of contained cells.

Table 16: Quantification results of BART test and qPCR. The ranking of the qPCR is separated into three parts to compare this ranking with the ranking of the BART tests, so that it is possible to make a statement about the trend of the results.

Rank BART	Sample	Rank qPCR	Sample
1	SCL	1	NGM
	BS1	2	BS1
2	E12	3	N14
3	N14	4	CDE
4	E13	5	V2I
	V2I	6	GCL
	NGM	7	E12
	MSS	8	SDS
	GCL	9	E13
	LDM	10	V20
	BRI	11	SCL
	W18	12	W18
5	SH8	13	VFO
6	CDE	14	TDW
	SDS	15	SH8
7	E01	16	BRI
	FND	17	MSS
	VFO	18	FND
8	V20	19	TDD
	TDW	20	E01
	TDD	21	LDM

A conversion factor of 3.6 can be used to transfer the amount of copies into the number of cells³. Because of the given circumstances, the quantification by qPCR only allows to say, that all samples contain between 1 and 0.1 ng mL⁻¹ 16S rDNA. To make a quantitative statement thereof is not meaningful. Nevertheless, it is possible to make a statement about the tendency of the BART test. Regarding Table 16, the seven samples with the highest concentration of DNA according to the qPCR results are marked grey. Almost all of them are under the BART

tests with the highest number of predictive active cells. Only CDE is an outlier. The other two parts are mixed up and no clear statement can be made. The red marked samples are the one with the smallest amount of DNA according to the qPCR results. In the results of the BART tests, none of these samples can be found under the samples with the highest number of predictive active cells. A slight tendency can be recognized in this way, but it is not meaningful. To isolate the mistake, it would be helpful to perform the qPCR with the Femto™ Bacterial DNA Quantification Kit with another instrument, e.g. the ABI PRISM® of Thermo Fisher Scientific. As an alternative, it would be also possible to use another quantification kit with another fluorescence dye, e.g. SYBR GREEN or EvaGreen. In this case, BSA or other substances have to be added to prevent inhibition.

However, as it is possible to make predictions of the water quality by measuring on-site parameters and performing an ICP-MS scan, it cannot be done by microbiological studies.

A perfect example therefore are the sampling locations SDS and CDE. The samples from SDS are taken from a river which is the drinking water source for Sabie. CDE is a direct mine water discharge into a wetland on a paddock. For the comparison, the most important data can be found in Table 17.

Table 17: On-site parameters for the comparison of SDS and CDE

Sample	pH	E _H / mV	EC / $\mu\text{S cm}^{-1}$	TDS / mg L^{-1}	Fe / mg L^{-1}
SDS	6.75	392	228	130	0.051
CDE	4.30	346	1480.5	1420	3.89

Next to the pH and the redox potential, the electrical conductivity is an important factor. Together with the TDS, a reference value and the knowledge of the possible contamination, the EC can give a hint at the amount of potentially toxic substances contained in the water. As drinking water, SDS is a good reference value, which has a near neutral pH, a low redox potential and also a low electrical conductivity. Having a look at the TDS, the low EC is explained. As an example value for the TDS, the amount of iron is contained in Table 17 as well. CDE has a lower pH, almost the same redox potential but a higher EC just as a higher amount of TDS and iron. Referring to the BART test, both contain the same number of active cells. Comparing that with the qPCR results, CDE contains a bit more DNA than SDS. So in general it can be said, that the microbiological consortium has to be different, but only the number of cells does not make a clear statement about the water quality.

5.2 Microbiological Diversity

Many investigations about the microbiological diversity of mine drainage and by mine drainage influenced water were done. In one paper, Schippers et al. reviewed about 70 studies about microorganisms in this environment.¹⁵ Mostly bacteria were contained, but some archaea and eukarya as well. As pyrite oxidiser, *Acidimicrobium*, *Acidithiobacillus*, *Alicyclobacillus*, *Leptospirillum* and *Sulfobacillus* could be detected. As iron-oxidiser, *Gallionella* was discovered additionally. Bacteria originating from the order *Desulfobacterales* were found as sulfate-reducing bacteria. Ferric iron-reducer were detected as well, such as *Acidiphilium*, *Acidithiobacillus*, *Alicyclobacillus*, *Bacillus*, *Ferribacterium* and some of the *Desulfobacterales*. To assume that the results are based on 70 different studies, it is very likely that these bacteria are contained in the water samples as well. To make a clear statement about the consortia in the water discharges, a screening needs to be done. Nevertheless, only a small amount of the contained bacteria can be proved. So the BART tests cannot tell specifically, which orders and families of microorganism are contained, but it is possible to say whether a type of bacteria is contained or not. The BART test also enables one to make a general statement about the environment in which the bacteria live.

5.3 Example Case 1: Passive Treatment System in Carolina

As an example of how the BART tests could be applied in the future, a case study of the passive treatment system in Carolina is done. The system there is based on a vertical flow reactor (VFR), which are used to filter iron-(III)-hydroxide and to catalyse the oxidation of ferrous iron to ferric iron on the hydroxide surface.⁴⁵ In Figure 37, the setup of a VFR is explained.

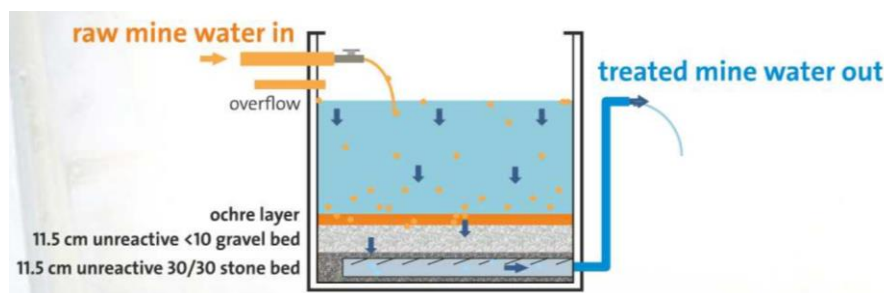


Figure 37: Scheme of a vertical flow reactor (from Wolkersdorfer: 'From Ground to Mine Water')

The raw mine water flows into the basin. The $\text{Fe}(\text{OH})_3$ precipitates on an ochre layer and the water is filtered through unreactive stone beds before it flows out. The oxidation of ferrous iron is not only surface catalysed, the iron-oxidising bacteria contained in the raw material

also add to that. Depending of the other solids and nutrients contained in the mine water, other bacteria are contained in the basin as well and continue with their metabolism. Since the educts are transferred to the metabolism products before the water is filtered, they stay in the reactor and the filtered water contains measurably less of the substance. Because of that, the respective bacteria should not be present in the outflow.

The Carolina passive treatment plant (Figure 15) has two vertical flow reactors. The first one is fed by mine drainage from FND and the outflow goes into a lake that is used for some studies about water treatment plants as well. A part of the outflow (V2I) of this lake flows into the second basin. The outflow of this one is called V2O.

Table 18: On-site parameters of FND, VFO, V2I and V2O for the case example 1.

Sample	pH	E_H / mV	EC / $\mu\text{S cm}^{-1}$	TDS / mg L^{-1}	Fe / mg L^{-1}	Mg / mg L^{-1}	Ca / mg L^{-1}	IRB-BART / pac mL^{-1}
FND	3.22	564	1905	- ^a	- ^a	- ^a	- ^a	2,200
VFO	3.02	658	2008.5	1802	18	89	165	2,200
V2I	3.68	549	1879	1798	126	42	190	566,000
V2O	3.65	577	1885.5	1724	119	43	196	-

^a The values could not be identified by reference to the sample names on the report due some writing mistake

From the first to the second VFR, the pH rises as well as the iron content, but responsible therefore is the lake in between. For this example case, the second reactor is the most interesting one, especially by looking at the BART test results of the IRB-BART (the SRB-BART was negative). Here it can be seen clearly, that the inflow contains a lot of iron-reducing or oxidising bacteria, while the outflow does not contain any of them.

Regarding the green colour of the medium, anaerobe iron-reducing bacteria are mainly contained in the samples V2I, V2O and VFO. The green staining is the result of the reduction to ferrous iron. Another proof therefore is the small brown ring around the ball. Having a look at samples with a distinct brown ring or samples, which turned brown completely (see Appendix), the medium is yellowish because of the oxidising conditions. According to the ICP-MS scan, both samples have a high calcium and magnesium amount as well.

Therefore, if the IRB-BART is suddenly positive in the outflow, something has to be wrong with the filter bed. In addition, if the SRB-BART should be positive at the inflow, something changed the water composition, e.g. a new discharge. For this reason, further investigations need to be initiated.

5.4 Example Case 2: Cradle of Humankind – UNESCO World Heritage Site

The Cradle of Humankind (COHWHS) in South Africa, close to Krugersdorp, is an important UNESCO World Heritage Site for the country. Because of this, the concern about a possible destruction of the karst landscape through environmental pollution is very high. Several studies were implemented to examine if there are any influences from acid mine drainage on the karst ^{39,46,47}. As a carbonate rock, the karst is threatened by chemical weathering in particular. The sulfuric acid originating from the chemical and biological pyrite oxidation constitutes a threat. AMD from the West Rand discharges into the Tweeloupiespruit the Wonderfonteinspruit and the Bloubankspruit and flows through the COHWHS, whereby the contaminated water affects the karst ^{29,46}. However, only less than 30 % of the ground water resources in this region are threatened by AMD in fact ³⁹.

Table 19: On-site parameters of SCL and GCL for the case example 2.

Sample	pH	E _H / mV	EC / $\mu\text{S cm}^{-1}$	TDS / mg L^{-1}	Fe / mg L^{-1}	Mg / mg L^{-1}
SCL	6.96	401	792	498	0.031	40
GCL	6.90	389	557	334	<0.025	29
Sample	Ca / mg L^{-1}	S / mg L^{-1}	SO ₄ ²⁻ / mg L^{-1}	IRB-BART / pac mL^{-1}	SRB-BART / pac mL^{-1}	
SCL	67	76	168	566,000	466,000	
GCL	50	38	73	566,000	-	

In analysing Table 19, the values of the samples are quite moderate, especially compared to the values of V2I in Table 18, which has a comparable BART test result. At this pH, ferrous iron is not stable, so mainly ferric iron is contained. However, at this point, a weakness of the BART test occurs. The result of the BART test is almost the same as the result of V2I, that means from 'pure' acid mine drainage. By only referring to these results, a statement about the contamination with AMD cannot be made. Therefore, the other parameters need to be considered as well. So in this case, the difference in the consortia between acid mine drainage and water samples out of the caves is more important than the vague quantification by BART tests.

5.5 Example Case 3: Active Mining

Another application possibility for the BART tests is the extension of routine checks in mining companies. Changing the mindsets about environmental protection starts slowly. Very few companies have begun to note down the on-site parameters regularly to improve the water

quality. Table 20 shows the on-site parameters and BART test results of a mining company close to Krugersdorp. The company began improving the water quality with unspecified methods. The samples were taken from three different mine water discharges on the area.

Table 20: On-site parameters of SH8, W18 and BRI for the case example 3.

Sample	pH	E _H / mV	EC / $\mu\text{S cm}^{-1}$	TDS / mg L^{-1}	Fe / mg L^{-1}	Mg / mg L^{-1}
W18	6.23	113	3541	3770	49	149
SH8	6.07	155	3552.5	3588	54	106
BRI	6.14	153	3469	3714	81	157

Sample	Ca / mg L^{-1}	S / mg L^{-1}	SO ₄ ²⁻ / mg L^{-1}	IRB-BART / pac mL^{-1}	SRB-BART / pac mL^{-1}
W18	616	1030	2455	566,000	-
SH8	637	833	2410	8,820	910
BRI	628	1029	2449	566,000	-

Despite the high electrical conductivity and the amount of total dissolved solids, the pH is near neutral and the iron content is not too high. Regarding the BART test results, only in one sample (SH8) are sulfate-reducing bacteria contained. As obligate anaerobic bacteria, sulfate-reducer can be present in all three samples, especially since the samples were taken directly from the outflow of the underground water source. Since the amount of SRB in SH8 is low compared to others, this fact is not really pivotal for a discrimination between this three samples. In conjunction with the result of the IRB-BART test, it is possible to use the test in the same way as in the example case 1.

5.6 Future Work

To evaluate the routinely performance of the BART test, it is necessary to integrate them in a bigger project. Therefore, a longer-term thesis e.g. about a water treatment plant would be suitable. Especially further examinations about the precision of the tests when these are performed by different people are relevant for a possible application in the daily routine.

It would be interesting to observe an integration of the BART test in the daily work routine of an employee of a mining company, in order to see how untrained staff copes with the test.

For understanding the exact processes in a vertical flow reactor, a detailed microbiological screening needs to be done.

6 Conclusions

The BART test is a cheap test which is easy to perform. It is definitely suitable for routine checks and can be applied by non-trained staff as well. Therefore, a broad observation of problem areas is possible. The implementation is obviously a political task.

However, for further investigations, specialists and more precise methods are necessary. The first thing is that the BART test is a test which always needs a reference. If different people perform the test, photographs of a standard reference are needed, because of individuals' differing visual perceptions. The test also has to be performed at the same time after sample taking. Otherwise, big differences in the results appear and the comparability of the results cannot be secured. This is also a weakness of the test relating to field trips which last longer than one day. The samples need to be stored from the point of sampling to the point of performing the test and as cool as possible to reduce bacterial growth in between, at least. Except for sampling in the Arctic or Antarctic it is impossible to achieve this cooling point with an ordinary cool box. Moreover, the real amount of the tested bacteria can also not be determined. Most of the bacteria, especially the slime-forming ones grow on surfaces and do not move freely in the water.

7 References

- (1) Davenport, J. *Digging deep: A history of mining in South Africa, 1852-2002*; Jonathan Ball Publishers: Johannesburg, 2013.
- (2) motsie, refilee. *South Africas Mineral Industry 2012 2013*; Pretoria, 2013.
- (3) Kock, D.; Schippers, A. Geomicrobiological investigation of two different mine waste tailings generating acid mine drainage. *Hydrometallurgy* **2006**, 83 (1-4), 167–175. DOI: 10.1016/j.hydromet.2006.03.022.
- (4) Südafrika. *The mineral resources of South Africa*, 6. ed.; Handbook / Council for Geoscience 16; Council for Geoscience: Pretoria, 1998.
- (5) A.L. Mills. The Role of Bacteria in Environmental Geochemistry.
- (6) Stumm, W.; Morgan, J. J. *Aquatic Chemistry: Chemical Equilibria and Rates in Natural Waters*, 3rd ed.; Environmental Science and Technology; Wiley: Hoboken, 2012.
- (7) Johnson, D. B. Chemical and Microbiological Characteristics of Mineral Spoils and Drainage Waters at Abandoned Coal and Metal Mines. *Water, Air and Soil Pollution: Focus* **2003**, 3 (1), 47–66. DOI: 10.1023/A:1022107520836.
- (8) McCarthy, T. S.; Humphries, M. S. Contamination of the water supply to the town of Carolina, Mpumalanga, January 2012. *S. Afr. J. Sci.* **2013**, 109, 112. DOI: 10.1590/sajs.2013/20120112.
- (9) McCarthy, T. S. The impact of acid mine drainage in South Africa. *S. Afr. J. Sci.* **2011**, 107, 712. DOI: 10.4102/sajs.v107i5/6.712.
- (10) Hobbs, Philip J., Cobbing, Jude E. *A Hydrogeological Assessment of Acid Mine Drainage Impacts in the West Rand Basin, Gauteng Province*; Pretoria, 2007.
- (11) Naicker, K.; Cukrowska, E.; McCarthy, T. S. Acid mine drainage arising from gold mining activity in Johannesburg, South Africa and environs. *Environ. Pollut.* **2003**, 122, 29–40. DOI: 10.1016/S0269-7491(02)00281-6.
- (12) Wolkersdorfer, C. *Water Management at Abandoned Flooded Underground Mines: Fundamentals, Tracer Tests, Modelling, Water Treatment*; Mining and the Environment; Springer-Verlag Berlin Heidelberg: Berlin, Heidelberg, 2008.
- (13) Cypionka, H. *Grundlagen der Mikrobiologie*, 4., überarb. und aktual. Aufl.; Springer-Lehrbuch; Springer: Heidelberg, 2010.

-
- (14) Madigan, M. T.; Martinko, J. M.; Brock, T. D.; Lazar, T.; Thomm, M. *Brock Mikrobiologie: [Studentengetestet]*, 11., aktualisierte Aufl. 2009, [Nachdr.]; bc - biologie/chemie; Pearson Studium: München, 20]12 [erschienen] 2011.
- (15) Schippers, A.; Breuker, A.; Blazejak, A.; Bosecker, K.; Kock, D.; Wright, T. L. The biogeochemistry and microbiology of sulfidic mine waste and bioleaching dumps and heaps, and novel Fe(II)-oxidizing bacteria. *Hydrometallurgy* **2010**, *104* (3-4), 342–350. DOI: 10.1016/j.hydromet.2010.01.012.
- (16) Singer, P. C.; Stumm, W. Acidic mine drainage: the rate-determining step. *Science (New York, N.Y.)* **1970**, *167* (3921), 1121–1123. DOI: 10.1126/science.167.3921.1121.
- (17) Johnson, D. B. Geomicrobiology of extremely acidic subsurface environments. *FEMS Microbiology Ecology* **2012**, *81* (1), 2–12. DOI: 10.1111/j.1574-6941.2011.01293.x.
- (18) Kamika, I.; Momba, M. N. B. Microbial Diversity of Emalahleni Mine Water in South Africa and Tolerance Ability of the Predominant Organism to Vanadium and Nickel. *PLoS One* **2014**, *9*, 1. DOI: 10.1371/journal.pone.0086189.
- (19) Aytar, P.; Kay, C. M.; Mutlu, M. B.; Cabuk, A.; Johnson, D. B. Diversity of acidophilic prokaryotes at two acid mine drainage sites in Turkey. *Environmental science and pollution research international* **2015**, *22* (8), 5995–6003. DOI: 10.1007/s11356-014-3789-4.
- (20) *Biological sulphate removal using hydrogen as the energy source*; Eloff, E., Ed., 2003.
- (21) *Biological sulphate reduction of acid mine drainage using primary sewage sludge*; Poinapen, J., Ed., 2012.
- (22) *Verification of a Semi-Passive Microbially-Assisted Biotechnology for Large-Scale Treatment of Acid Mine Drainage*; Wade, P. W., Ed.; Abstracts of the International Mine Water Conference, 2009.
- (23) Coetzee, H. *Rapid field based analytical techniques for the environmental screening of abandoned mine sites*; Reliable Mine Water Technology; International Mine Water Association: Golden, 2013.
- (24) Fyffe, L.; Coetzee, H.; Wolkersdorfer, C. Cost effective screening of mine waters using accessible field test kits – Experience with a high school project in the Wonderfonteinspruit Catchment, South Africa. In *Uranium – Past and Future Challenges*; Merkel, B. J., Arab, A., Eds., 2015; pp 565–572.

- (25) Jin, S.; Fallgren, P. H.; Morris, J. M.; Gossard, R. B. Biological Source Treatment of Acid Mine Drainage Using Microbial and Substrate Amendments: Microcosm Studies. *Mine Water Environ* **2008**, *27* (1), 20–30. DOI: 10.1007/s10230-007-0026-0.
- (26) Strosnider, W. H.; Winfrey, B. K.; Nairn, R. W. Alkalinity Generation in a Novel Multi-stage High-strength Acid Mine Drainage and Municipal Wastewater Passive Co-treatment System. *Mine Water Environ* **2011**, *30* (1), 47–53. DOI: 10.1007/s10230-010-0124-2.
- (27) Tsipa, A. The impact of mobile science laboratories in the performance of Grade 12 learners in Mpumalanga Province. In *Optimization Principles*; Rau, N. S., Ed.; IEEE, 2003.
- (28) Turton, A. Managing the Unintended Consequences of Mining: Acid Mine Drainage in Johannesburg. In *Urban Water Reuse Handbook*; Eslamian, S., Ed.; CRC Press, 2015; pp 551–561.
- (29) Durand, J. F. The impact of gold mining on the Witwatersrand on the rivers and karst system of Gauteng and North West Province, South Africa. *J. Afr. Earth Sci.* **2012**, *68*, 24–43. DOI: 10.1016/j.jafrearsci.2012.03.013.
- (30) Rösner, T.; van Schalkwyk, A. The environmental impact of gold mine tailings footprints in the Johannesburg region, South Africa. *Bull Eng Geol Env* **2000**, *59*, 137–148. DOI: 10.1007/s100640000037.
- (31) Cullimore, D. R. *Microbiology of well biofouling*; The sustainable well series; Lewis: Boca Raton, Fla, 2000.
- (32) Lottspeich, F. *Bioanalytik*, 2., [aktualisierte und erw.] Aufl., [Nachdr.]; Spektrum Akad. Verl.: Heidelberg, 2009.
- (33) *Gentechnische Methoden: Eine Sammlung von Arbeitsanleitungen für das molekularbiologische Labor*, 4. Aufl.; Elsevier Spektrum Akad. Verl.: München, 2007.
- (34) 05450110990_DE_EA_LightCycler-480-Quantifizierungsstrategien-Broschüre_DE.
- (35) Lösel, R. *Bioanalytik*. Vorlesungsskript, Technische Hochschule Nürnberg Georg-Simon-Ohm, Nürnberg, 2015.
- (36) TURNER, S.; PRYER, K. M.; MIAO, V. P. W.; PALMER, J. D. Investigating Deep Phylogenetic Relationships among Cyanobacteria and Plastids by Small Subunit rRNA Sequence Analysis. *J Eukaryotic Microbiology* **1999**, *46* (4), 327–338. DOI: 10.1111/j.1550-7408.1999.tb04612.x.

- (37) Armougom, F. Exploring Microbial Diversity Using 16S rRNA High-Throughput Methods. *J Comput Sci Syst Biol* **2009**, 02 (01). DOI: 10.4172/jcsb.1000019.
- (38) McKenna, P.; Hoffmann, C.; Minkah, N.; Aye, P. P.; Lackner, A.; Liu, Z.; Lozupone, C. A.; Hamady, M.; Knight, R.; Bushman, F. D. The macaque gut microbiome in health, lentiviral infection, and chronic enterocolitis. *PLoS pathogens* [Online] **2008**, 4 (2), e20. <http://www.ncbi.nlm.nih.gov/pmc/articles/PMC2222957/pdf/ppat.0040020.pdf> (accessed August 5, 2016).
- (39) Holland, M.; Witthüser, K. T. Geochemical characterization of karst groundwater in the cradle of humankind world heritage site, South Africa. *Environmental Geology* **2009**, 57, 513–524. DOI: 10.1007/s00254-008-1320-2.
- (40) Wu, X.; Liu, L.; Zhang, Z.; Deng, F.; Liu, X. Phylogenetic and genetic characterization of *Acidithiobacillus* strains isolated from different environments. *World journal of microbiology & biotechnology* [Online] **2014**, 30 (12), 3197–3209. https://my.ohmportal.de/service/home/~art_10.1007_s11274-014-1747-4.pdf?auth=co&loc=en_US&id=0771-644C-emsg-A63B7CE98A741216E0404B8D6CED07BC00000F335B57&part=2 (accessed August 1, 2016).
- (41) Kesberg, A. I.; Schleheck, D. Improved protocol for recovery of bacterial DNA from water filters: Sonication and backflushing of commercial syringe filters. *Journal of microbiological methods* [Online] **2013**, 93 (1), 55–57. https://my.ohmportal.de/service/home/~DNA_aus_Filtern_Kesberg_2013.pdf?auth=co&loc=en_US&id=0771-644C-emsg-A63B7CE98A741216E0404B8D6CED07BC00000F335B57&part=3 (accessed August 1, 2016).
- (42) Sandstrom, M.; Jalilehvand, F.; Persson, I.; Gelius, U.; Frank, P.; Hall-Roth, I. Deterioration of the seventeenth-century warship Vasa by internal formation of sulphuric acid. *Nature* **2002**, 415 (6874), 893–897. DOI: 10.1038/415893a.
- (43) Monis, P. T.; Giglio, S.; Saint, C. P. Comparison of SYTO9 and SYBR Green I for real-time polymerase chain reaction and investigation of the effect of dye concentration on amplification and DNA melting curve analysis. *Analytical biochemistry* [Online] **2005**, 340 (1), 24–34. <http://www.gene-quantification.com/monis-sytor-sybr-hrm-2005.pdf> (accessed August 8, 2016).
- (44) Eischeid, A. C. SYTO dyes and EvaGreen outperform SYBR Green in real-time PCR. *BMC*

research notes [Online] **2011**, 4, 263. http://download.springer.com/static/pdf/820/art%253A10.1186%252F1756-0500-4-263.pdf?originUrl=http%3A%2F%2Fbmcrenotes.biomedcentral.com%2Farticle%2F10.1186%2F1756-0500-4-263&token2=exp=1470647146~acl=%2Fstatic%2Fpdf%2F820%2Fart%25253A10.1186%25252F1756-0500-4-263.pdf*~hmac=c2504c7c41de9eabf2a47d0f1259750fddbff97f9a7fcc3cddcc4b72130809f3 (accessed August 8, 2016).

(45) *A novel method for passive treatment of mine water using a vertical flow accretion system*; Sapsford, D. J., Ed., 2005.

(46) Durand, J. F.; Meeuvis, J.; Fourie, M. Environmental management and the threat of mine effluent to the UNESCO status of the Cradle of Humankind World Heritage Site. *TD The Journal for Transdisciplinary Research in Southern Africa* **2010**, 6.

(47) Hobbs, P. J.; Mills, P. J. Managing the Threats to the Karst Water Resources of the Cradle of Humankind World Heritage Site, South Africa. In *Protected karst territories – monitoring and management*; Yordanova, M., Stefanova, D., Mikhova, D., Eds., 2012; pp 1–11.

8 Appendix

8.1 Standard Curves of the Agarose Gel Electrophoresis

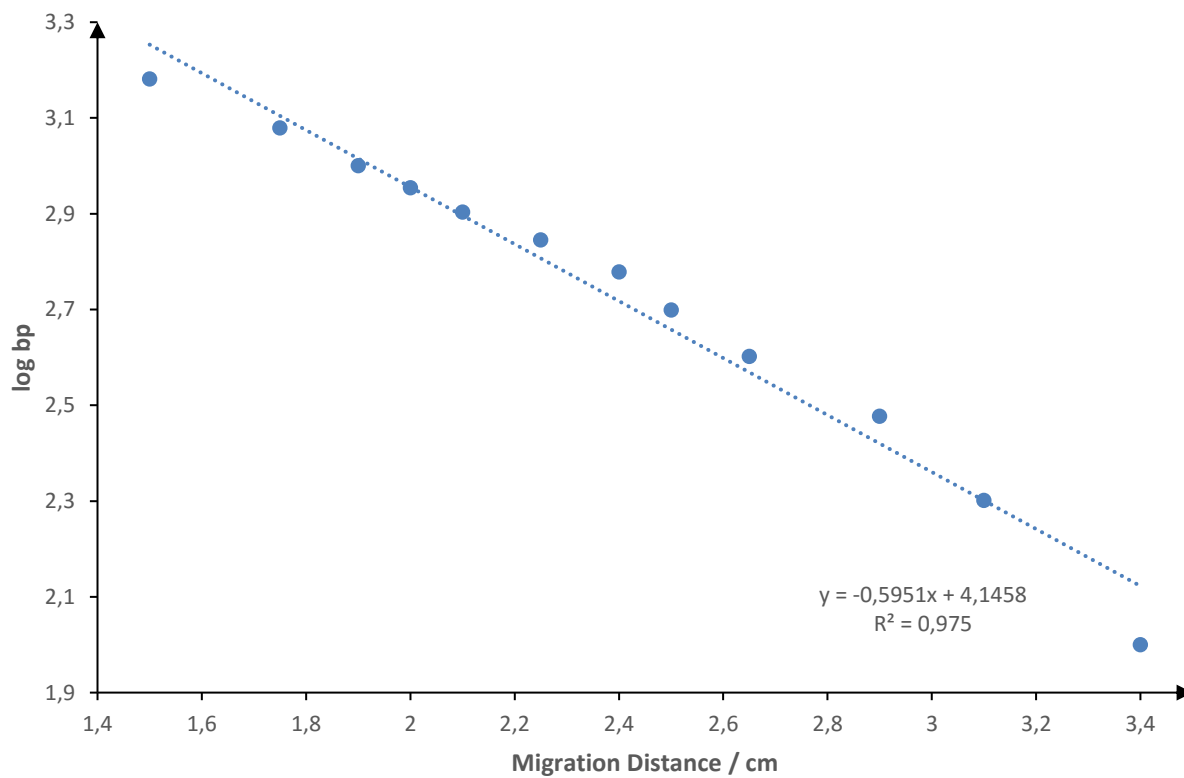


Figure A.1: Standard curve of gel 1, upper line.

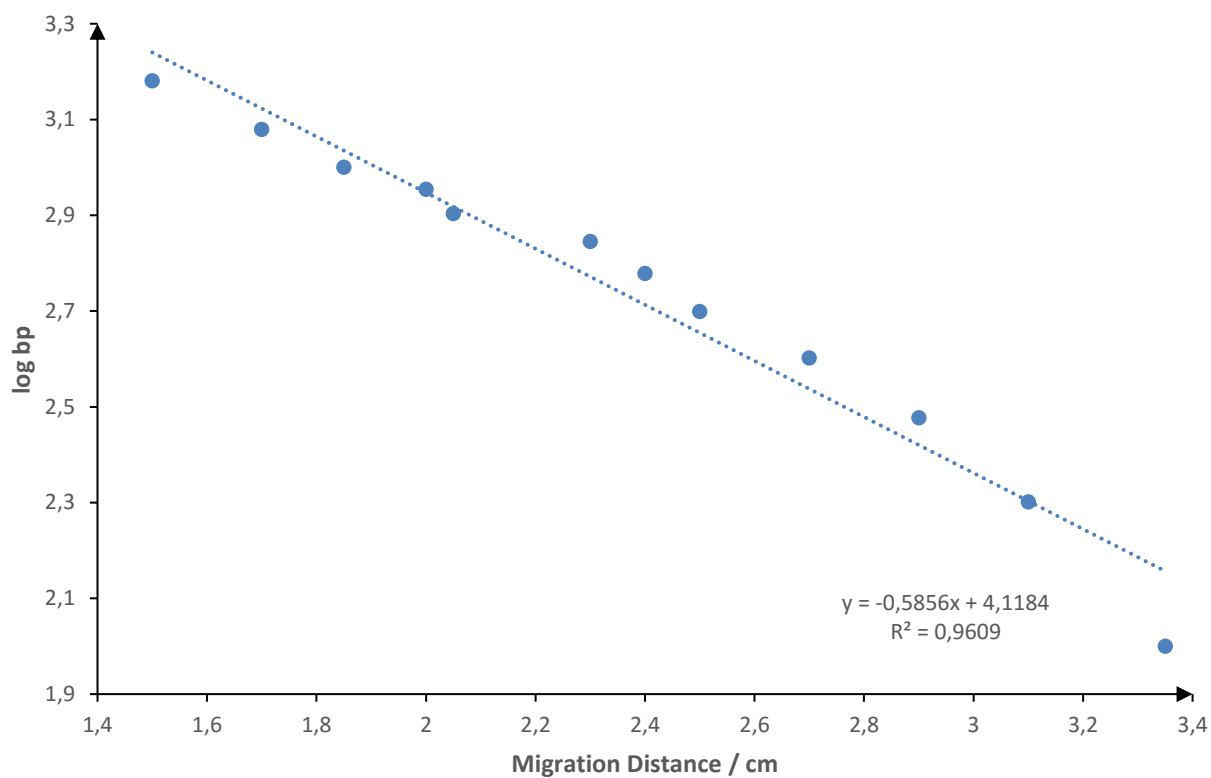


Figure A.2: Standard curve of gel 1, line down.

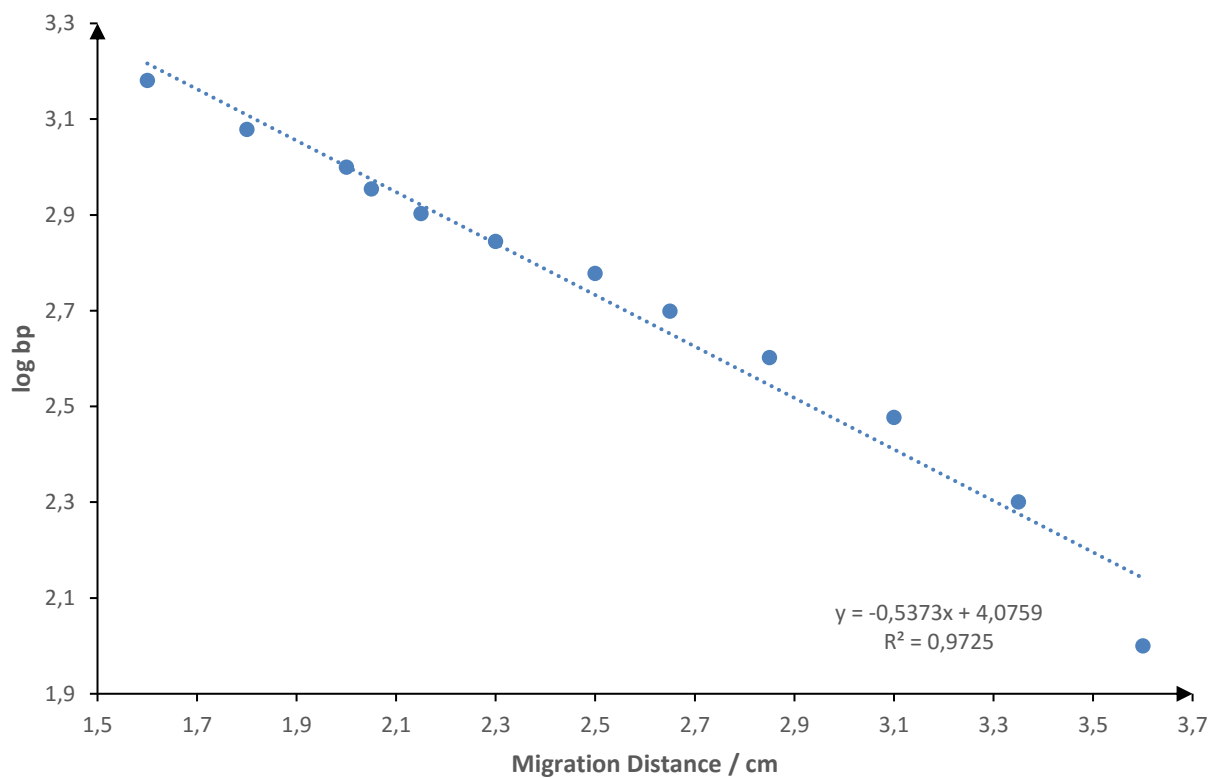


Figure A.3: Standard curve of gel 2, upper line.

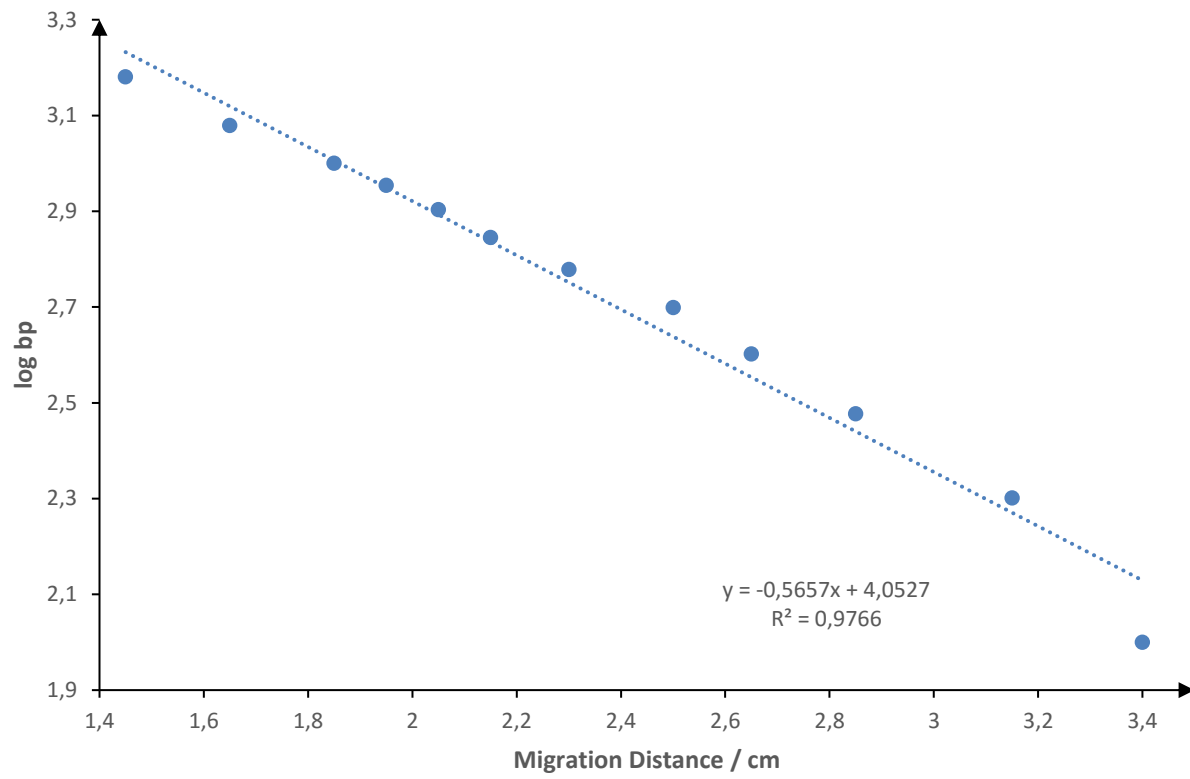
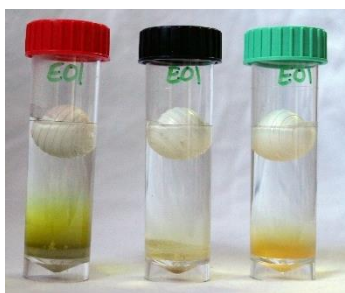


Figure A.4: Standard curve of gel 2, line down.

8.2 Process of BART Test

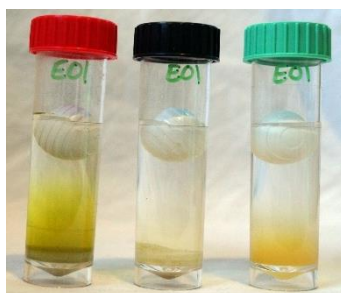


Day 1

IRB: -

SRB: Cloudy Gel-Like

SLYM: Dense Slime, Cloudy Plates layering

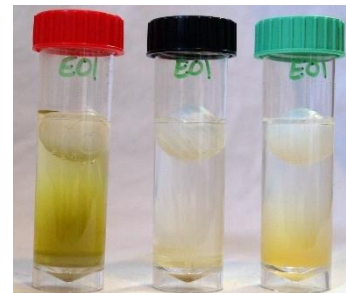


Day 2

IRB: -

SRB: Cloudy Gel-Like

SLYM: Dense Slime, Cloudy Plates layering

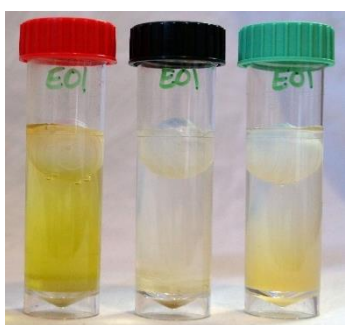


Day 3

IRB: -

SRB: Cloudy Gel-Like

SLYM: Dense Slime, Cloudy Plates layering

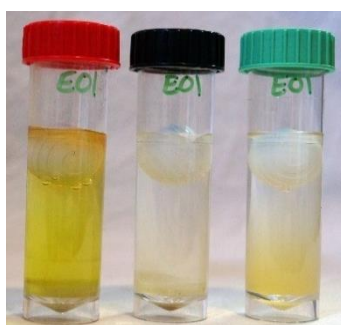


Day 4

IRB: -

SRB: Cloudy Gel-Like

SLYM: Dense Slime, Cloudy Plates layering

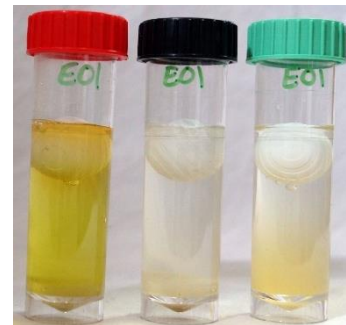


Day 5

IRB: Brown Ring

SRB: Cloudy Gel-Like

SLYM: Dense Slime, Cloudy Plates layering

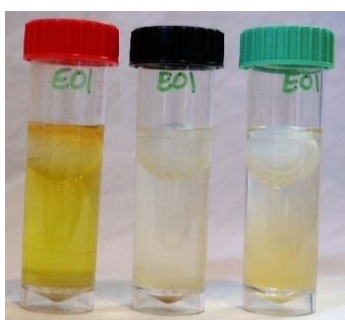


Day 6

IRB: Brown Ring

SRB: Cloudy Gel-Like

SLYM: Dense Slime, Cloudy Plates layering

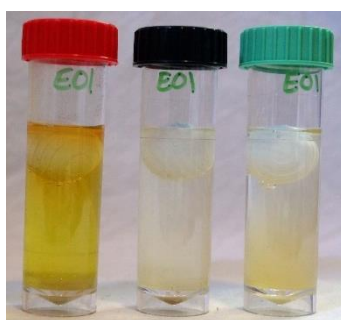


Day 7

IRB: Brown Ring, Foam

SRB: Cloudy Gel-Like

SLYM: Dense Slime, Cloudy Plates layering



Day 8

IRB: Brown Ring, Foam

SRB: Cloudy Gel-Like

SLYM: Dense Slime, Cloudy Plates layering



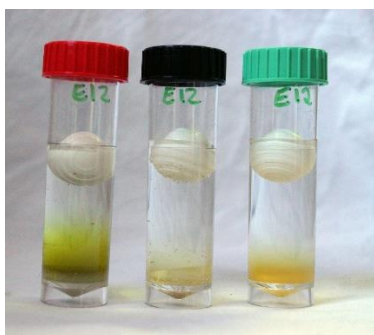
Day 9

IRB: Brown Ring, Foam

SRB: Cloudy Gel-Like

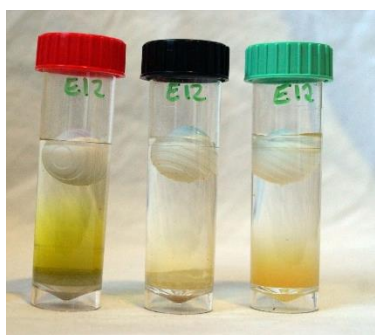
SLYM: Dense Slime, Cloudy Plates layering

Figure A.5: Progress of the BART test of E01.



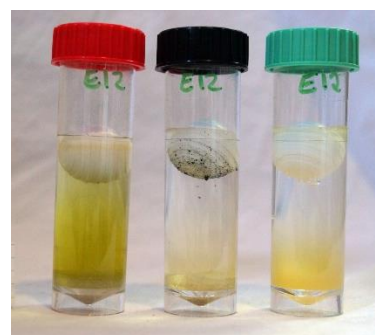
Day 1

IRB: Cloudy
SRB: Cloudy Gel-Like
SLYM: Dense Slime, Cloudy Plates layering



Day 2

IRB: Cloudy
SRB: Cloudy Gel-Like
SLYM: Dense Slime, Cloudy Plates layering



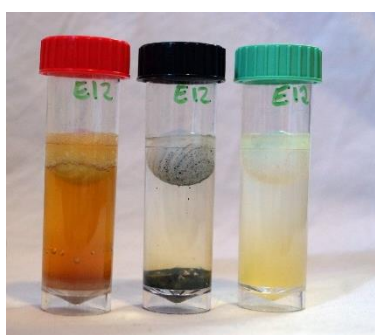
Day 3

IRB: Cloudy
SRB: Cloudy Gel-Like, Black Top
SLYM: Dense Slime, Cloudy Plates layering, Pale Blue Glow



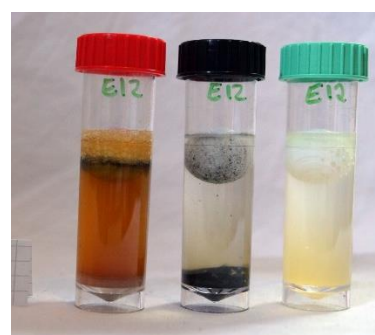
Day 4

IRB: Cloudy, Brown Ring
SRB: Cloudy Gel-Like, Black Top, Black Base
SLYM: Dense Slime, Cloudy Plates layering, Pale Blue Glow



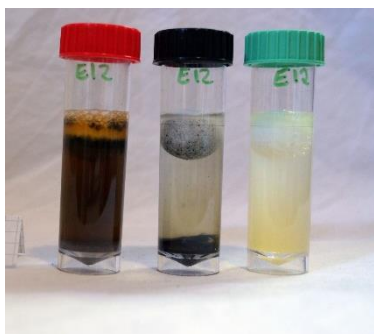
Day 5

IRB: Cloudy, Brown Complete, Foam
SRB: Cloudy Gel-Like, Black Top, Black Base
SLYM: Dense Slime, Cloudy Plates layering, Pale Blue Glow



Day 6

IRB: Cloudy, Brown Complete, Foam
SRB: Cloudy Gel-Like, Black Top, Black Base
SLYM: Dense Slime, Cloudy Plates layering, Pale Blue Glow



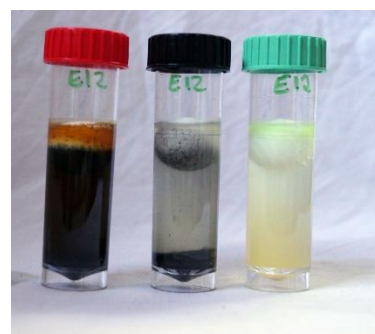
Day 7

IRB: Cloudy, Blackened Liquid, Foam
SRB: Cloudy Gel-Like, Black Top, Black Base
SLYM: Dense Slime, Cloudy Plates layering, Pale Blue Glow



Day 8

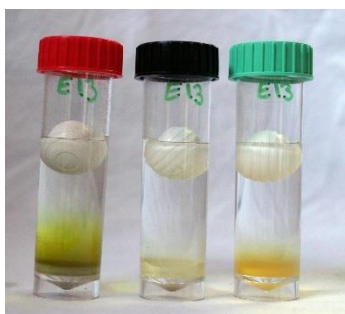
IRB: Cloudy, Blackened Liquid, Foam
SRB: Cloudy Gel-Like, Black Top, Black Base
SLYM: Dense Slime, Cloudy Plates layering, Pale Blue Glow



Day 9

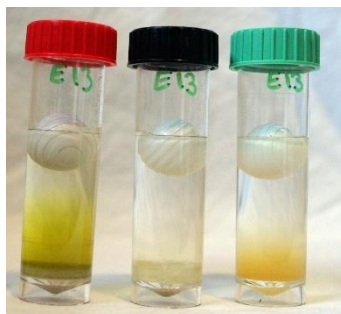
IRB: Cloudy, Blackened Liquid, Foam
SRB: Cloudy Gel-Like, Black Top, Black Base
SLYM: Dense Slime, Cloudy Plates layering, Pale Blue Glow

Figure A.6: Progress of the BART test of E12.



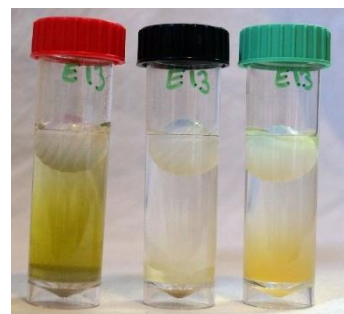
Day 1

IRB: -
SRB: Cloudy Gel-Like
SLYM: Dense Slime, Thread-Like Strings



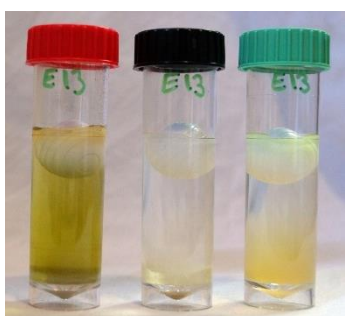
Day 2

IRB: Cloudy
SRB: Cloudy Gel-Like
SLYM: Dense Slime, Thread-Like Strings



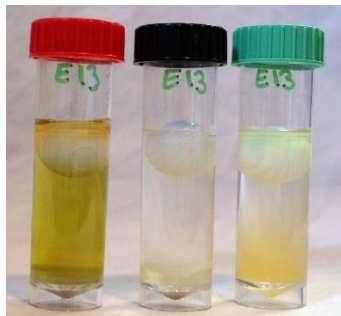
Day 3

IRB: Cloudy
SRB: Cloudy Gel-Like
SLYM: Dense Slime, Thread-Like Strings
Pale Blue Glow



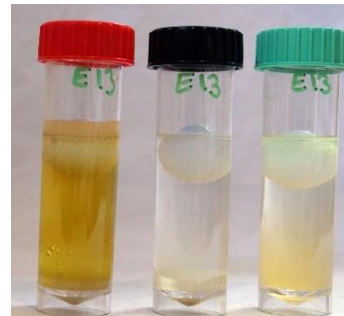
Day 4

IRB: Cloudy, Brown Ring
SRB: Cloudy Gel-Like, Black Top, Black Base
SLYM: Dense Slime, Thread-Like Strings
Pale Blue Glow



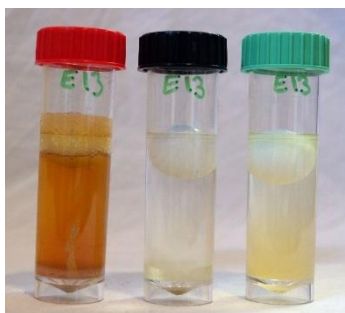
Day 5

IRB: Cloudy, Brown Ring
SRB: Cloudy Gel-Like, Black Top, Black Base
SLYM: Dense Slime, Thread-Like Strings
Pale Blue Glow



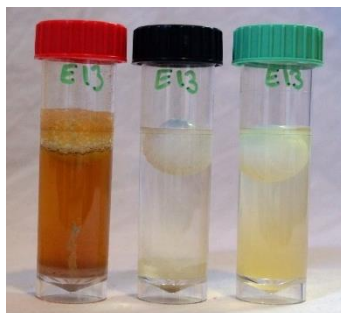
Day 6

IRB: Cloudy, Brown Ring, Foam
SRB: Cloudy Gel-Like, Black Top, Black Base
SLYM: Dense Slime, Thread-Like Strings
Pale Blue Glow



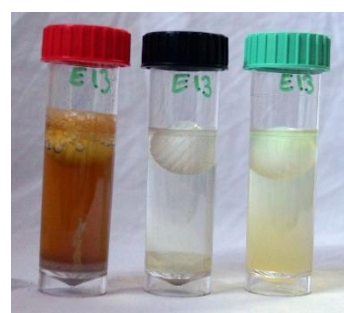
Day 7

IRB: Cloudy, Brown Ring, Foam
SRB: Cloudy Gel-Like, Black Top, Black Base
SLYM: Dense Slime, Thread-Like Strings
Pale Blue Glow



Day 8

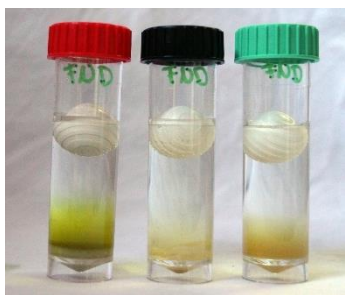
IRB: Cloudy, Brown Ring, Foam
SRB: Cloudy Gel-Like, Black Top, Black Base
SLYM: Dense Slime, Thread-Like Strings
Pale Blue Glow



Day 9

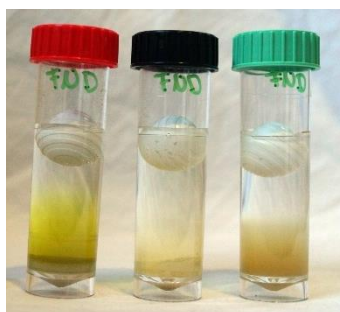
IRB: Cloudy, Brown Ring, Foam
SRB: Cloudy Gel-Like, Black Top, Black Base
SLYM: Dense Slime, Thread-Like Strings
Pale Blue Glow

Figure A.7: Progress of the BART test of E13.



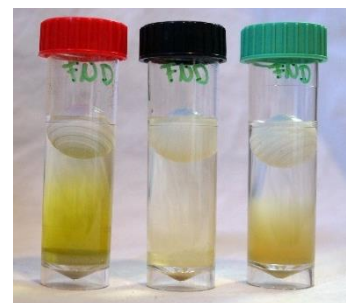
Day 1

IRB: -
SRB: Cloudy Gel-Like
SLYM: Dense Slime, Cloudy Plates layering



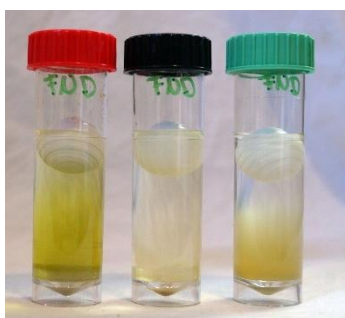
Day 2

IRB: -
SRB: Cloudy Gel-Like
SLYM: Dense Slime, Cloudy Plates layering



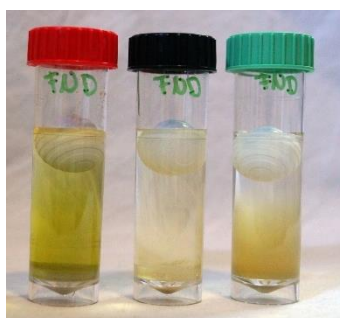
Day 3

IRB: -
SRB: Cloudy Gel-Like
SLYM: Dense Slime, Cloudy Plates layering



Day 4

IRB: -
SRB: Cloudy Gel-Like
SLYM: Dense Slime, Cloudy Plates layering



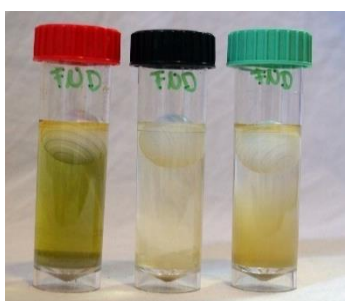
Day 5

IRB: Brown Ring
SRB: Cloudy Gel-Like
SLYM: Dense Slime, Cloudy Plates layering



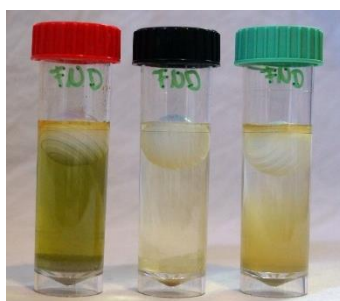
Day 6

IRB: Brown Ring
SRB: Cloudy Gel-Like
SLYM: Dense Slime, Cloudy Plates layering



Day 7

IRB: Brown Ring
SRB: Cloudy Gel-Like
SLYM: Dense Slime, Cloudy Plates layering



Day 8

IRB: Brown Ring
SRB: Cloudy Gel-Like
SLYM: Dense Slime, Cloudy Plates layering



Day 9

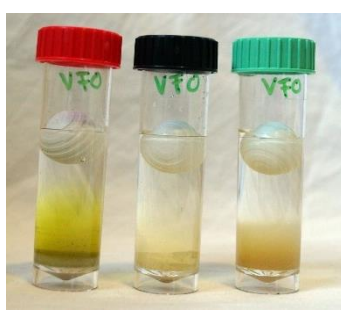
IRB: Brown Ring
SRB: Cloudy Gel-Like
SLYM: Dense Slime, Cloudy Plates layering

Figure A.8: Progress of the BART test of FND.



Day 1

IRB: -
SRB: Cloudy Gel-Like
SLYM: Dense Slime, Cloudy Plates layering



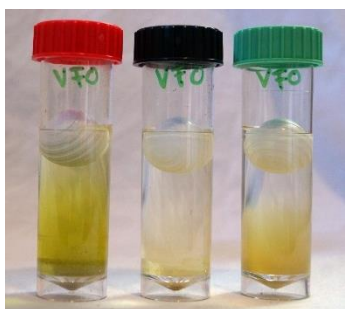
Day 2

IRB: -
SRB: Cloudy Gel-Like
SLYM: Dense Slime, Cloudy Plates layering



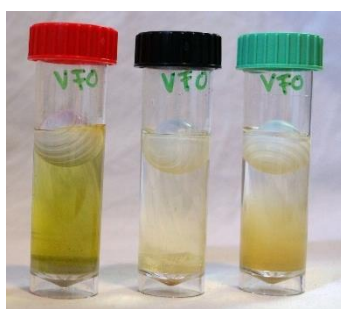
Day 3

IRB: -
SRB: Cloudy Gel-Like
SLYM: Dense Slime, Cloudy Plates layering



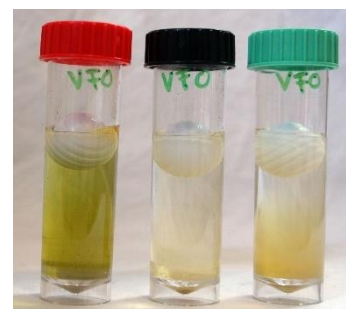
Day 4

IRB: -
SRB: Cloudy Gel-Like
SLYM: Dense Slime, Cloudy Plates layering



Day 5

IRB: Brown Ring
SRB: Cloudy Gel-Like
SLYM: Dense Slime, Cloudy Plates layering



Day 6

IRB: Brown Ring
SRB: Cloudy Gel-Like
SLYM: Dense Slime, Cloudy Plates layering



Day 7

IRB: Brown Ring
SRB: Cloudy Gel-Like
SLYM: Dense Slime, Cloudy Plates layering



Day 8

IRB: Brown Ring
SRB: Cloudy Gel-Like
SLYM: Dense Slime, Cloudy Plates layering



Day 9

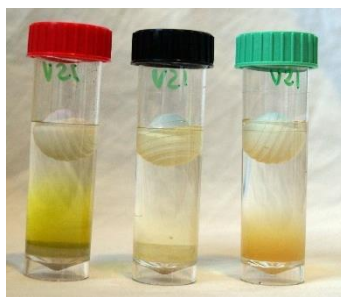
IRB: Brown Ring
SRB: Cloudy Gel-Like
SLYM: Dense Slime, Cloudy Plates layering

Figure A.9: Progress of the BART test of VFO.



Day 1

IRB: Cloudy
SRB: Cloudy Gel-Like
SLYM: Dense Slime, Cloudy Growth



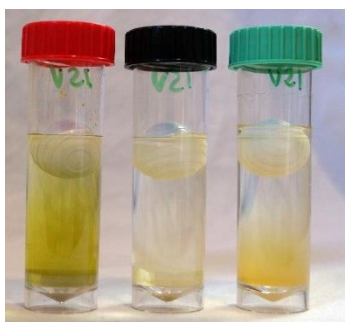
Day 2

IRB: Cloudy
SRB: Cloudy Gel-Like
SLYM: Dense Slime, Cloudy Growth



Day 3

IRB: Cloudy
SRB: Cloudy Gel-Like
SLYM: Dense Slime, Cloudy Growth



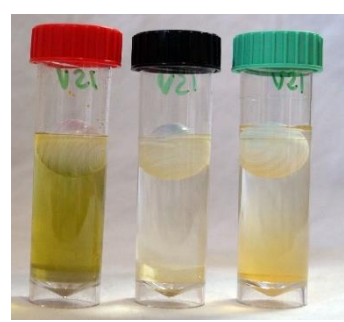
Day 4

IRB: Cloudy, Brown Ring
SRB: Cloudy Gel-Like
SLYM: Dense Slime, Cloudy Growth



Day 5

IRB: Cloudy
SRB: Cloudy Gel-Like
SLYM: Dense Slime, Cloudy Growth



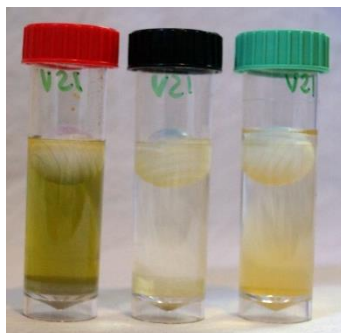
Day 6

IRB: Cloudy, Brown Ring
SRB: Cloudy Gel-Like
SLYM: Dense Slime, Cloudy Growth



Day 7

IRB: Cloudy, Brown Ring
SRB: Cloudy Gel-Like
SLYM: Dense Slime, Cloudy Growth



Day 8

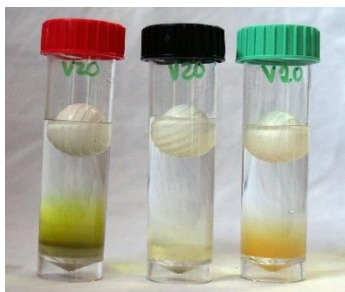
IRB: Cloudy, Brown Ring
SRB: Cloudy Gel-Like
SLYM: Dense Slime, Cloudy Growth



Day 9

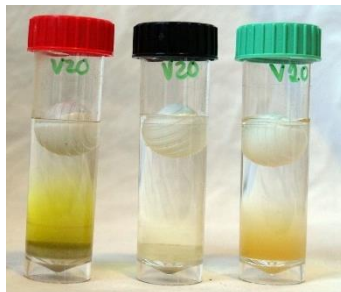
IRB: Cloudy, Brown Ring
SRB: Cloudy Gel-Like
SLYM: Dense Slime, Cloudy Growth

Figure A.10: Progress of the BART test of V21.



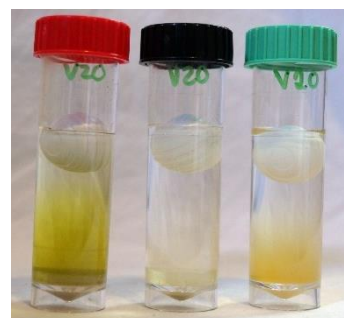
Day 1

IRB: -
SRB: Cloudy Gel-Like
SLYM: Dense Slime, Cloudy Plates layering



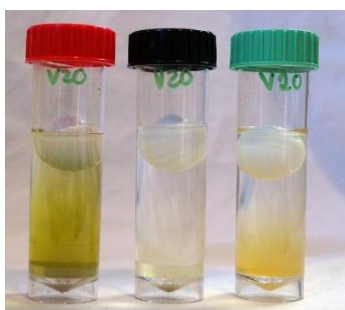
Day 2

IRB: -
SRB: Cloudy Gel-Like
SLYM: Dense Slime, Cloudy Plates layering



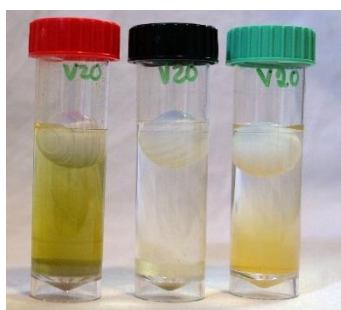
Day 3

IRB: -
SRB: Cloudy Gel-Like
SLYM: Dense Slime, Cloudy Plates layering,



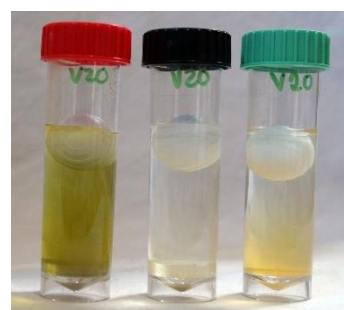
Day 4

IRB: -
SRB: Cloudy Gel-Like
SLYM: Dense Slime, Cloudy Plates layering



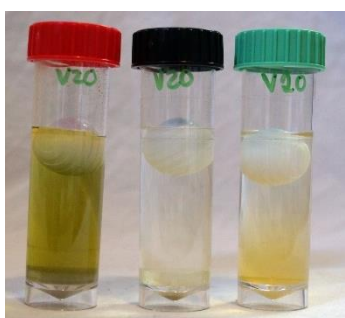
Day 5

IRB: -
SRB: Cloudy Gel-Like
SLYM: Dense Slime, Cloudy Plates layering



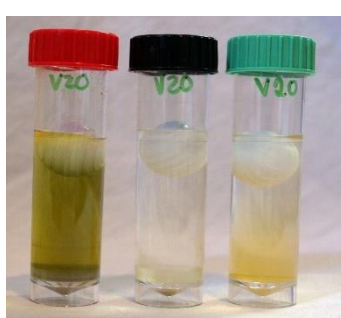
Day 6

IRB: -
SRB: Cloudy Gel-Like
SLYM: Dense Slime, Cloudy Plates layering,



Day 7

IRB: -
SRB: Cloudy Gel-Like
SLYM: Dense Slime, Cloudy Plates layering



Day 8

IRB: -
SRB: Cloudy Gel-Like
SLYM: Dense Slime, Cloudy Plates layering



Day 9

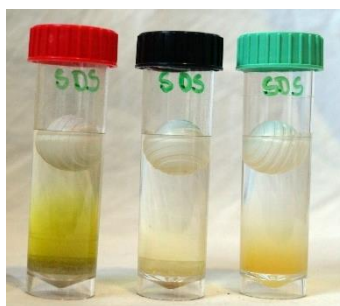
IRB: -
SRB: Cloudy Gel-Like
SLYM: Dense Slime, Cloudy Plates layering

Figure A.11: Progress of the BART test of V20.



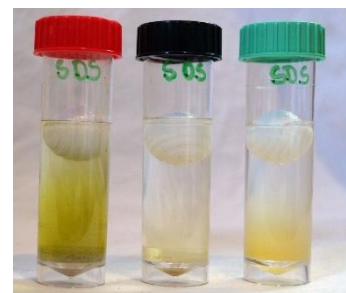
Day 1

IRB: -
SRB: Cloudy Gel-Like
SLYM: Dense Slime, Cloudy Plates layering



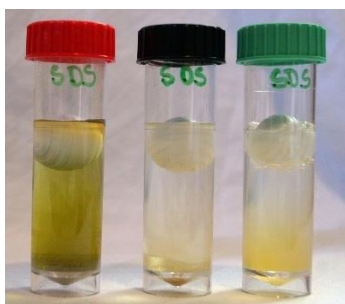
Day 2

IRB: -
SRB: Cloudy Gel-Like
SLYM: Dense Slime, Cloudy Plates layering



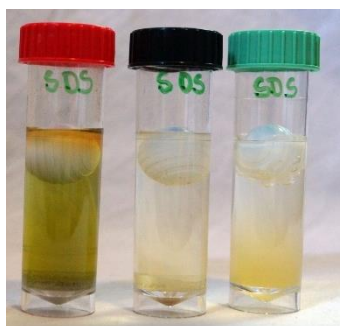
Day 3

IRB: -
SRB: Cloudy Gel-Like
SLYM: Dense Slime, Cloudy Plates layering



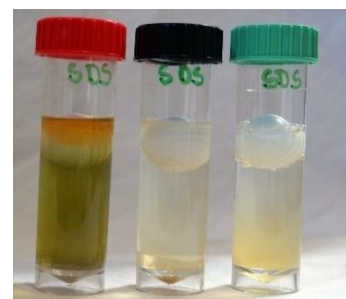
Day 4

IRB: Brown Ring
SRB: Cloudy Gel-Like
SLYM: Dense Slime, Cloudy Plates layering



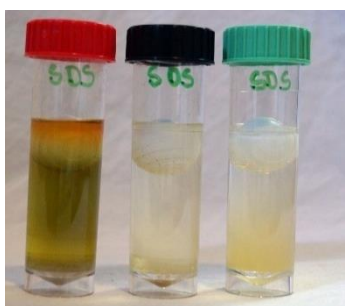
Day 5

IRB: Brown Ring
SRB: Cloudy Gel-Like
SLYM: Dense Slime, Cloudy Plates layering



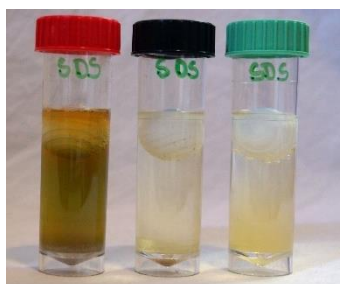
Day 6

IRB: Brown Ring
SRB: Cloudy Gel-Like
SLYM: Dense Slime, Cloudy Plates layering



Day 7

IRB: Brown Ring
SRB: Cloudy Gel-Like
SLYM: Dense Slime, Cloudy Plates layering



Day 8

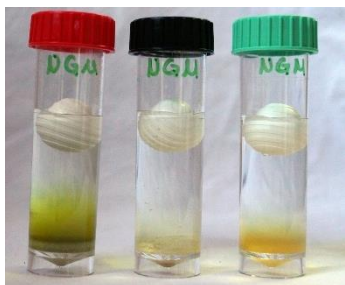
IRB: Brown Ring, Foam
SRB: Cloudy Gel-Like
SLYM: Dense Slime, Cloudy Plates layering



Day 9

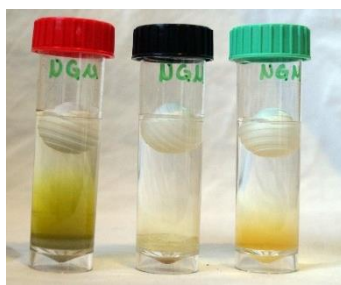
IRB: Brown Complete, Foam
SRB: Cloudy Gel-Like
SLYM: Dense Slime, Cloudy Plates layering,

Figure A.12: Progress of the BART test of SDS.



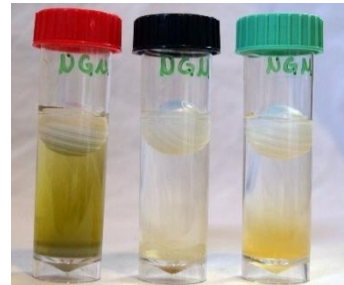
Day 1

IRB: Cloudy
SRB: Cloudy Gel-Like
SLYM: Dense Slime, Cloudy Plates layering



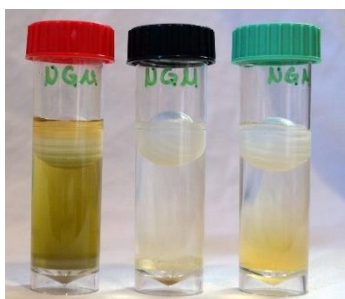
Day 2

IRB: Cloudy
SRB: Cloudy Gel-Like
SLYM: Dense Slime, Cloudy Plates layering



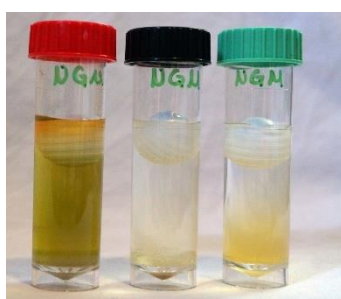
Day 3

IRB: Cloudy
SRB: Cloudy Gel-Like, Black Top
SLYM: Dense Slime, Cloudy Plates layering



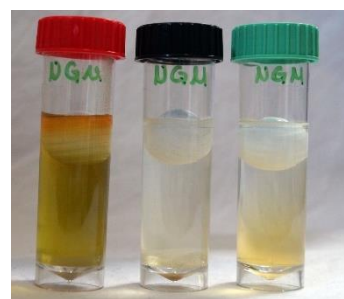
Day 4

IRB: Cloudy, Brown Ring
SRB: Cloudy Gel-Like, Black Top, Black Base
SLYM: Dense Slime, Cloudy Plates layering



Day 5

IRB: Cloudy, Brown Ring
SRB: Cloudy Gel-Like, Black Top, Black Base
SLYM: Dense Slime, Cloudy Plates layering



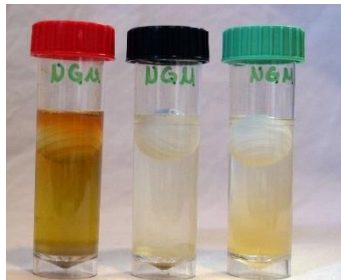
Day 6

IRB: Cloudy, Brown Ring
SRB: Cloudy Gel-Like, Black Top, Black Base
SLYM: Dense Slime, Cloudy Plates layering



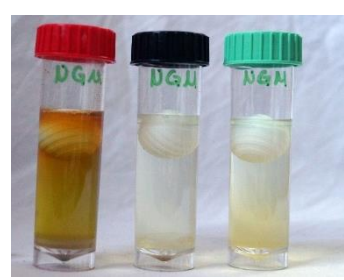
Day 7

IRB: Cloudy, Brown Ring
SRB: Cloudy Gel-Like, Black Top, Black Base
SLYM: Dense Slime, Cloudy Plates layering, Pale Blue Glow



Day 8

IRB: Cloudy, Brown Ring
SRB: Cloudy Gel-Like, Black Top, Black Base
SLYM: Dense Slime, Cloudy Plates layering, Pale Blue Glow



Day 9

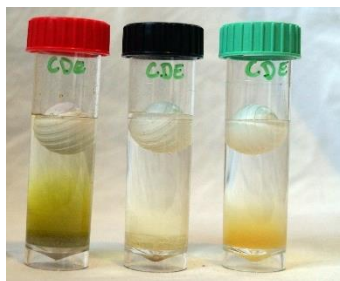
IRB: Cloudy, Brown Complete
SRB: Cloudy Gel-Like, Black Top, Black Base
SLYM: Dense Slime, Cloudy Plates layering, Pale Blue Glow

Figure A.13: Progress of the BART test of NGM.



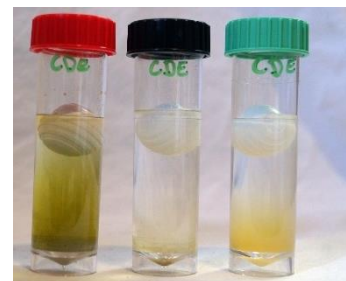
Day 1

IRB: -
SRB: Cloudy Gel-Like
SLYM: Dense Slime, Cloudy Growth



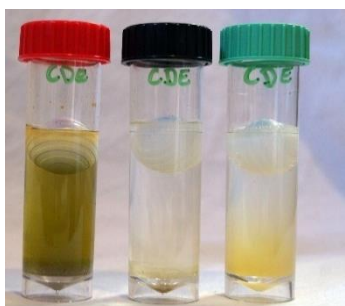
Day 2

IRB: -
SRB: Cloudy Gel-Like
SLYM: Dense Slime, Cloudy Growth



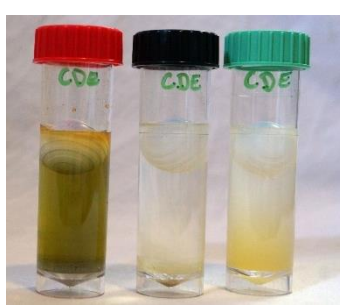
Day 3

IRB: -
SRB: Cloudy Gel-Like
SLYM: Dense Slime, Cloudy Growth



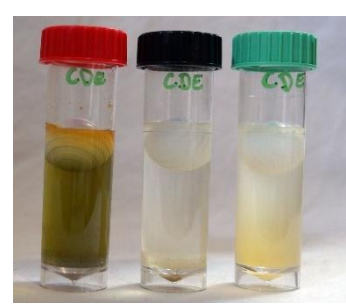
Day 4

IRB: Brown Ring
SRB: Cloudy Gel-Like
SLYM: Dense Slime, Cloudy Growth



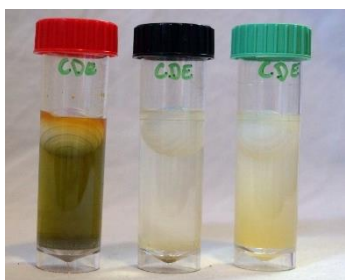
Day 5

IRB: Brown Ring
SRB: Cloudy Gel-Like
SLYM: Dense Slime, Cloudy Growth



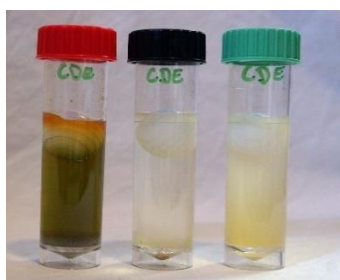
Day 6

IRB: Brown Ring
SRB: Cloudy Gel-Like
SLYM: Dense Slime, Cloudy Growth



Day 7

IRB: Brown Ring
SRB: Cloudy Gel-Like
SLYM: Dense Slime, Cloudy Growth



Day 8

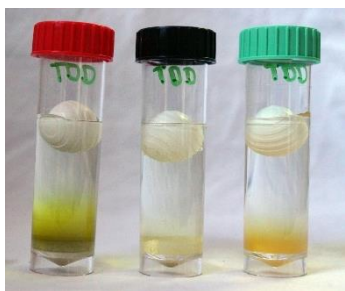
IRB: Brown Ring
SRB: Cloudy Gel-Like
SLYM: Dense Slime, Cloudy Growth



Day 9

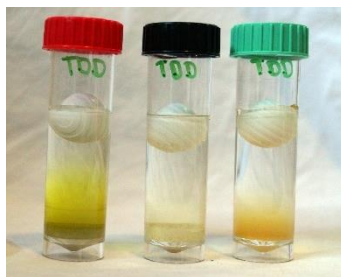
IRB: Brown Ring, Foam
SRB: Cloudy Gel-Like
SLYM: Dense Slime, Cloudy Growth

Figure A.14: Progress of the BART test of CDE.



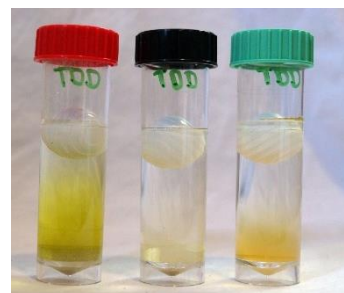
Day 1

IRB: -
SRB: Cloudy Gel-Like
SLYM: Dense Slime, Cloudy Growth



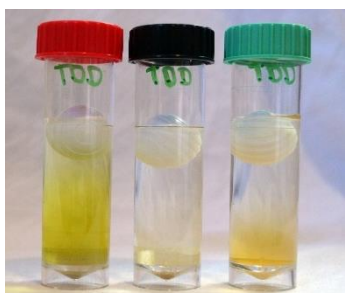
Day 2

IRB: -
SRB: Cloudy Gel-Like
SLYM: Dense Slime, Cloudy Growth



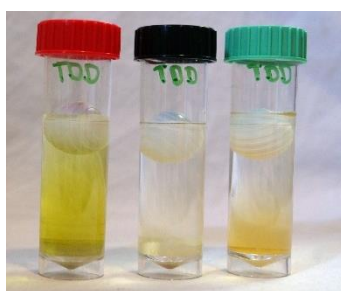
Day 3

IRB: -
SRB: Cloudy Gel-Like
SLYM: Dense Slime, Cloudy Growth



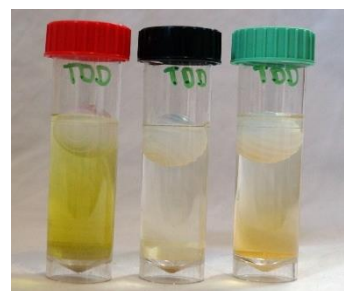
Day 4

IRB: -
SRB: Cloudy Gel-Like
SLYM: Dense Slime, Cloudy Growth



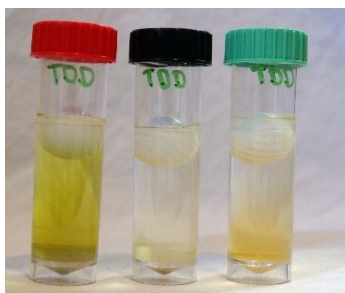
Day 5

IRB: -
SRB: Cloudy Gel-Like
SLYM: Dense Slime, Cloudy Growth



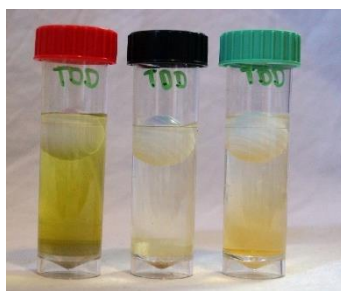
Day 6

IRB: -
SRB: Cloudy Gel-Like
SLYM: Dense Slime, Cloudy Growth



Day 7

IRB: -
SRB: Cloudy Gel-Like
SLYM: Dense Slime, Cloudy Growth



Day 8

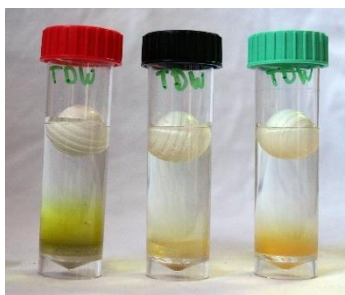
IRB: -
SRB: Cloudy Gel-Like
SLYM: Dense Slime, Cloudy Growth



Day 9

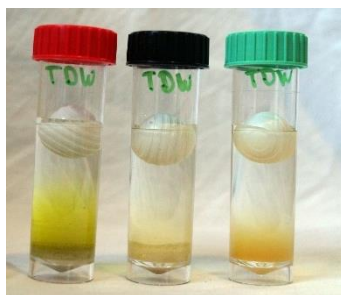
IRB: -
SRB: Cloudy Gel-Like
SLYM: Dense Slime, Cloudy Growth

Figure A.15: Progress of the BART test of TDD.



Day 1

IRB: -
SRB: Cloudy Gel-Like
SLYM: Dense Slime, Cloudy Plates layering



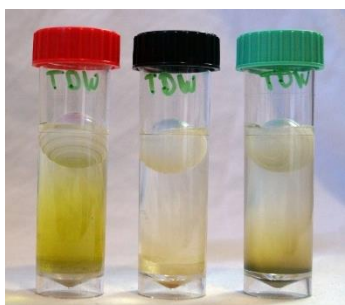
Day 2

IRB: -
SRB: Cloudy Gel-Like
SLYM: Dense Slime, Cloudy Plates layering



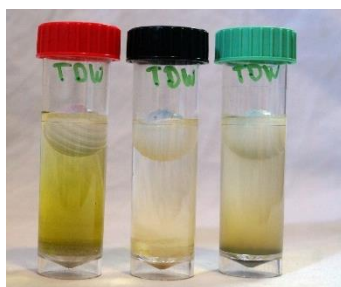
Day 3

IRB: -
SRB: Cloudy Gel-Like
SLYM: Dense Slime, Cloudy Plates layering



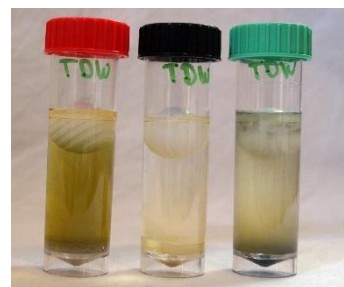
Day 4

IRB: -
SRB: Cloudy Gel-Like
SLYM: Dense Slime, Cloudy Plates layering



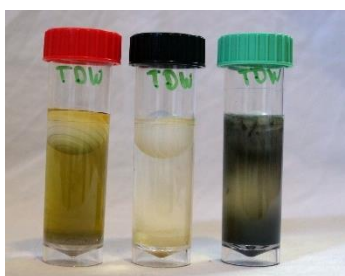
Day 5

IRB: -
SRB: Cloudy Gel-Like
SLYM: Dense Slime, Cloudy Plates layering



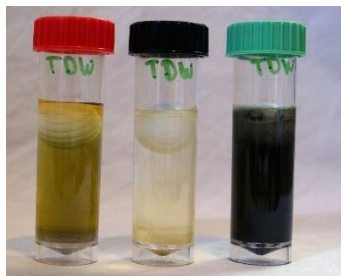
Day 6

IRB: -
SRB: Cloudy Gel-Lik
SLYM: Dense Slime, Cloudy Plates layering



Day 7

IRB: -
SRB: Cloudy Gel-Like
SLYM: Dense Slime, Cloudy Plates layering



Day 8

IRB: -
SRB: Cloudy Gel-Like
SLYM: Dense Slime, Cloudy Plates layering



Day 9

IRB: -
SRB: Cloudy Gel-Like
SLYM: Dense Slime, Cloudy Plates layering

Figure A.16: Progress of the BART test of TDW.



Day 1

IRB: Cloudy
SRB: Cloudy Gel-Like
SLYM: Dense Slime, Cloudy Plates layering



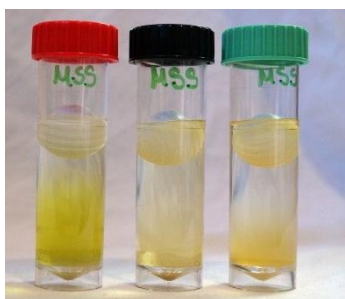
Day 2

IRB: Cloudy
SRB: Cloudy Gel-Like
SLYM: Dense Slime, Cloudy Plates layering



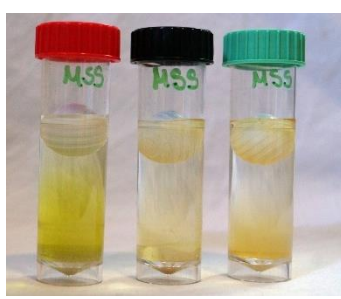
Day 3

IRB: Cloudy
SRB: Cloudy Gel-Like
SLYM: Dense Slime, Cloudy Plates layering



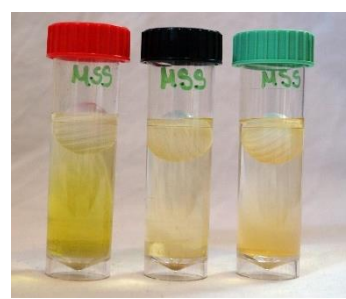
Day 4

IRB: Cloudy
SRB: Cloudy Gel-Like
SLYM: Dense Slime, Cloudy Plates layering



Day 5

IRB: Cloudy
SRB: Cloudy Gel-Like
SLYM: Dense Slime, Cloudy Plates layering



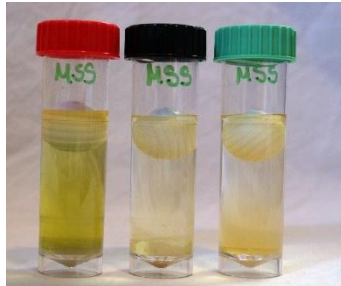
Day 6

IRB: Cloudy
SRB: Cloudy Gel-Like
SLYM: Dense Slime, Cloudy Plates layering



Day 7

IRB: Cloudy
SRB: Cloudy Gel-Like
SLYM: Dense Slime, Cloudy Plates layering



Day 8

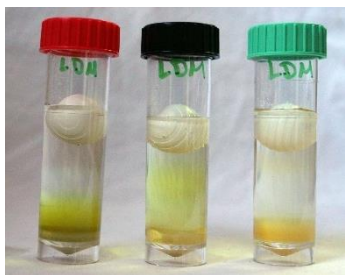
IRB: Cloudy
SRB: Cloudy Gel-Like
SLYM: Dense Slime, Cloudy Plates layering



Day 9

IRB: Cloudy
SRB: Cloudy Gel-Like
SLYM: Dense Slime, Cloudy Plates layering

Figure A.17: Progress of the BART test of MSS.



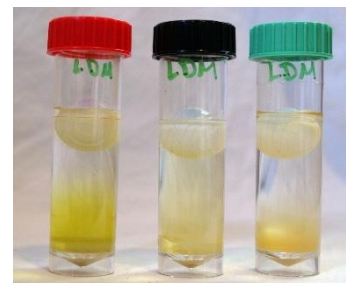
Day 1

IRB: Cloudy
SRB: Cloudy Gel-Like
SLYM: Dense Slime, Cloudy Plates layering



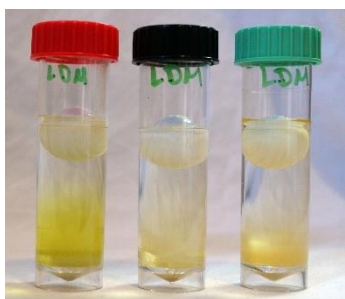
Day 2

IRB: Cloudy
SRB: Cloudy Gel-Like
SLYM: Dense Slime, Cloudy Plates layering



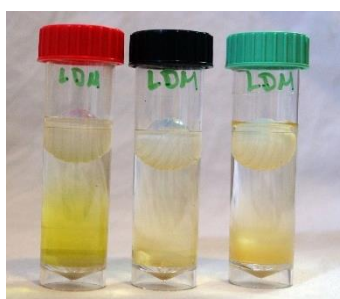
Day 3

IRB: Cloudy
SRB: Cloudy Gel-Like
SLYM: Dense Slime, Cloudy Plates layering



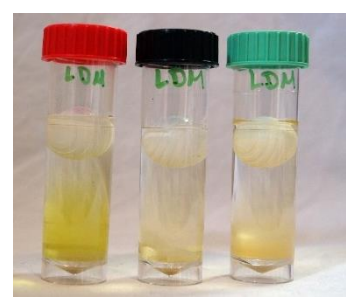
Day 4

IRB: Cloudy
SRB: Cloudy Gel-Like
SLYM: Dense Slime, Cloudy Plates layering



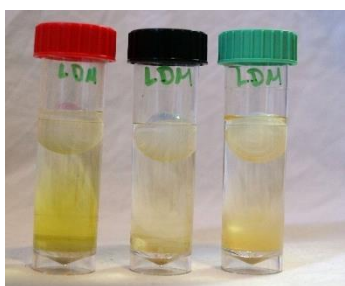
Day 5

IRB: Cloudy
SRB: Cloudy Gel-Like
SLYM: Dense Slime, Cloudy Plates layering



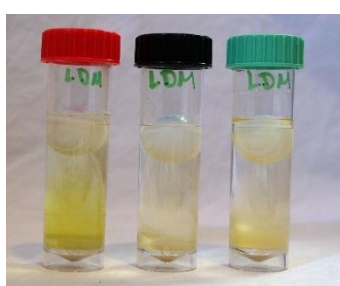
Day 6

IRB: Cloudy
SRB: Cloudy Gel-Like
SLYM: Dense Slime, Cloudy Plates layering



Day 7

IRB: Cloudy
SRB: Cloudy Gel-Like
SLYM: Dense Slime, Cloudy Plates layering



Day 8

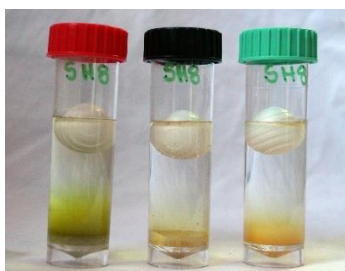
IRB: Cloudy
SRB: Cloudy Gel-Like
SLYM: Dense Slime, Cloudy Plates layering



Day 9

IRB: Cloudy
SRB: Cloudy Gel-Like
SLYM: Dense Slime, Cloudy Plates layering

Figure A.18: Progress of the BART test of LDM.

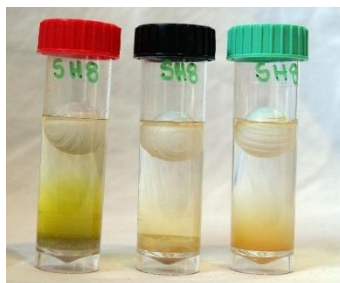


Day 1

IRB: -

SRB: Cloudy Gel-Like

SLYM: Dense Slime, Cloudy Growth, Slime Ring

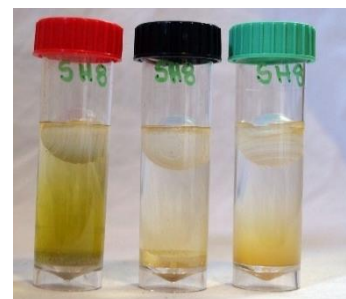


Day 2

IRB: -

SRB: Cloudy Gel-Like

SLYM: Dense Slime, Cloudy Growth, Slime Ring

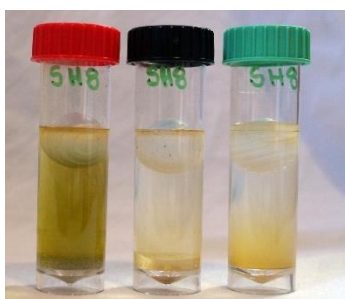


Day 3

IRB: -

SRB: Cloudy Gel-Like

SLYM: Dense Slime, Cloudy Growth, Slime Ring

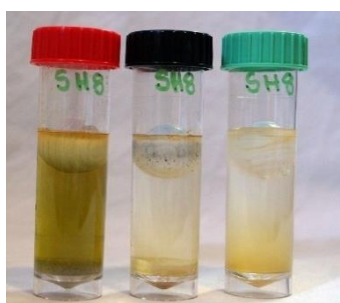


Day 4

IRB: Brown Ring

SRB: Cloudy Gel-Like

SLYM: Dense Slime, Cloudy Growth, Slime Ring



Day 5

IRB: Brown Ring

SRB: Cloudy Gel-Like, Black Top

SLYM: Dense Slime, Cloudy Growth, Slime Ring



Day 6

IRB: Brown Ring

SRB: Cloudy Gel-Like, Black Top

SLYM: Dense Slime, Cloudy Growth, Slime Ring

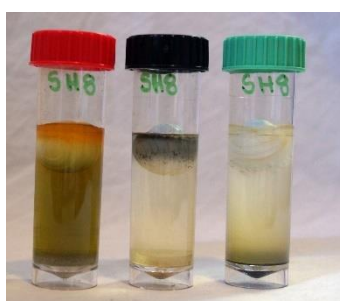


Day 7

IRB: Brown Ring

SRB: Cloudy Gel-Like, Black Top

SLYM: Dense Slime, Cloudy Growth, Slime Ring



Day 8

IRB: Brown Ring

SRB: Cloudy Gel-Like, Black Top

SLYM: Dense Slime, Cloudy Growth, Slime Ring



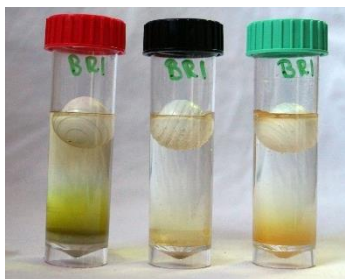
Day 9

IRB: Brown Ring

SRB: Cloudy Gel-Like, Black Top

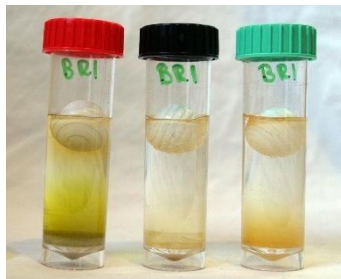
SLYM: Dense Slime, Cloudy Growth, Slime Ring

Figure A.19: Progress of the BART test of SH8.



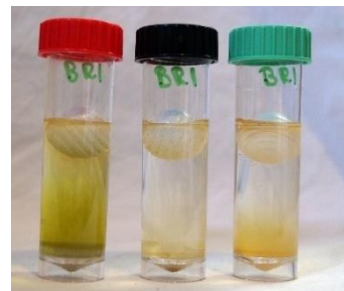
Day 1

IRB: Cloudy
SRB: Cloudy Gel-Like
SLYM: Dense Slime, Cloudy Growth, Slime Ring



Day 2

IRB: Cloudy
SRB: Cloudy Gel-Like
SLYM: Dense Slime, Cloudy Growth, Slime Ring



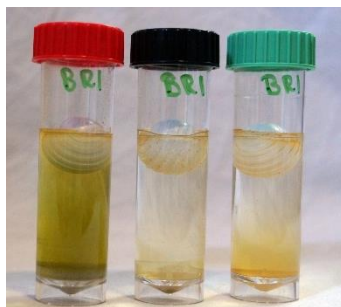
Day 3

IRB: Cloudy, Brown Ring
SRB: Cloudy Gel-Like
SLYM: Dense Slime, Cloudy Growth, Slime Ring



Day 4

IRB: Cloudy, Brown Ring
SRB: Cloudy Gel-Like
SLYM: Dense Slime, Cloudy Growth, Slime Ring



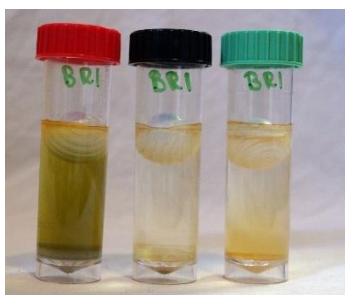
Day 5

IRB: Cloudy, Brown Ring
SRB: Cloudy Gel-Like
SLYM: Dense Slime, Cloudy Growth, Slime Ring



Day 6

IRB: Cloudy, Brown Ring
SRB: Cloudy Gel-Like
SLYM: Dense Slime, Cloudy Growth, Slime Ring



Day 7

IRB: Cloudy, Brown Ring
SRB: Cloudy Gel-Like
SLYM: Dense Slime, Cloudy Growth, Slime Ring



Day 8

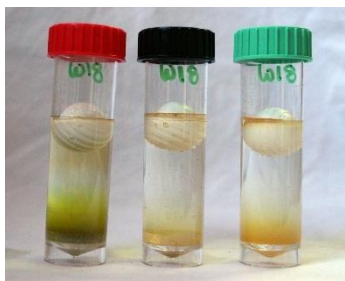
IRB: Cloudy, Brown Ring
SRB: Cloudy Gel-Like
SLYM: Dense Slime, Cloudy Growth, Slime Ring



Day 9

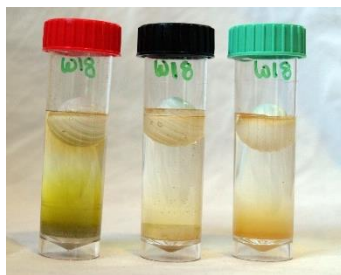
IRB: Cloudy, Brown Ring, Foam
SRB: Cloudy Gel-Like
SLYM: Dense Slime, Cloudy Growth, Slime Ring

Figure A.20: Progress of the BART test of BRI.



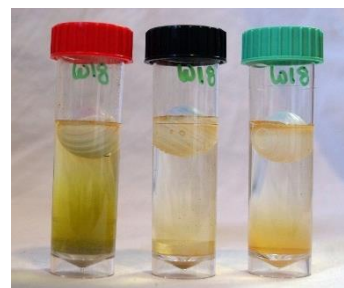
Day 1

IRB: Cloudy
SRB: Cloudy Gel-Like
SLYM: Dense Slime, Cloudy Growth, Slime Ring



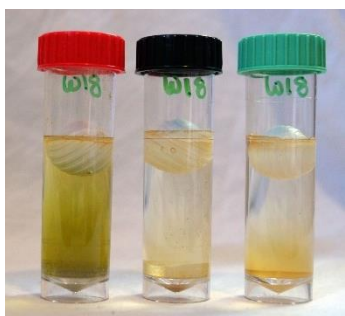
Day 2

IRB: Cloudy
SRB: Cloudy Gel-Like
SLYM: Dense Slime, Cloudy Growth, Slime Ring



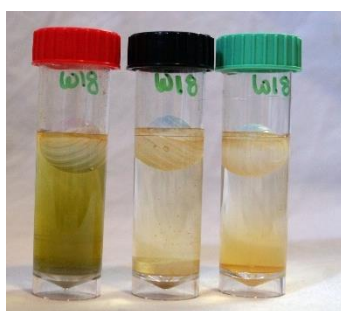
Day 3

IRB: Cloudy, Brown Ring
SRB: Cloudy Gel-Like
SLYM: Dense Slime, Cloudy Growth, Slime Ring



Day 4

IRB: Cloudy, Brown Ring
SRB: Cloudy Gel-Like
SLYM: Dense Slime, Cloudy Growth, Slime Ring



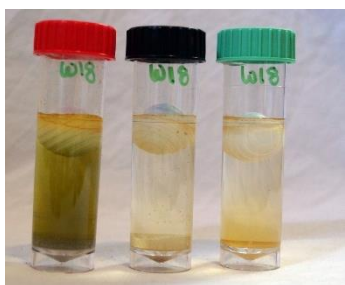
Day 5

IRB: Cloudy, Brown Ring
SRB: Cloudy Gel-Like
SLYM: Dense Slime, Cloudy Growth, Slime Ring



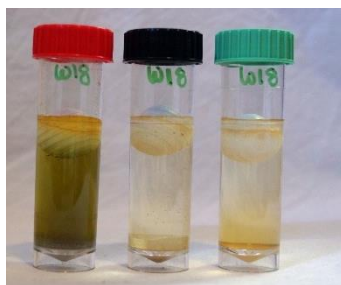
Day 6

IRB: Cloudy, Brown Ring
SRB: Cloudy Gel-Like
SLYM: Dense Slime, Cloudy Growth, Slime Ring



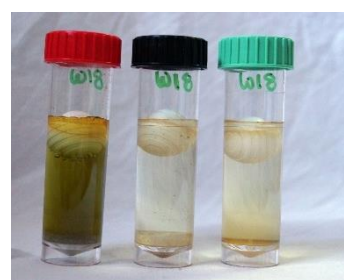
Day 7

IRB: Cloudy, Brown Ring
SRB: Cloudy Gel-Like
SLYM: Dense Slime, Cloudy Growth, Slime Ring



Day 8

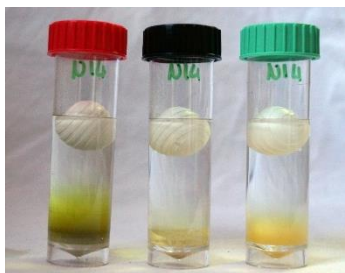
IRB: Cloudy, Brown Ring
SRB: Cloudy Gel-Like
SLYM: Dense Slime, Cloudy Growth, Slime Ring



Day 9

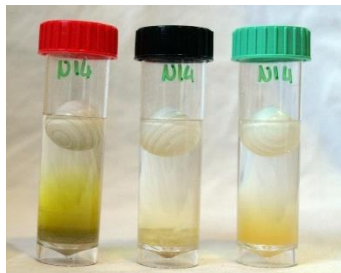
IRB: Cloudy, Brown Ring
SRB: Cloudy Gel-Like
SLYM: Dense Slime, Cloudy Growth, Slime Ring

Figure A.21: Progress of the BART test of W18.



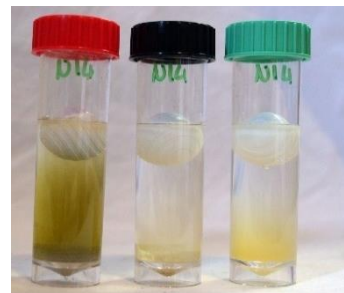
Day 1

IRB: Cloudy
SRB: Cloudy Gel-Like
SLYM: Dense Slime, Cloudy Growth



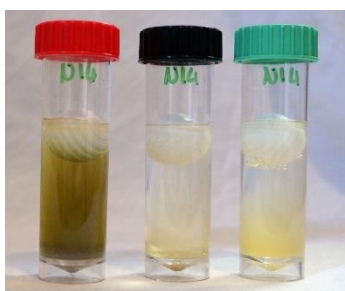
Day 2

IRB: Cloudy
SRB: Cloudy Gel-Like
SLYM: Dense Slime, Cloudy Growth, Pale Blue Glow



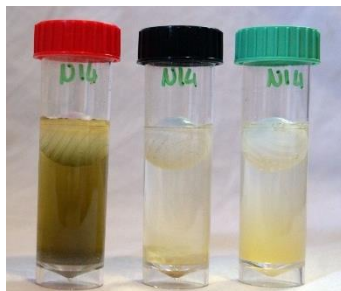
Day 3

IRB: Cloudy
SRB: Cloudy Gel-Like
SLYM: Dense Slime, Cloudy Growth, Pale Blue Glow



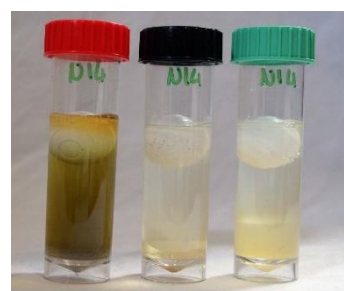
Day 4

IRB: Cloudy
SRB: Cloudy Gel-Like
SLYM: Dense Slime, Cloudy Growth, Pale Blue Glow



Day 5

IRB: Cloudy
SRB: Cloudy Gel-Like
SLYM: Dense Slime, Cloudy Growth, Pale Blue Glow



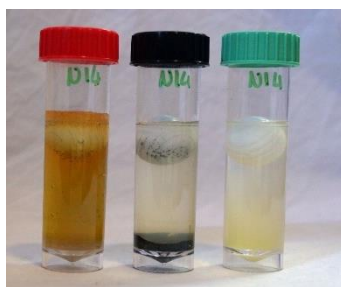
Day 6

IRB: Cloudy
SRB: Cloudy Gel-Like
SLYM: Dense Slime, Cloudy Growth, Pale Blue Glow



Day 7

IRB: Cloudy
SRB: Cloudy Gel-Like, Black Top
SLYM: Dense Slime, Cloudy Growth, Pale Blue Glow



Day 8

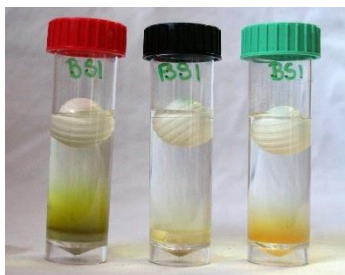
IRB: Cloudy, Brown Complete, Foam
SRB: Cloudy Gel-Like, Black Top, Black Base
SLYM: Dense Slime, Cloudy Growth, Pale Blue Glow



Day 9

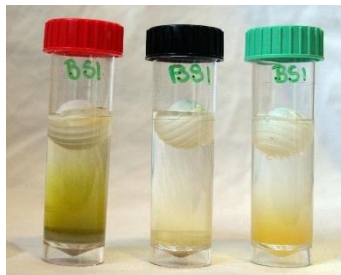
IRB: Cloudy, Brown Complete, Foam
SRB: Cloudy Gel-Like, Black Top, Black Base
SLYM: Dense Slime, Cloudy Growth, Pale Blue Glow

Figure A.22: Progress of the BART test of N14.



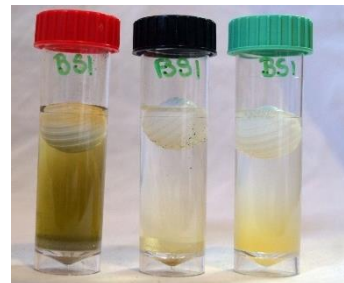
Day 1

IRB: Cloudy
SRB: Cloudy Gel-Like
SLYM: Dense Slime, Cloudy Plates layering



Day 2

IRB: Cloudy
SRB: Cloudy Gel-Like
SLYM: Dense Slime, Cloudy Plates layering



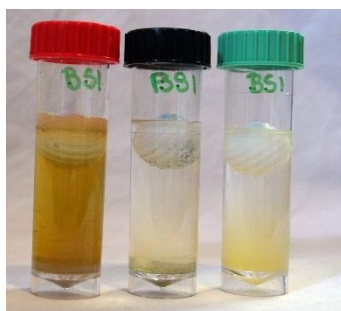
Day 3

IRB: Cloudy, Brown Ring
SRB: Cloudy Gel-Like, Black Top
SLYM: Dense Slime, Cloudy Plates layering



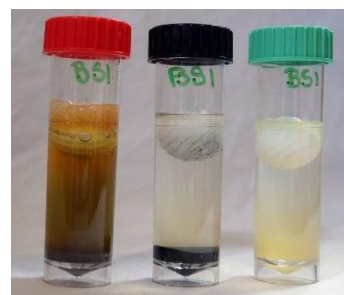
Day 4

IRB: Cloudy, Brown Ring
SRB: Cloudy Gel-Like, Black Top
SLYM: Dense Slime, Cloudy Plates layering



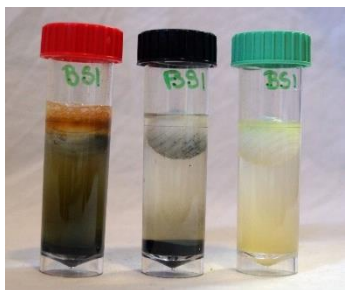
Day 5

IRB: Cloudy, Brown Complete, Foam
SRB: Cloudy Gel-Like, Black Top, Black Base
SLYM: Dense Slime, Cloudy Plates layering



Day 6

IRB: Cloudy, Brown Complete, Foam
SRB: Cloudy Gel-Like, Black Top, Black Base
SLYM: Dense Slime, Cloudy Plates layering



Day 7

IRB: Cloudy, Blackened Liquid, Foam
SRB: Cloudy Gel-Like, Black Top, Black Base
SLYM: Dense Slime, Cloudy Plates layering



Day 8

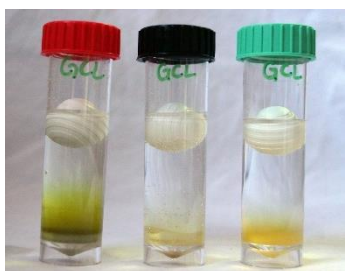
IRB: Cloudy, Blackened Liquid, Foam
SRB: Cloudy Gel-Like, Black Top, Black Base
SLYM: Dense Slime, Cloudy Plates layering



Day 9

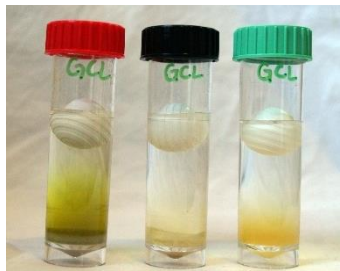
IRB: Cloudy, Blackened Liquid, Foam
SRB: Cloudy Gel-Like, Black Top, Black Base
SLYM: Dense Slime, Cloudy Plates layering

Figure A.23: Progress of the BART test of BS1.



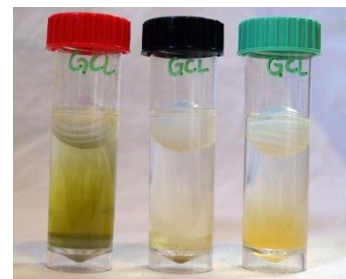
Day 1

IRB: Cloudy
SRB: Cloudy Gel-Like
SLYM: Dense Slime, Thread-Like Strings



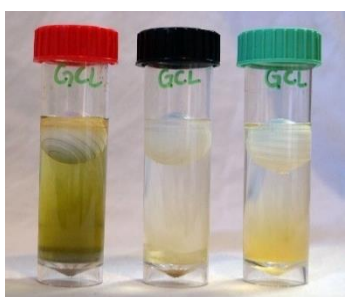
Day 2

IRB: Cloudy
SRB: Cloudy Gel-Like
SLYM: Dense Slime, Thread-Like Strings, Pale Blue Glow



Day 3

IRB: Cloudy
SRB: Cloudy Gel-Like
SLYM: Dense Slime, Thread-Like Strings, Pale Blue Glow



Day 4

IRB: Cloudy, Brown Ring
SRB: Cloudy Gel-Like
SLYM: Dense Slime, Thread-Like Strings, Pale Blue Glow



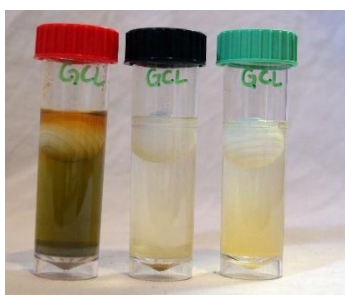
Day 5

IRB: Cloudy, Brown Ring
SRB: Cloudy Gel-Like
SLYM: Dense Slime, Thread-Like Strings, Pale Blue Glow



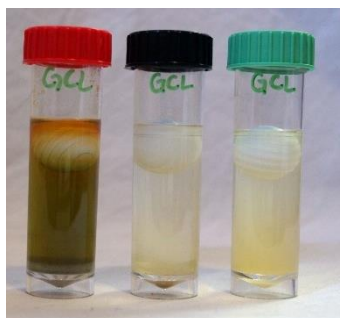
Day 6

IRB: Cloudy, Brown Ring
SRB: Cloudy Gel-Like
SLYM: Dense Slime, Thread-Like Strings, Pale Blue Glow



Day 7

IRB: Cloudy, Brown Ring
SRB: Cloudy Gel-Like
SLYM: Dense Slime, Thread-Like Strings, Pale Blue Glow



Day 8

IRB: Cloudy, Brown Ring
SRB: Cloudy Gel-Like
SLYM: Dense Slime, Thread-Like Strings, Pale Blue Glow



Day 9

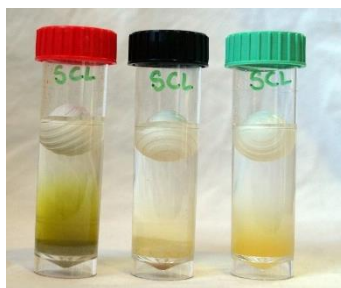
IRB: Cloudy, Brown Ring
SRB: Cloudy Gel-Like
SLYM: Dense Slime, Thread-Like Strings, Pale Blue Glow

Figure A.24: Progress of the BART test of GCL.



Day 1

IRB: Cloudy
SRB: Cloudy Gel-Like
SLYM: Dense Slime, Cloudy Plates layering



Day 2

IRB: Cloudy
SRB: Cloudy Gel-Like
SLYM: Dense Slime, Cloudy Plates layering, Pale Blue Glow



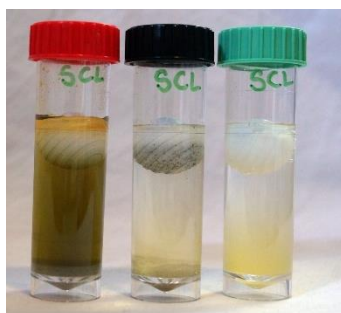
Day 3

IRB: Cloudy
SRB: Cloudy Gel-Like, Black Top
SLYM: Dense Slime, Cloudy Plates layering, Pale Blue Glow



Day 4

IRB: Cloudy, Brown Ring
SRB: Cloudy Gel-Like, Black Top
SLYM: Dense Slime, Cloudy Plates layering, Pale Blue Glow



Day 5

IRB: Cloudy, Brown Ring
SRB: Cloudy Gel-Like, Black Top
SLYM: Dense Slime, Cloudy Plates layering, Pale Blue Glow



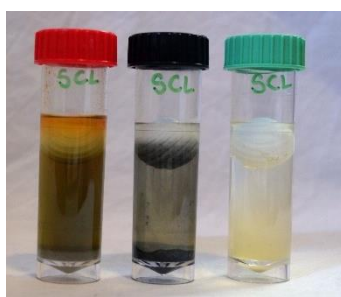
Day 6

IRB: Cloudy, Brown Ring
SRB: Cloudy Gel-Like, Black Top, Black Base
SLYM: Dense Slime, Cloudy Plates layering, Pale Blue Glow



Day 7

IRB: Cloudy, Brown Ring
SRB: Cloudy Gel-Like, Black Top, Black Base
SLYM: Dense Slime, Cloudy Plates layering, Pale Blue Glow



Day 8

IRB: Cloudy, Brown Ring
SRB: Cloudy Gel-Like, Black Top, Black Base
SLYM: Dense Slime, Cloudy Plates layering, Pale Blue Glow



Day 9

IRB: Cloudy, Brown Ring
SRB: Cloudy Gel-Like, Black Top, Black Base
SLYM: Dense Slime, Cloudy Plates layering, Pale Blue Glow

Figure A.25: Progress of the BART test of SCL.